Spatial and Temporal Coherence; Coherent Undulator Radiation

David Attwood

University of California, Berkeley

(http://www.coe.berkeley.edu/AST/srms)

COHERENCE AT SHORT WAVELENGTHS

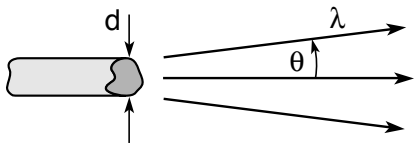

$$l_{coh} = \lambda^2/2\Delta\lambda \text{ \{temporal (longitudinal) coherence\}} \quad (8.3)$$

$$d \cdot \theta = \lambda/2\pi \text{ \{spatial (transverse) coherence\}} \quad (8.5)$$

$$\text{or } d \cdot 2\theta|_{FWHM} = 0.44\,\lambda \quad (8.5^*)$$

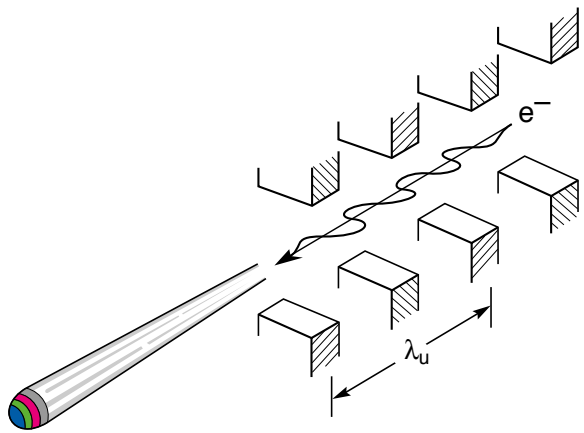

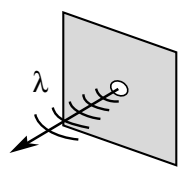

$$\bar{P}_{coh,N} = \frac{(\lambda/2\pi)^2}{(d_x\theta_x)(d_y\theta_y)}\bar{P}_{cen} \quad (8.6)$$

$$\bar{P}_{coh,\lambda/\Delta\lambda} = \frac{e\lambda_u I\eta(\Delta\lambda/\lambda)N^2}{8\pi\epsilon_0 d_x d_y} \cdot \left[1 - \frac{\hbar\omega}{\hbar\omega_0}\right] f(K) \quad (8.9)$$

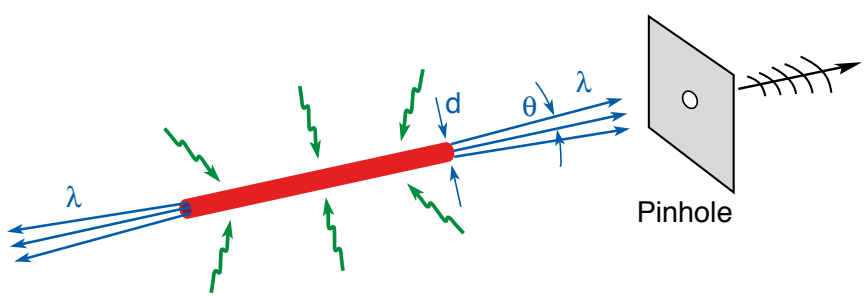

$$P_{coh} = \frac{(\lambda/2\pi)^2}{(d_x\theta_x)(d_y\theta_y)} P_{laser} \quad (8.11)$$

Professor David Attwood
Univ. California, Berkeley

Young's Double Slit Experiment: Spatial Coherence and the Persistence of Fringes

Persistence of fringes as the source grows from a point source to finite size.

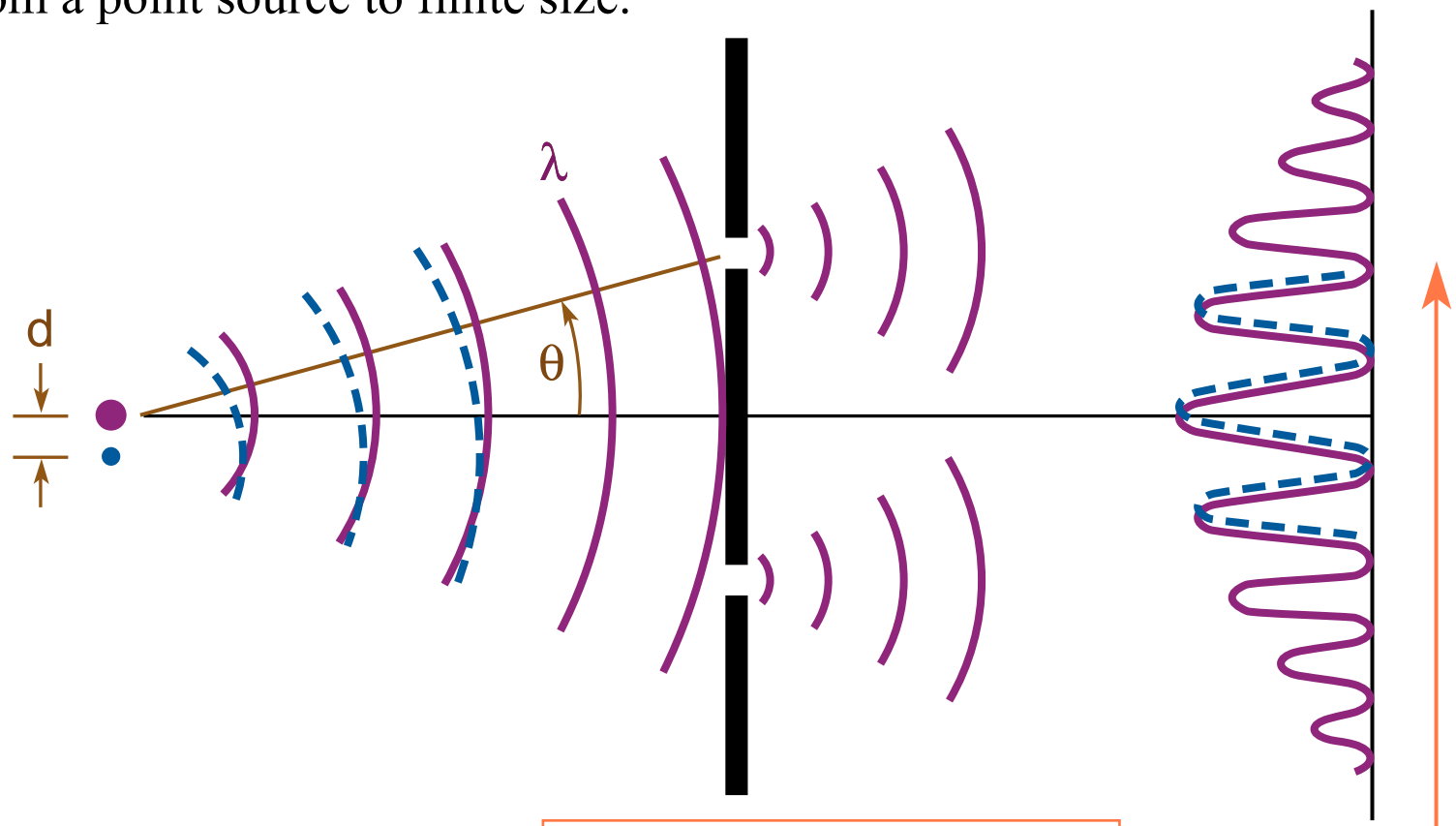

$$d \cdot 2\theta|_{FWHM} \simeq \lambda/2$$

$$\lambda_{coh} = \lambda^2/2\Delta\lambda = \frac{1}{2} N_{coh}\lambda$$

Professor David Attwood
Univ. California, Berkeley

Spatial and Spectral Filtering to Produce Coherent Radiation

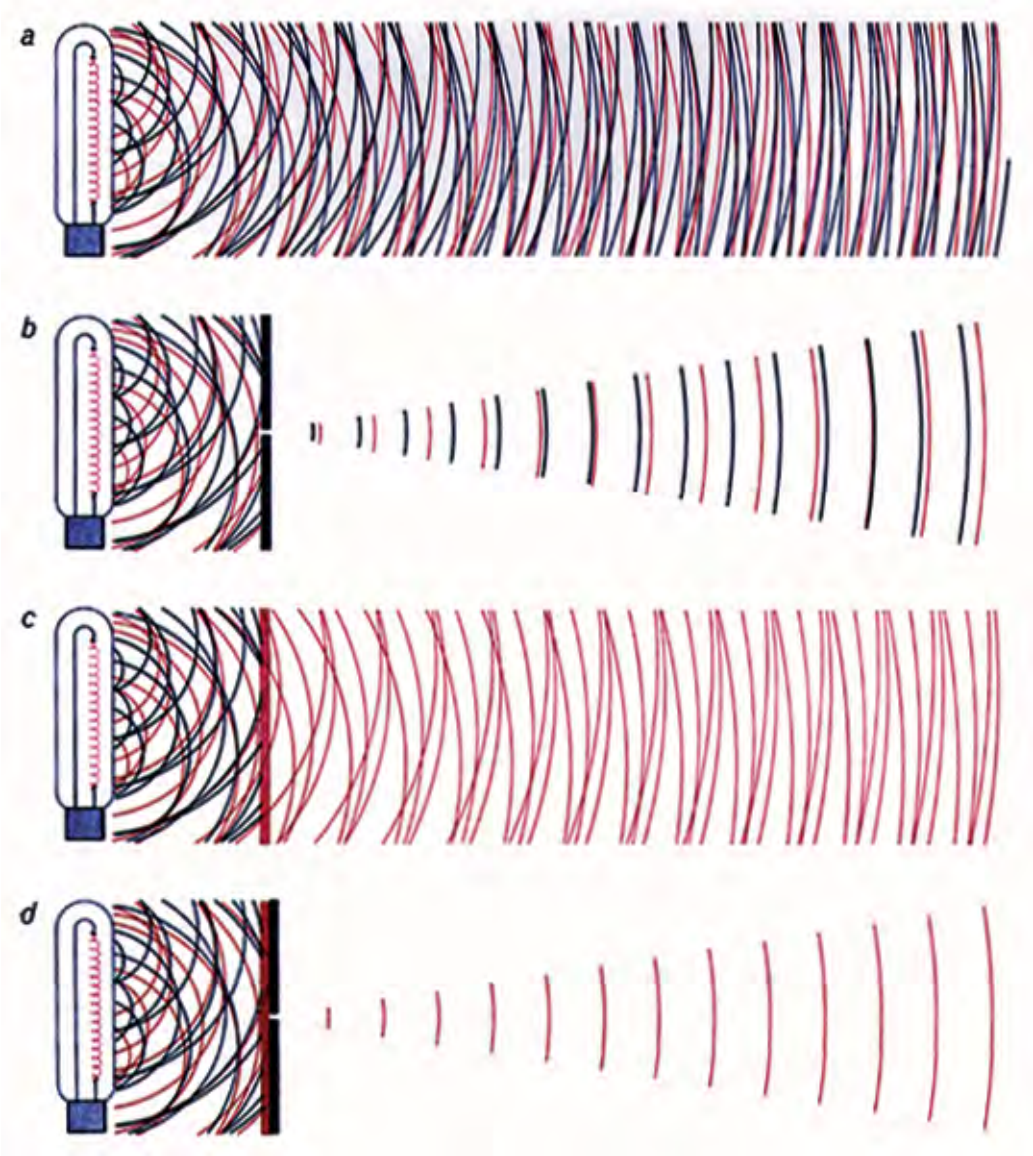

Courtesy of A. Schawlow, Stanford.

Coherence, Partial Coherence, and Incoherence

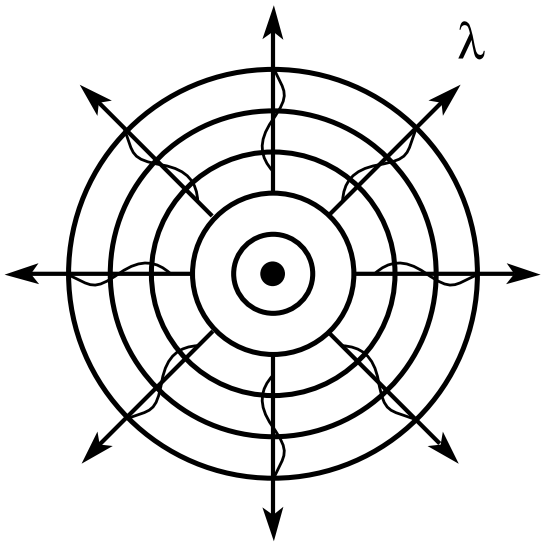

Point source oscillator
$-\infty < t < \infty$

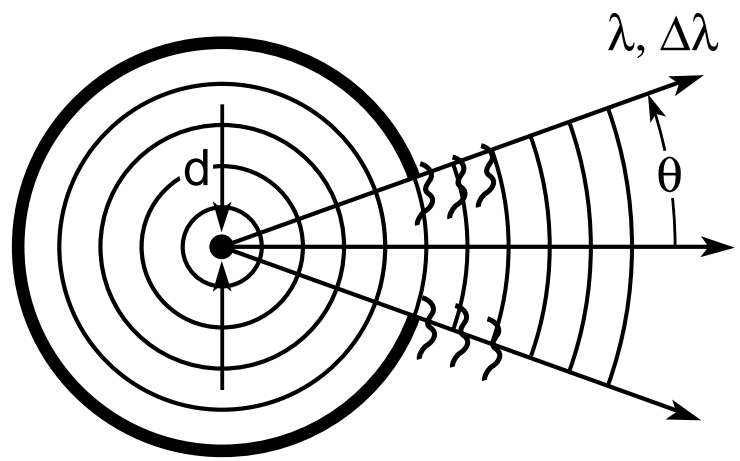

Source of finite size,
divergence, and duration

Spatial and Temporal Coherence

Mutual coherence factor

$$\Gamma_{12}(\tau) \equiv \langle E_1(t+\tau)E_2^*(t)\rangle \qquad (8.1)$$

Normalize degree of spatial coherence (complex coherence factor)

$$\mu_{12} = \frac{\langle E_1(t)E_2^*(t)\rangle}{\sqrt{\langle |E_1|^2\rangle}\sqrt{\langle |E_2|^2\rangle}} \qquad (8.12)$$

A high degree of coherence ($\mu \to 1$) implies an ability to form a high contrast interference (fringe) pattern. A low degree of coherence ($\mu \to 0$) implies an absence of interference, except with great care. In general radiation is partially coherent.

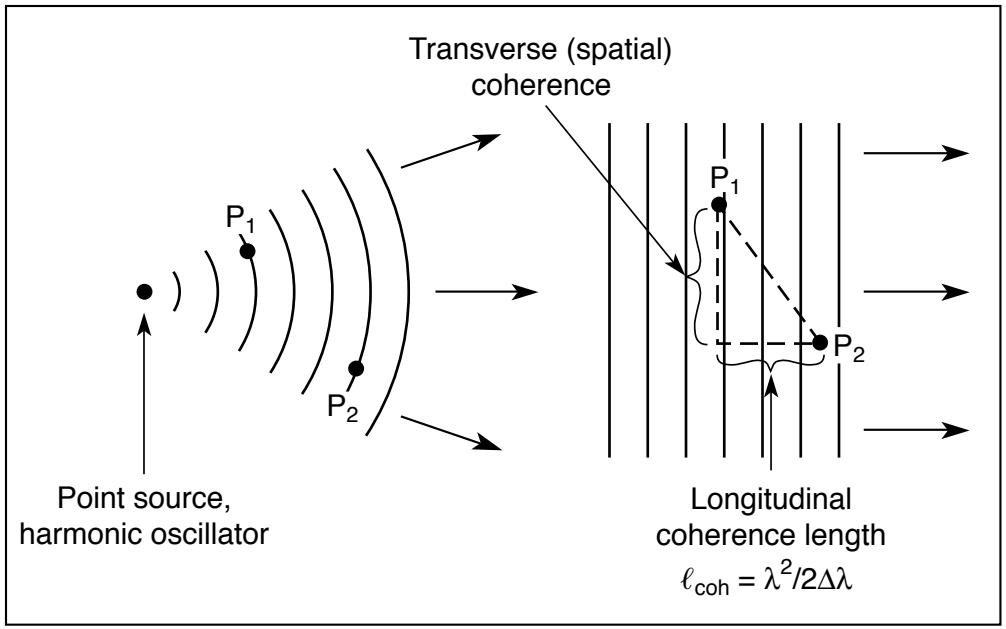

Longitudinal (temporal) coherence length

$$\ell_{coh} = \frac{\lambda^2}{2\,\Delta\lambda} \qquad (8.3)$$

Full spatial (transverse) coherence

$$d \cdot \theta = \lambda/2\pi \qquad (8.5)$$

Spectral Bandwidth and Longitudinal Coherence Length

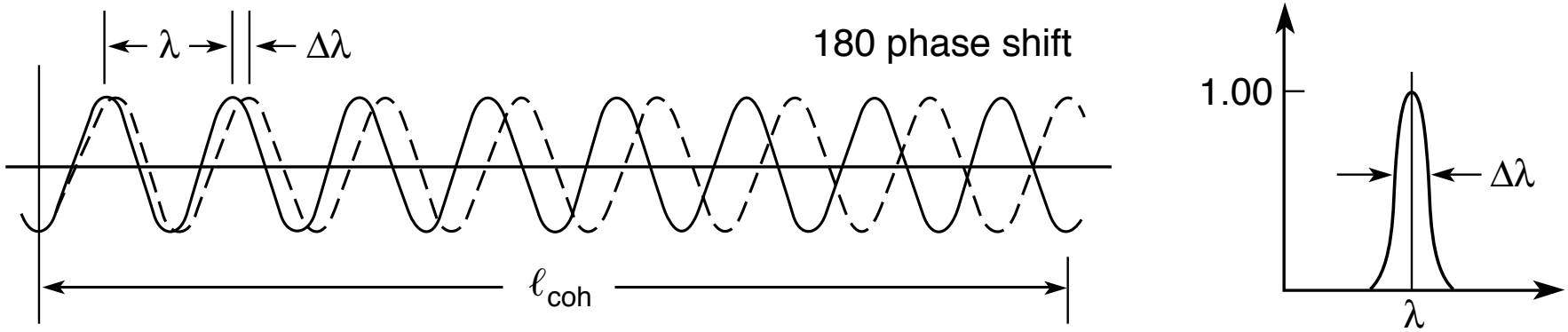

Define a coherence length ℓ_{coh} as the distance of propagation over which radiation of spectral width $\Delta\lambda$ becomes 180° out of phase. For a wavelength λ propagating through N cycles

$$\ell_{coh} = N\lambda$$

and for a wavelength $\lambda + \Delta\lambda$, a half cycle less $(N - \frac{1}{2})$

$$\ell_{coh} = (N - \tfrac{1}{2})\,(\lambda + \Delta\lambda)$$

Equating the two

$$N = \lambda/2\Delta\lambda$$

so that

$$\boxed{\ell_{coh} = \frac{\lambda^2}{2\,\Delta\lambda}} \qquad (8.3)$$

A Practical Interpretation of Spatial Coherence

- **Associate spatial coherence with a spherical wavefront.**
- **A spherical wavefront implies a point source.**
- **How small is a "point source"?**

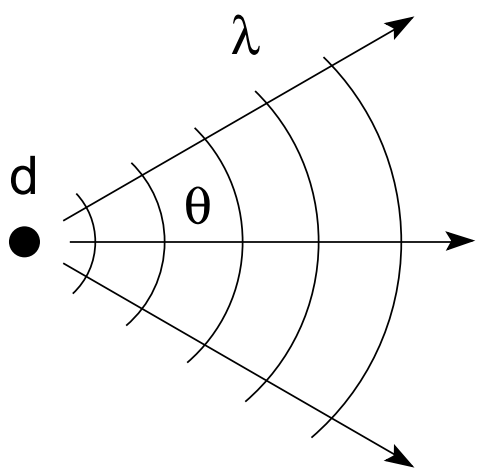

From Heisenberg's Uncertainty Principle ($\Delta x \cdot \Delta p \geq \frac{\hbar}{2}$), the smallest source size "d" you can resolve, with wavelength λ and half angle θ, is

$$d \cdot \theta = \frac{\lambda}{2\pi}$$

Partially Coherent Radiation Approaches Uncertainty Principle Limits

$\Delta\mathbf{x} \cdot \Delta\mathbf{p} \geq \hbar/2$ (8.4)

$\Delta\mathbf{x} \cdot \hbar\Delta\mathbf{k} \geq \hbar/2$

$\Delta\mathbf{x} \cdot \mathbf{k}\Delta\theta \geq 1/2$

$2\Delta\mathbf{x} \cdot \Delta\theta \geq \lambda/2\pi$

Standard deviations of Gaussian distributed functions (Tipler, 1978, pp. 174-189)

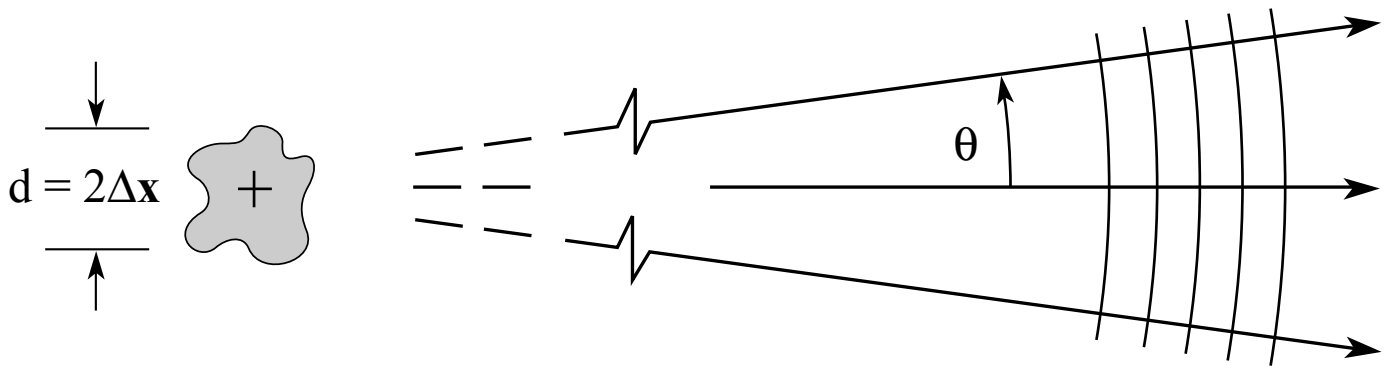

Spherical wavefronts occur in the limiting case

$$\boxed{d \cdot \theta = \lambda/2\pi}$$

(spatially coherent) $\Big\}$ $\frac{1}{\sqrt{e}}$ quantities

or

$(d \cdot 2\theta)_{FWHM} \simeq \lambda/2$ $\Big\}$ FWHM quantities

Note:

$\Delta\mathbf{p} = \hbar\Delta k$

$\Delta k = k\Delta\theta$

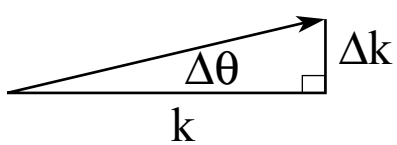

Propagation of a Gaussian Beam

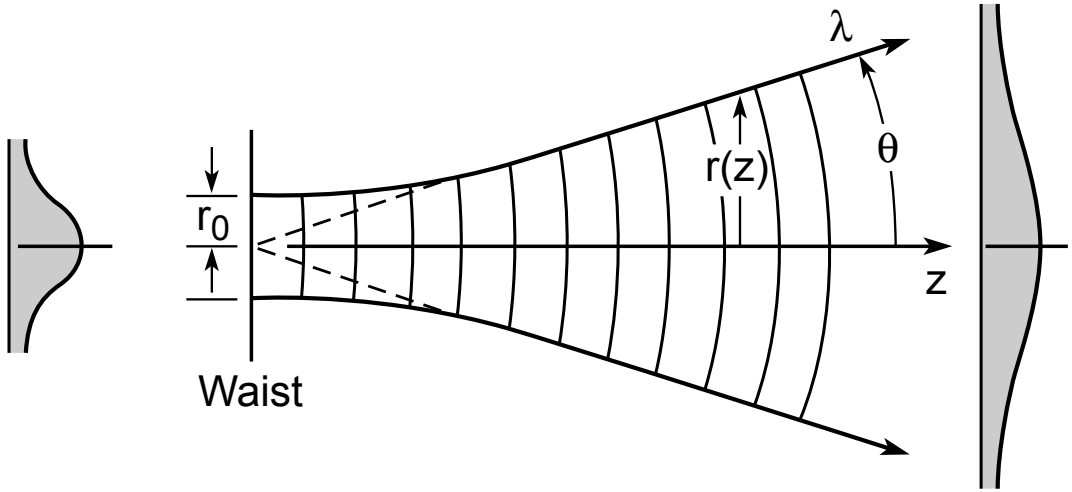

Gaussian intensity distribution, spherically propagating wave

For a spherical wave propagating with a Gaussian intensity distribution, $I/I_0 = \exp(-r^2/2r_0)$, where r_0 is the $1/\sqrt{e}$ waist radius at the origin ($z = 0$), the intensity distribution grows with a $1/\sqrt{e}$ radius given by (Siegman, Lasers)

$$r(z) = r_0\sqrt{1 + \left(\frac{\lambda z}{4\pi r_0^2}\right)^2}$$

In the far field, where $z \gg 4\pi r_0^2/\lambda$, the $1/\sqrt{e}$ divergence half angle is

$$\theta \equiv \frac{r(z)}{z} = \frac{\lambda}{4\pi r_0}$$

with waist diameter $d = 2r_0$, we have TEM_{00} radiation with $d \cdot \theta = \lambda/2\pi$

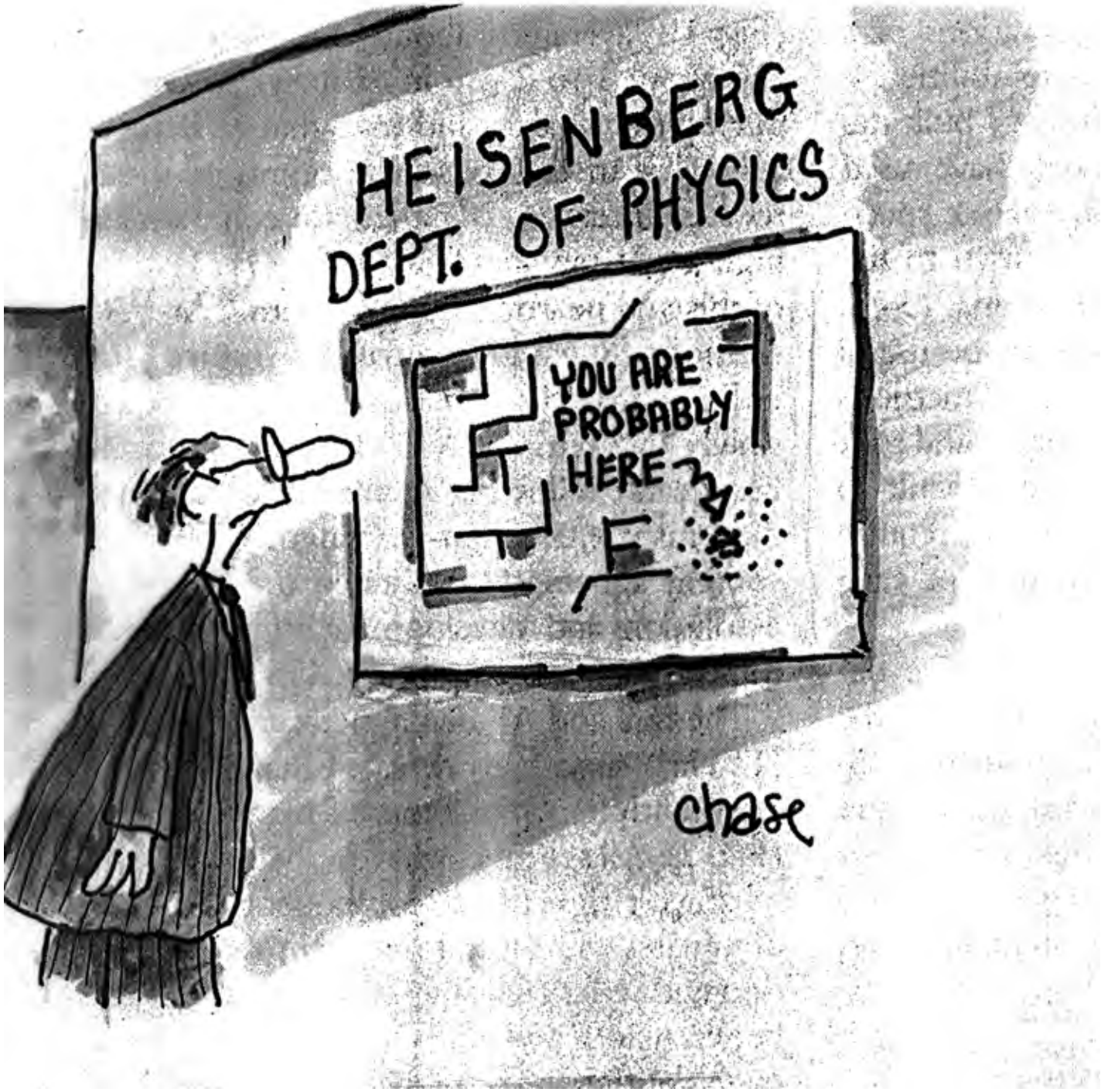
HEISENBERG
DEPT. OF PHYSICS
YOU ARE
PROBABLY
HERE
chase

Spatially Coherent Undulator Radiation

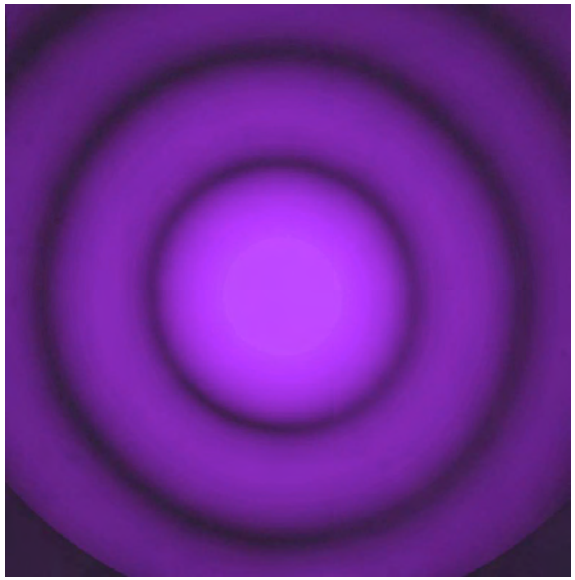

λ = 11.2 nm

λ = 13.4 nm

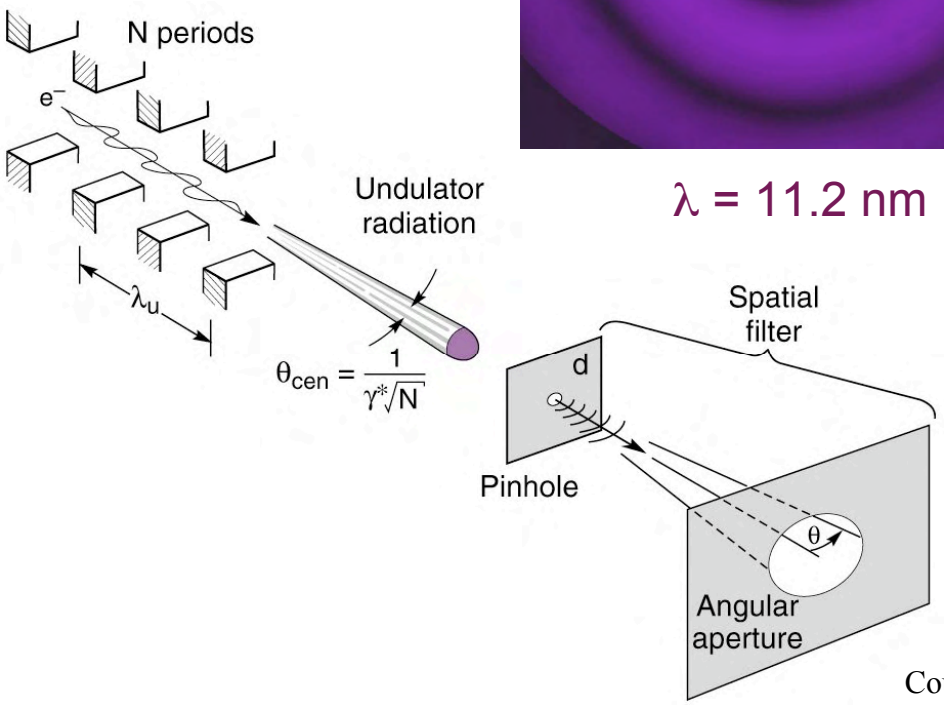

1 μm^D pinhole

25 mm wide CCD at 410 mm

Courtesy of Patrick Naulleau, LBNL.

Spatial Filtering of Undulator Radiation

Undulator central radiation cone ($\frac{\lambda}{\Delta\lambda} = N$; $\theta = \frac{1}{\gamma^* \sqrt{N}}$):

$$\bar{P}_{\text{cen}} = \frac{\pi e \gamma^2 I}{\epsilon_0 \lambda_u} \frac{K^2}{(1 + K^2/2)^2} f(K) \qquad (5.41a)$$

With spatial filtering (a pinhole and an angular aperture):

$$\bar{P}_{\text{coh},N} = \underbrace{\left(\frac{\lambda/2\pi}{d_x \theta_x}\right)}_{\leq 1} \underbrace{\left(\frac{\lambda/2\pi}{d_y \theta_y}\right)}_{\leq 1} \bar{P}_{\text{cen}} \qquad (8.6)$$

With eq.(5.28), $\lambda = \frac{\lambda_u}{2\gamma^2}\left(1 + \frac{K^2}{2} + \gamma^2\theta^2\right)$. Convert to photon energies where for $\theta = 0$, $\hbar\omega = \frac{\hbar\omega_0}{1 + K^2/2}$, and where $\hbar\omega_0 \equiv 4\pi\hbar c\gamma^2/\lambda_u$ corresponds to K = 0. For small electron beam diverence, $\sigma'^2_{x,y} << \theta^2_{\text{cen}}$, the spatially coherent power is

$$\boxed{\bar{P}_{\text{coh},N} = \frac{e\lambda_u I N}{8\pi\epsilon_0 d_x d_y}\left(1 - \frac{\hbar\omega}{\hbar\omega_0}\right) f(\hbar\omega/\hbar\omega_0)} \qquad (8.9)$$

Spatially Filtered Undulator Radiation

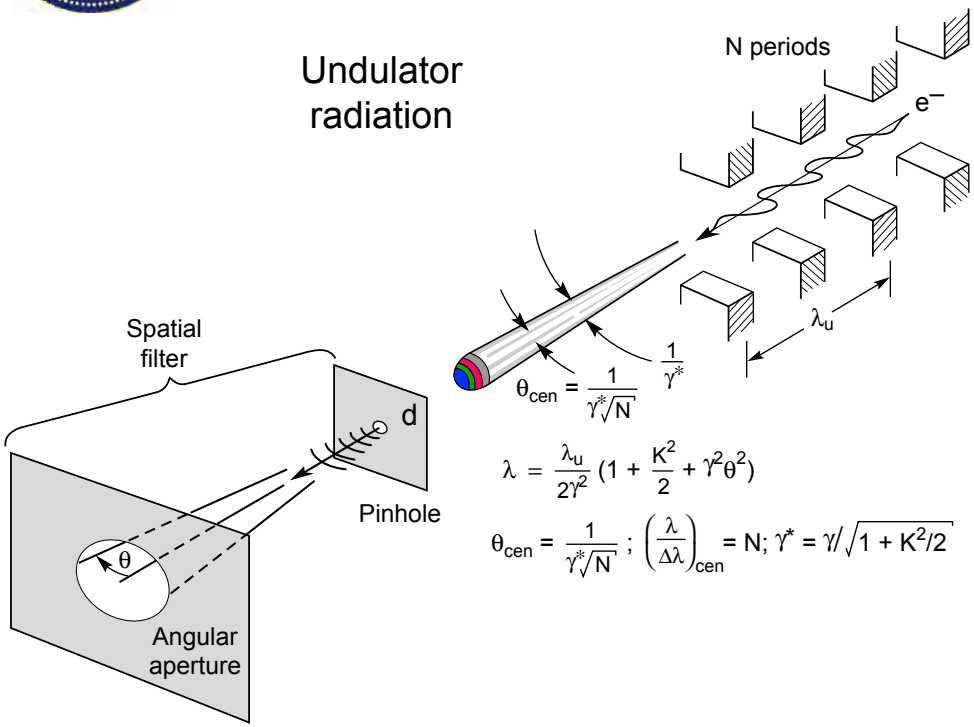

$$\lambda = \frac{\lambda_u}{2\gamma^2}\left(1 + \frac{K^2}{2} + \gamma^2\theta^2\right)$$

$$\theta_{cen} = \frac{1}{\gamma^*\sqrt{N}}\ ;\ \left(\frac{\lambda}{\Delta\lambda}\right)_{cen} = N;\ \gamma^* = \gamma/\sqrt{1 + K^2/2}$$

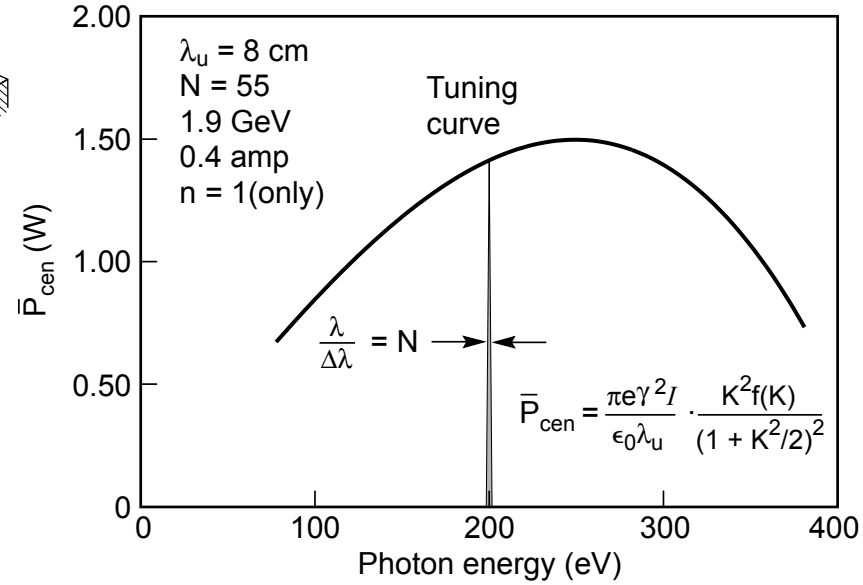

Using a pinhole-aperture spatial filter, passing only radiation that satisfies $d \cdot \theta = \lambda/2\pi$

$$\bar{P}_{\mathrm{coh},N} = \left(\frac{\lambda/2\pi}{d_x\theta_x}\right)\left(\frac{\lambda/2\pi}{d_y\theta_y}\right)\bar{P}_{\mathrm{cen}} \qquad (8.6)$$

$$\bar{P}_{\mathrm{coh},N} = \frac{e\lambda_u I N}{8\pi\epsilon_0 d_x d_y}\left(1 - \frac{\hbar\omega}{\hbar\omega_0}\right) f(\hbar\omega/\hbar\omega_0) \qquad (8.9)$$

for $d_x = 2\sigma_x$, $d_y = 2\sigma_y$, $\theta_{Tx} \to \theta_x$, $\theta_{Ty} \to \theta_y$, and $\sigma'^2 << \theta_{cen}^2$.

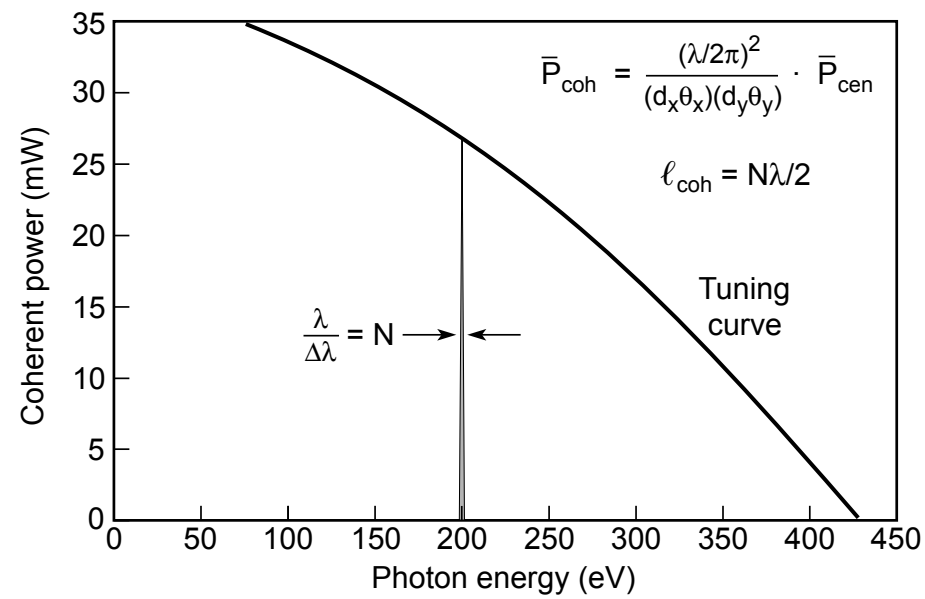

Spatial and Spectral Filtering of Undulater Radiation

In addition to the pinhole – angular aperture for spatial filtering and spatial coherence, add a monochromator for narrowed bandwidth and increased temporal coherence:

$$\bar{P}_{\mathrm{coh},\lambda/\Delta\lambda} = \underbrace{\eta}_{\substack{\text{beamline}\\ \text{efficiency}}} \underbrace{\frac{(\lambda/2\pi)^2}{(d_x\theta_x)(d_y,\theta_y)}}_{\substack{\text{spatial}\\ \text{filtering}}} \cdot \underbrace{N\frac{\Delta\lambda}{\lambda}}_{\substack{\text{spectral}\\ \text{filtering}}} \cdot \bar{P}_{\mathrm{cen}} \qquad (8.10a)$$

which for $\sigma'^2_{x,y} << \theta^2_{cen}$ (the undulator condition) gives the spatially and temporally coherent power ($d \cdot \theta = \lambda/2\pi$; $l_{\mathrm{coh}} = \dfrac{\lambda^2}{2\,\Delta\lambda}$)

$$\boxed{\bar{P}_{\mathrm{coh},\lambda/\Delta\lambda} = \frac{e\lambda_u I\eta(\Delta\lambda/\lambda)N^2}{8\pi\epsilon_0 d_x d_y} \cdot \left(1 - \frac{\hbar\omega}{\hbar\omega_0}\right) f(\hbar\omega/\hbar\omega_0)} \qquad (8.10c)$$

which we note scales as N^2.

Spatially and Spectrally Filtered Undulator Radiation

- Pinhole filtering for full spatial coherence
- Monochromator for spectral filtering to $\lambda/\Delta\lambda > N$

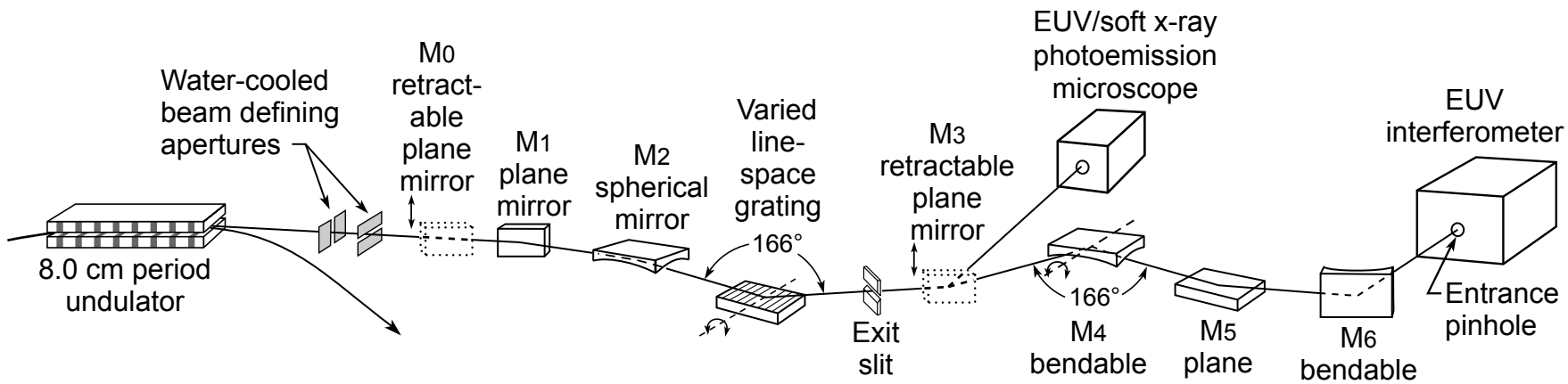

$$\bar{P}_{\mathrm{coh},\lambda/\Delta\lambda} = \underbrace{\eta}_{\substack{\text{beamline}\\ \text{efficiency}}} \underbrace{\frac{(\lambda/2\pi)^2}{(d_x\theta_x)(d_y\theta_y)}}_{\substack{\text{spatial}\\ \text{filtering}}} \cdot \underbrace{N\frac{\Delta\lambda}{\lambda}}_{\substack{\text{spectral}\\ \text{filtering}}} \cdot \bar{P}_{\mathrm{cen}} \qquad (8.10a)$$

$$\bar{P}_{\mathrm{coh},\lambda/\Delta\lambda} = \frac{e\lambda_u I\eta(\Delta\lambda/\lambda)N^2}{8\pi\epsilon_0 d_x d_y} \cdot \left(1 - \frac{\hbar\omega}{\hbar\omega_0}\right) f(\hbar\omega/\hbar\omega_0)$$

$$\left(\sigma'^2 \ll \theta_{\mathrm{cen}}^2\right) \qquad (8.10c)$$

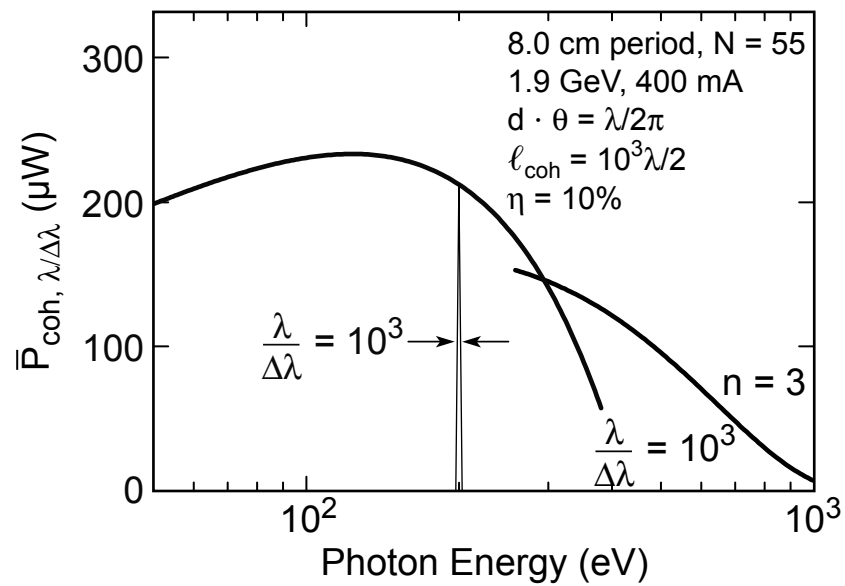

Coherent Soft X-Ray Beamline: Use of a Higher Harmonic (n = 3) to Access Shorter Wavelengths

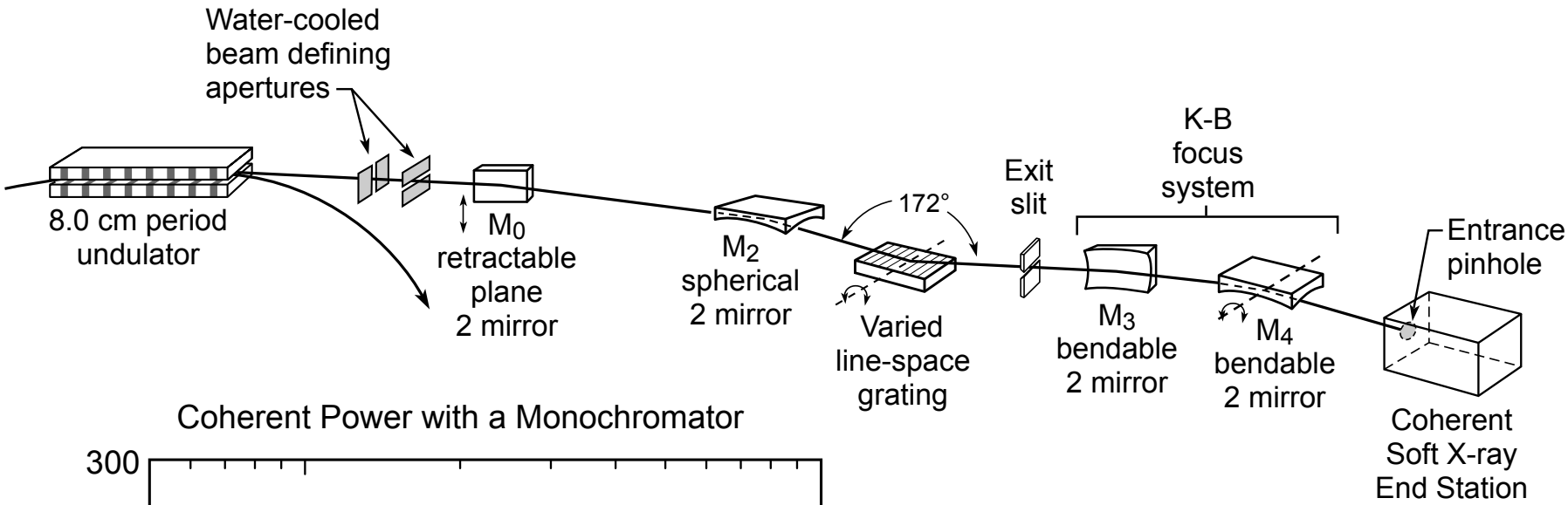

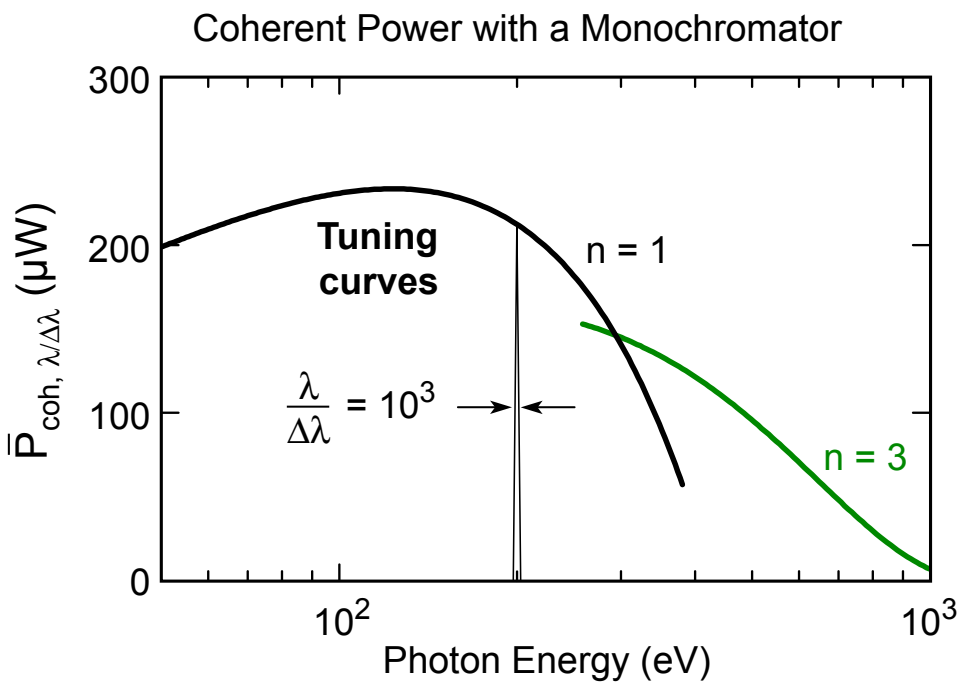

8.0 cm period, N = 55
1.9 GeV, 400 mA
$d \cdot \theta = \lambda/2\pi$
$\ell_{coh} = 1000\ \lambda/2$
$\eta_{euv} = 10\%$, $\eta_{sxr} = 10\%$

Coherent Power at the ALS

U8

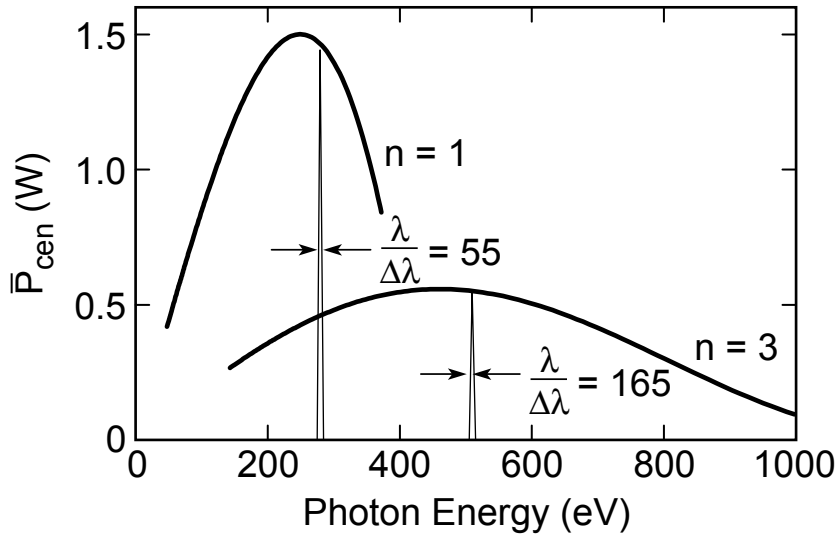

1.9 GeV, 400 mA

λ_u = 80 mm, N = 55

$0.5 \leq K \leq 4.0$

σ_x = 260 μm, σ_x' = 23 μr

σ_y = 16 μm, σ_y' = 3.9 μr

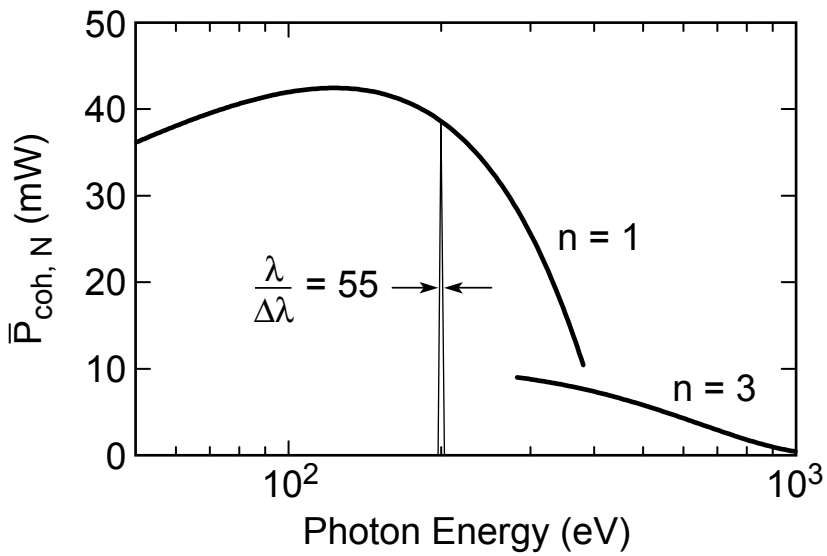

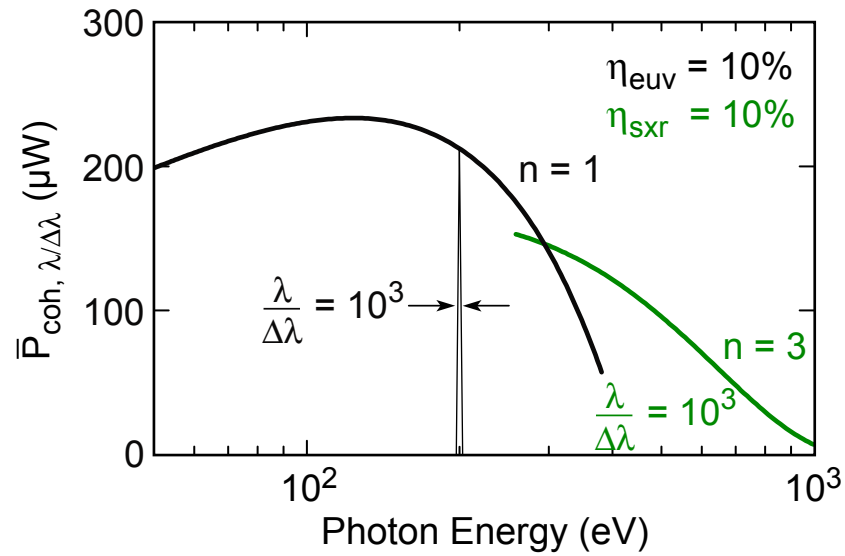

Coherent Power at the ALS

U5

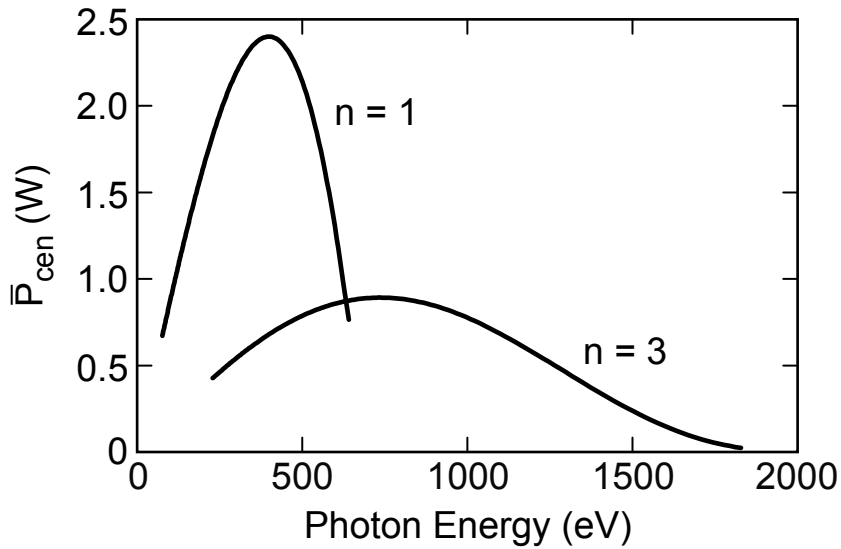

1.9 GeV, 400 mA

λ_u = 50 mm, N = 89

$0.5 \le K \le 4.0$

σ_x = 260 μm, σ_x' = 23 μr

σ_y = 16 μm, σ_y' = 3.9 μr

η = 10%

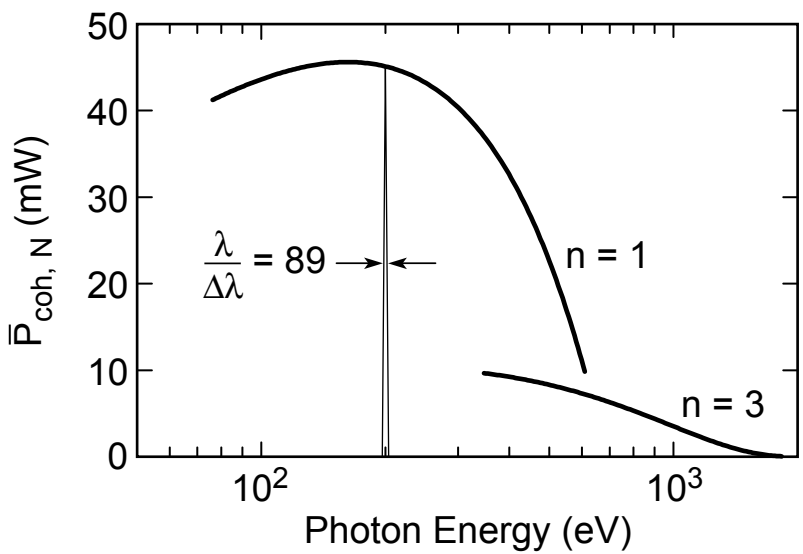

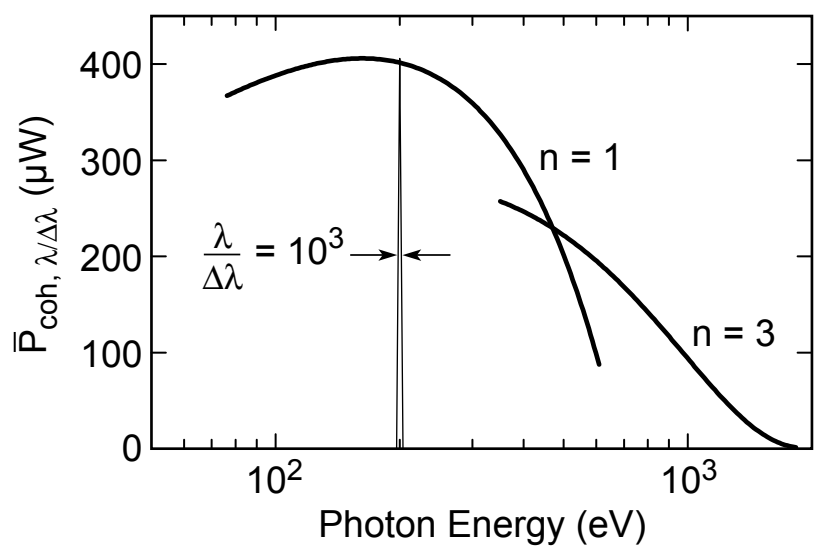

Coherent Power for an EPU at the ALS

U5 EPU

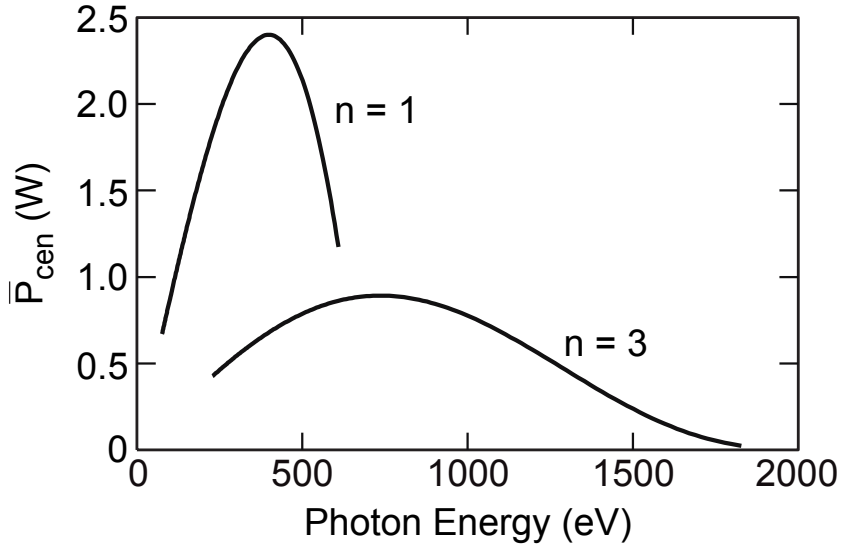

1.9 GeV, 400 mA

λ_u = 50 mm, N = 27

$0.5 \le K \le 4.0$

σ_x = 260 μm, σ_x' = 23 μr

σ_y = 16 μm, σ_y' = 3.9 μr

θ_{cen} = 61μr @ K = 0.87 (500 eV)

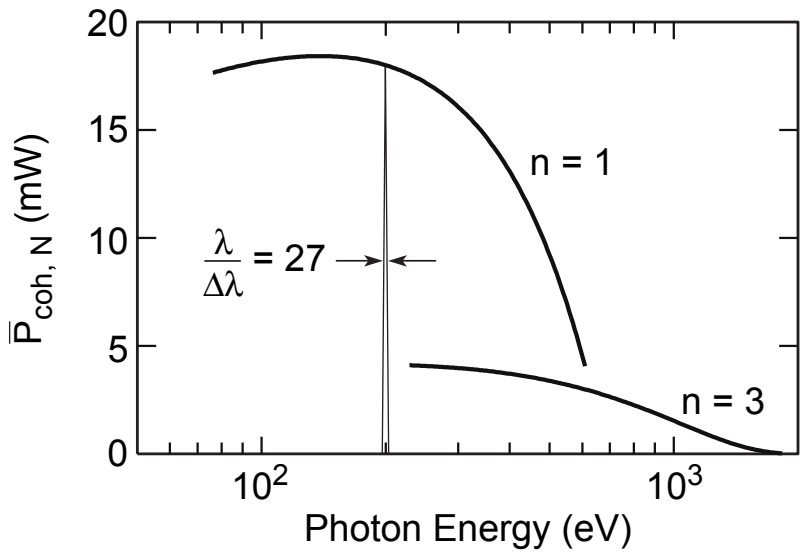

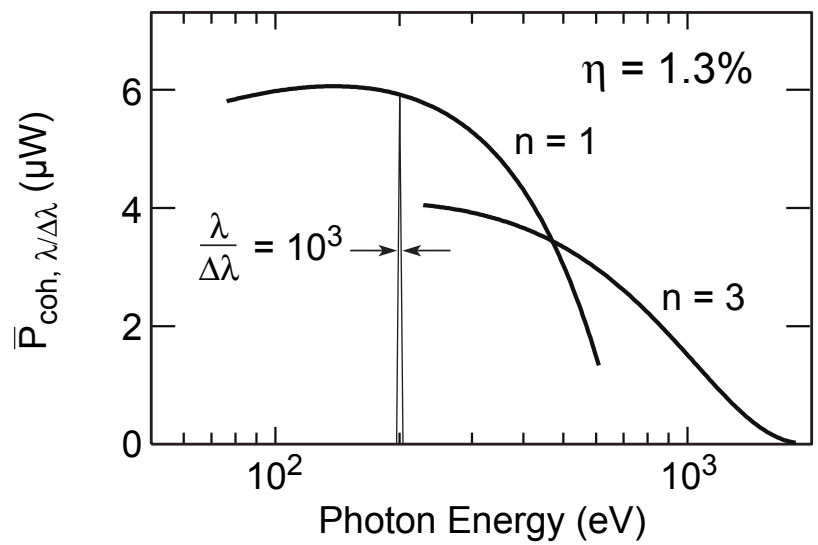

Coherent Power Predicted with SPEAR 3 at SSRL

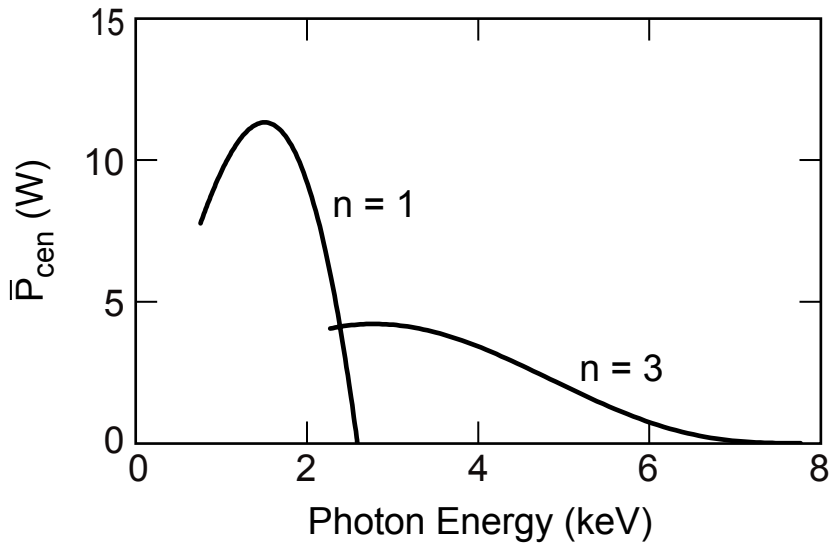

3.0 GeV, 500 mA

λ_u = 3.3 cm, N = 105

$0 \le K \le 2.2$

σ_x = 436 μm, σ_x' = 43 μrad

σ_y = 30 μm, σ_y' = 6.3 μrad

θ_{cen} = 17 μrad @ K = 1

η = 10%

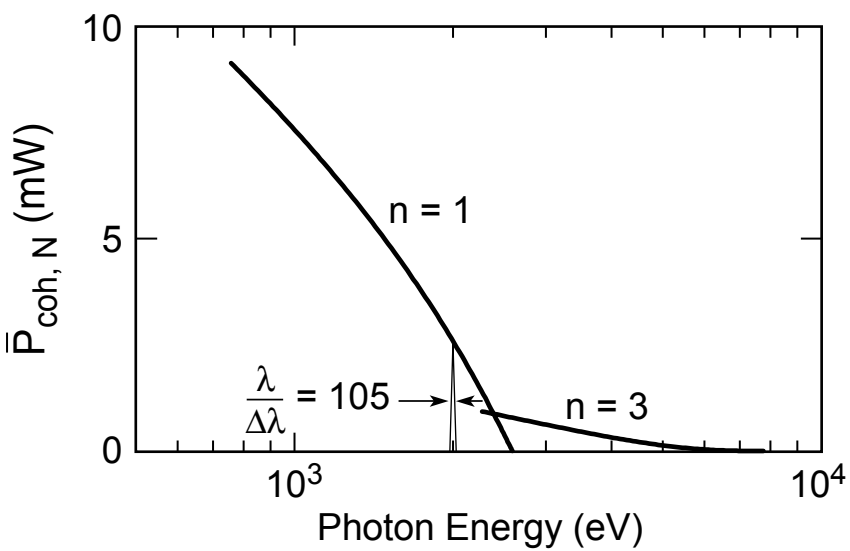

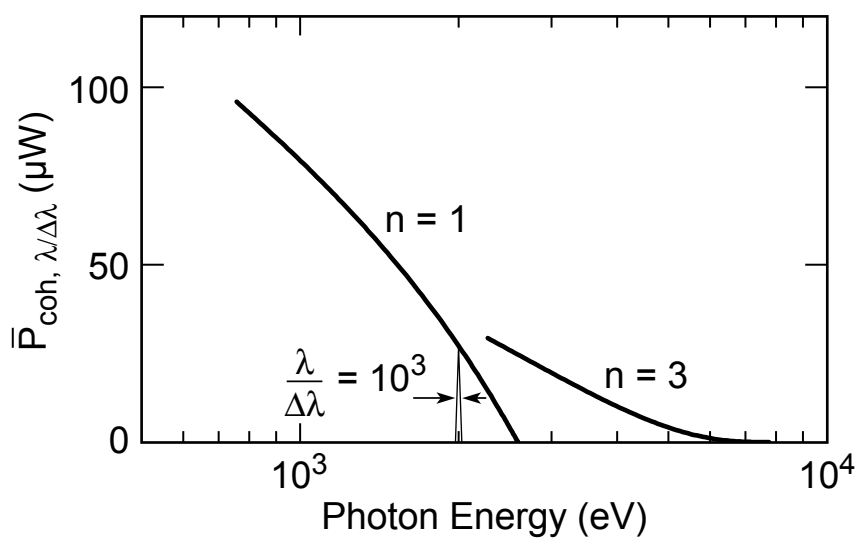

Coherent Power at the Australian Synchrotron

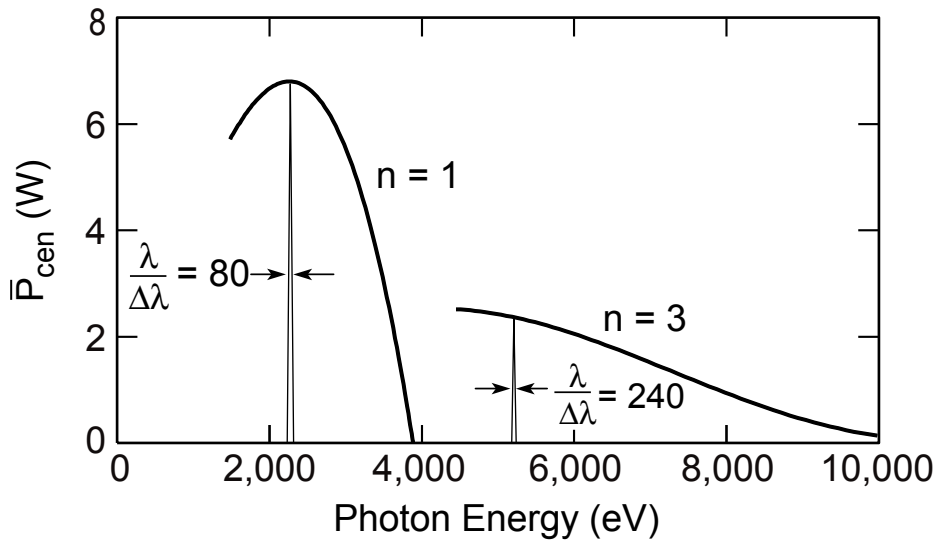

3.0 GeV, 200 mA

λ_u = 22 mm, N = 80

$0 \leq K \leq 1.8$

σ_x = 320 μm, σ_x' = 34 μrad

σ_y = 16 μm, σ_y' = 6 μrad

θ_{cen} = 23 μrad @ K = 1

η = 10%

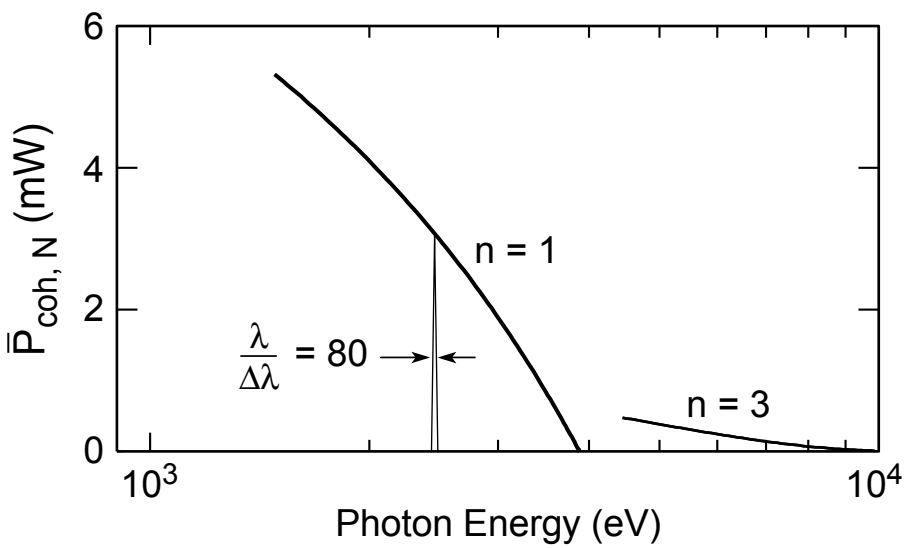

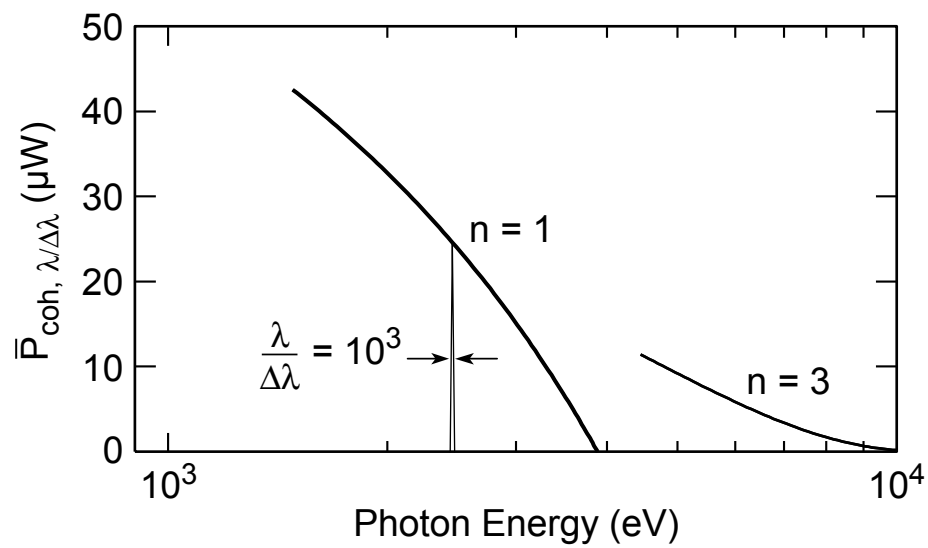

Professor David Attwood
Univ. California, Berkeley

Coherent Power at the UK's Diamond Synchrotron Facility

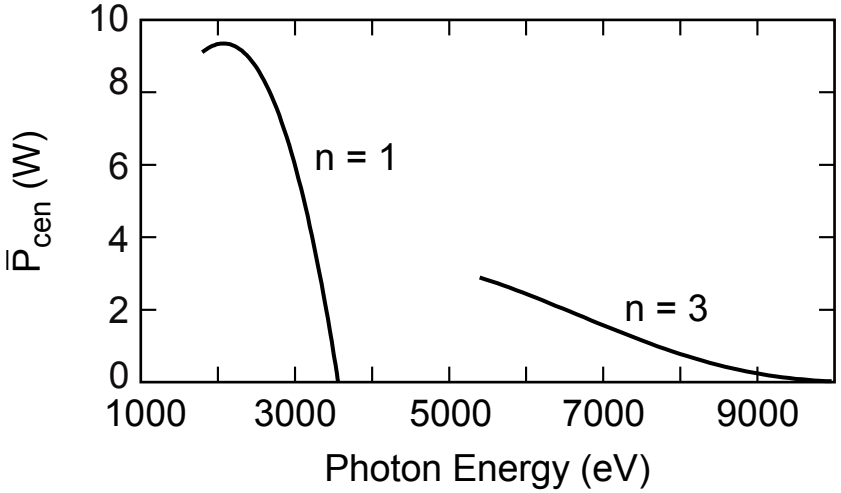

3.0 GeV, 300 mA

λ_u = 2.4 cm, N = 82

$0 \le K \le 1.4$

σ_x = 123 μm, σ_x' = 24 μr

σ_y = 6.4 μm, σ_y' = 4.2 μr

θ_{cen} = 23 μr @ K = 1

η = 10%

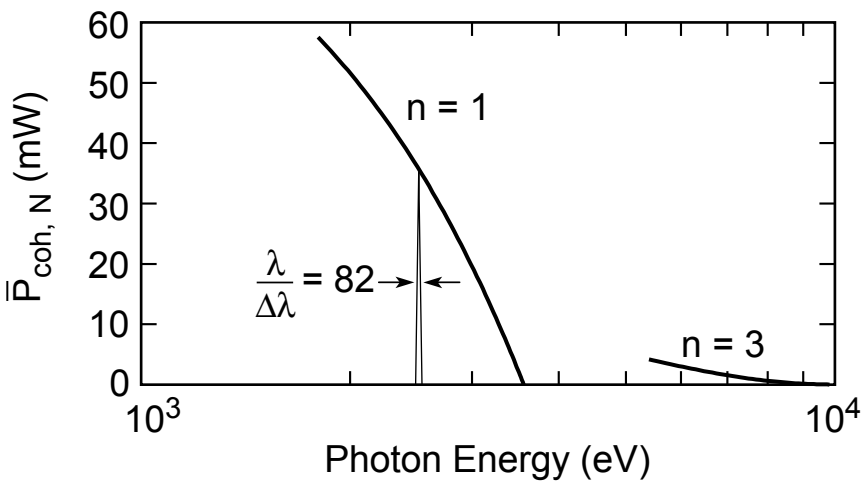

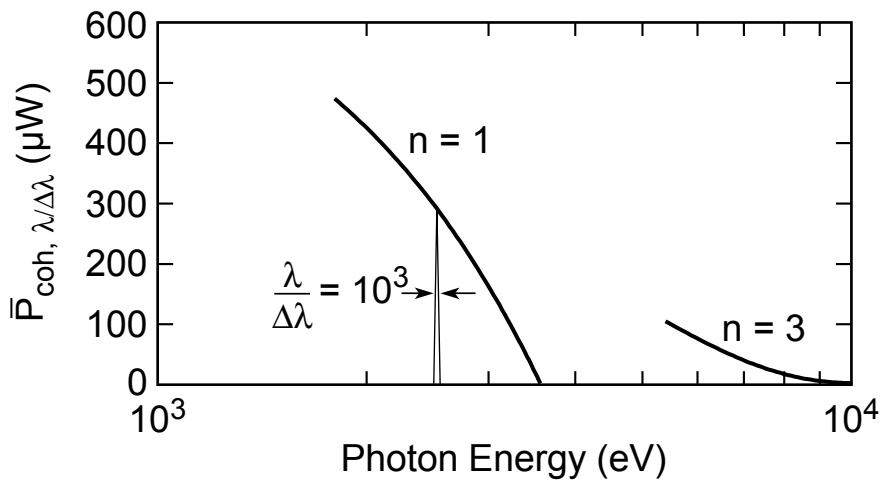

Courtesy of Brian Kennedy (King's College London), Susan Smith (Daresbury), and Yanwei Liu (LBNL)

Coherent Power at the APS

APS

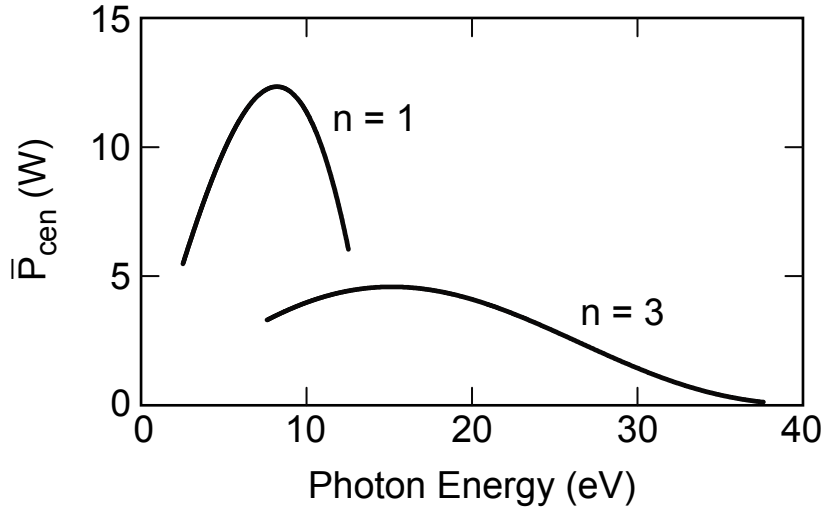

7.00 GeV, 100 mA

λ_u = 33 mm, N = 72

$0.5 \leq K \leq 3.0$

σ_x = 320 μm, σ_x' = 23 μr

σ_y = 50 μm, σ_y' = 7 μr

η = 10%

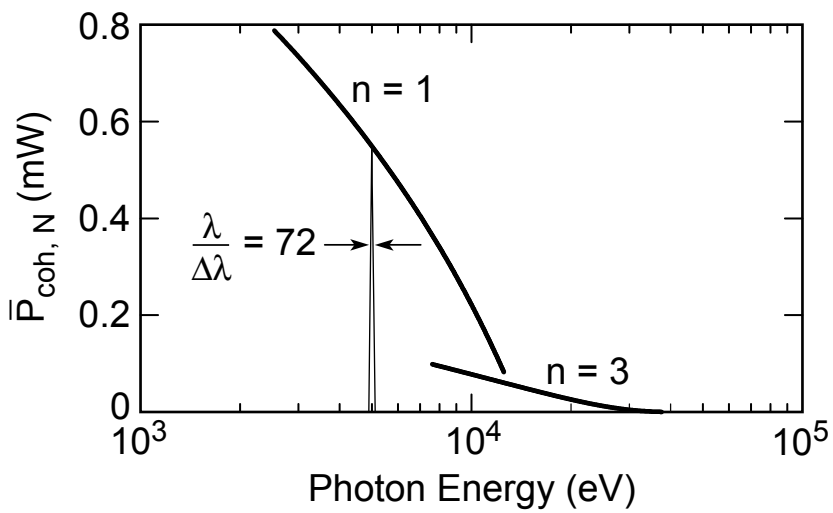

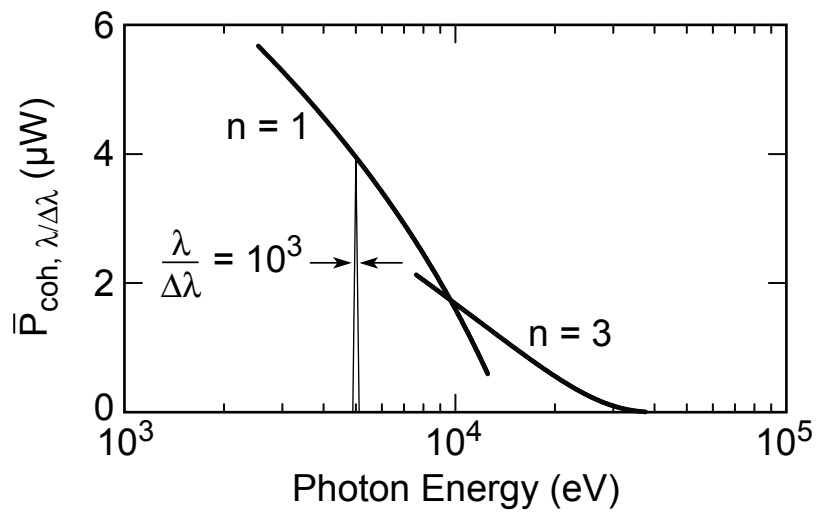

Coherent Power at SPring-8

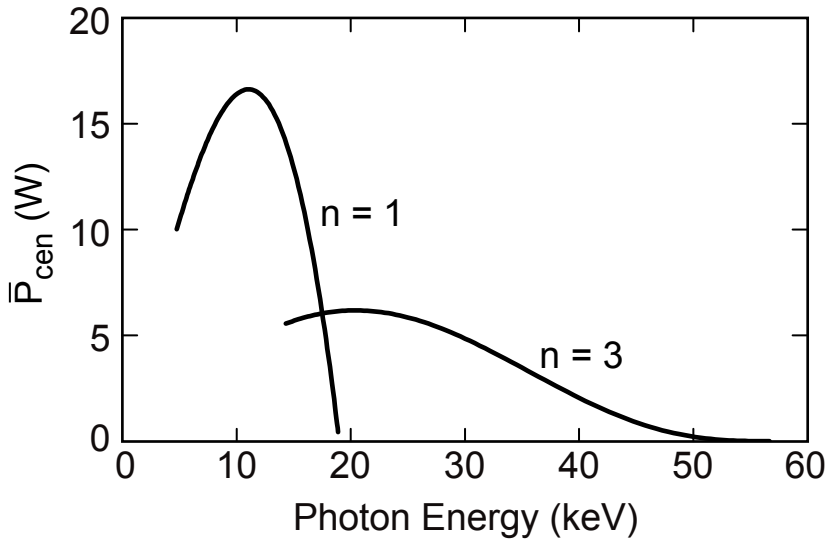

8 GeV, 100 mA

λ_u = 32 mm, N = 140

$0 \leq K \leq 2.46$

σ_x = 393 μm, σ_x' = 15.7 μr

σ_y = 4.98 μm, σ_y' = 1.24 μr

η = 10%

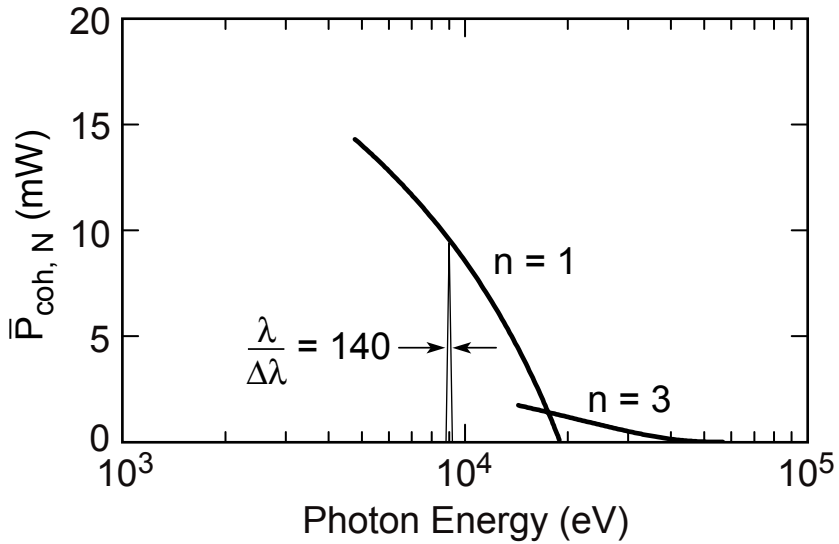

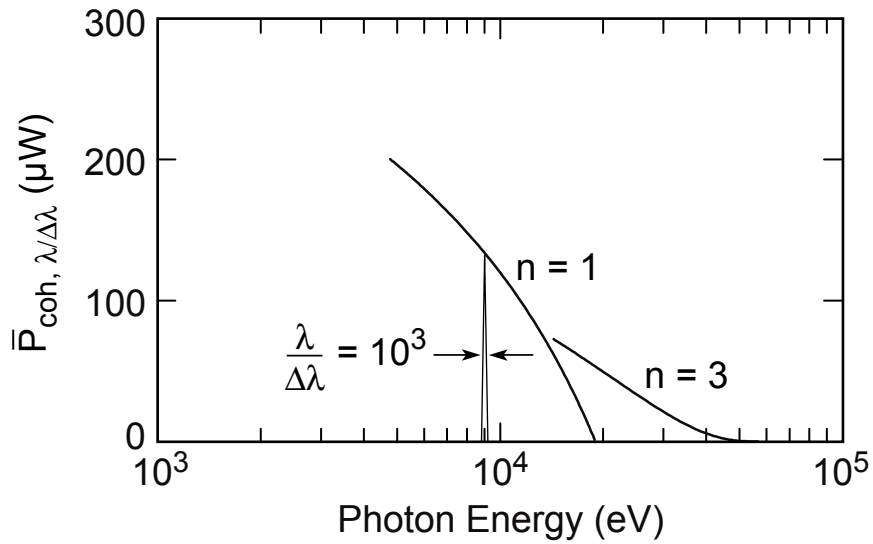

Spatially Coherent Undulator Radiation

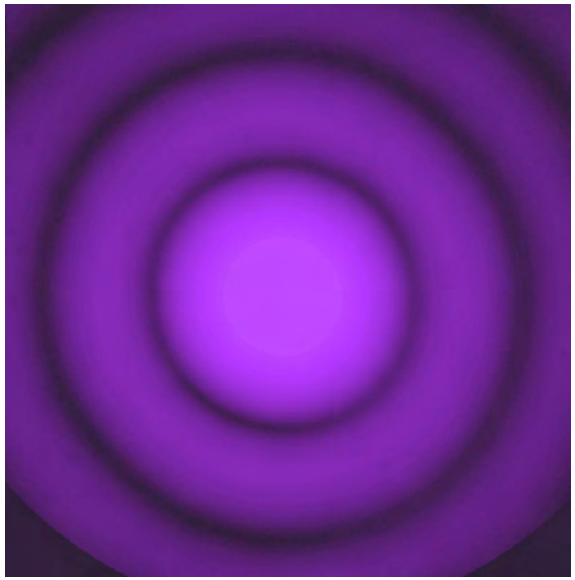

λ = 11.2 nm

λ = 13.4 nm

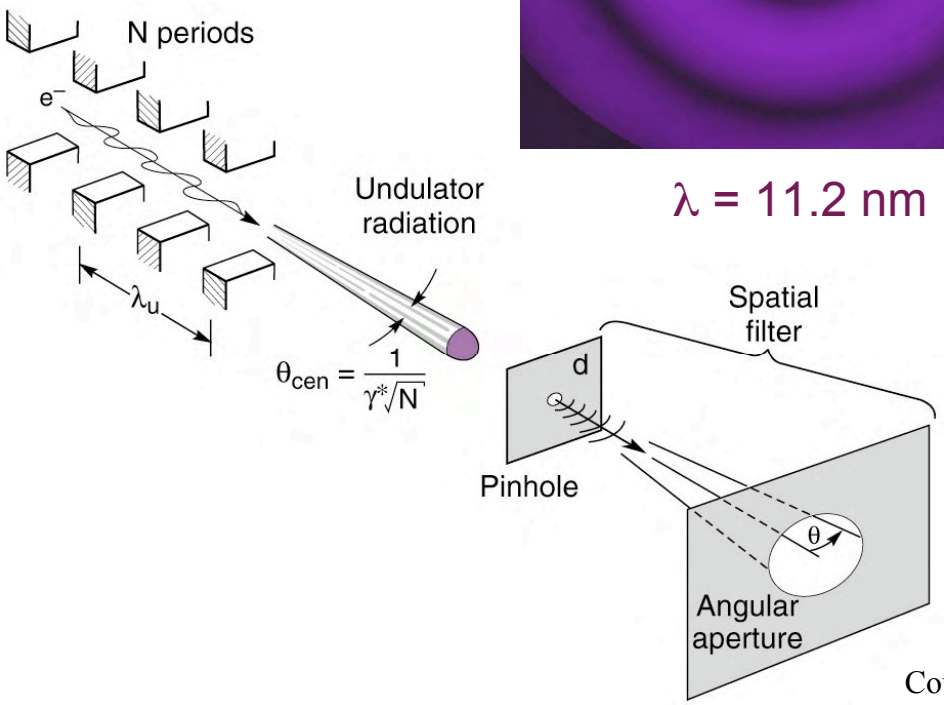

1 μm^D pinhole

25 mm wide CCD at 410 mm

Courtesy of Patrick Naulleau, LBNL.

Undulator Beamline for High Spatial Coherence Measurements

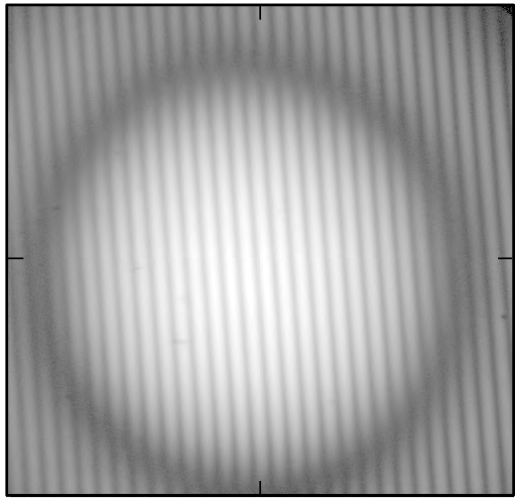

C. Chang

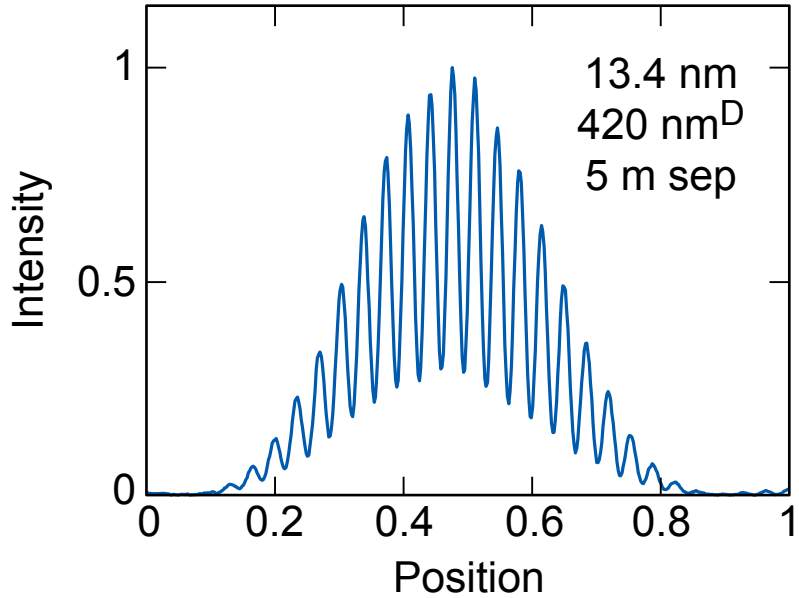

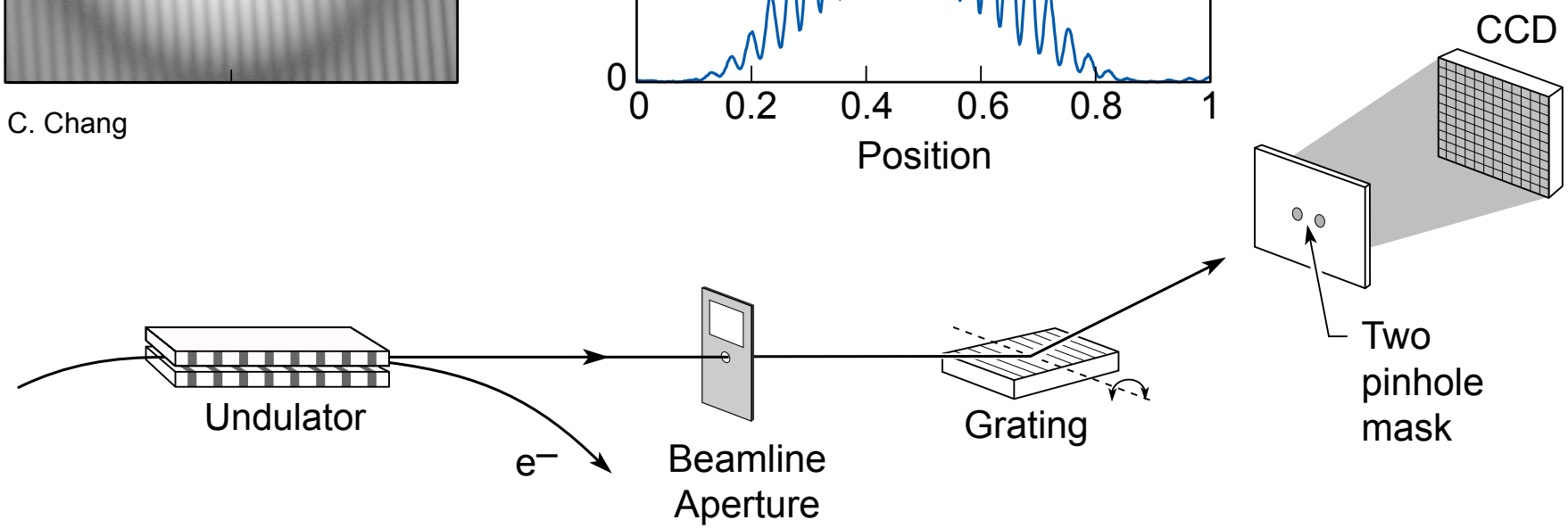

Spatial Coherence Measurements of Undulator Radiation Using the Classic 2-Pinhole Technique

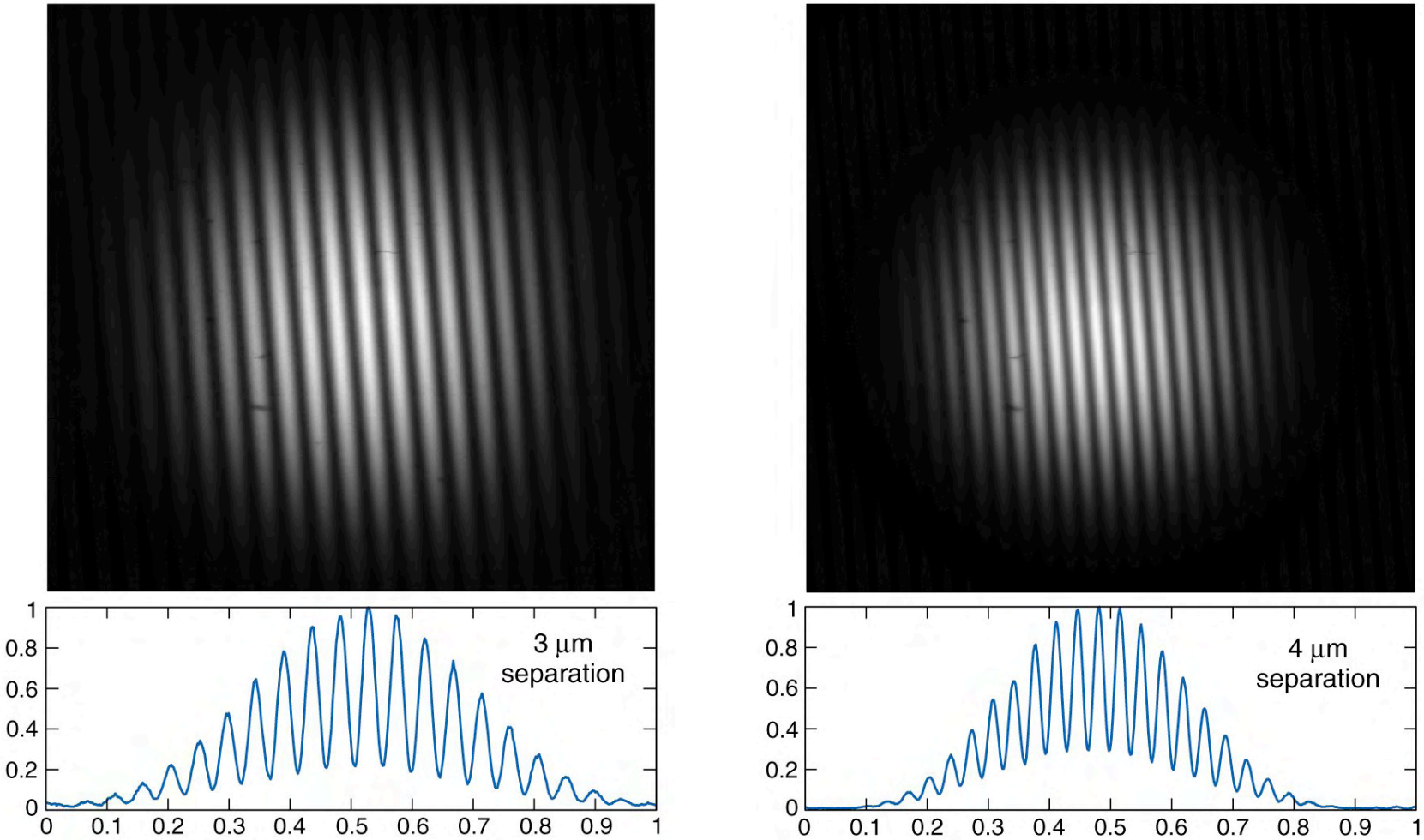

Courtesy of Chang Chang, UC Berkeley and LBNL.

λ = 13.4 nm, 450 nm diameter pinholes, 1024 x 1024 EUV/CCD at 26 cm ALS, 1.9 GeV, λ_u = 8 cm, N = 55

Spatial Coherence Measurements of Undulator Radiation Using the Classic 2-Pinhole Technique

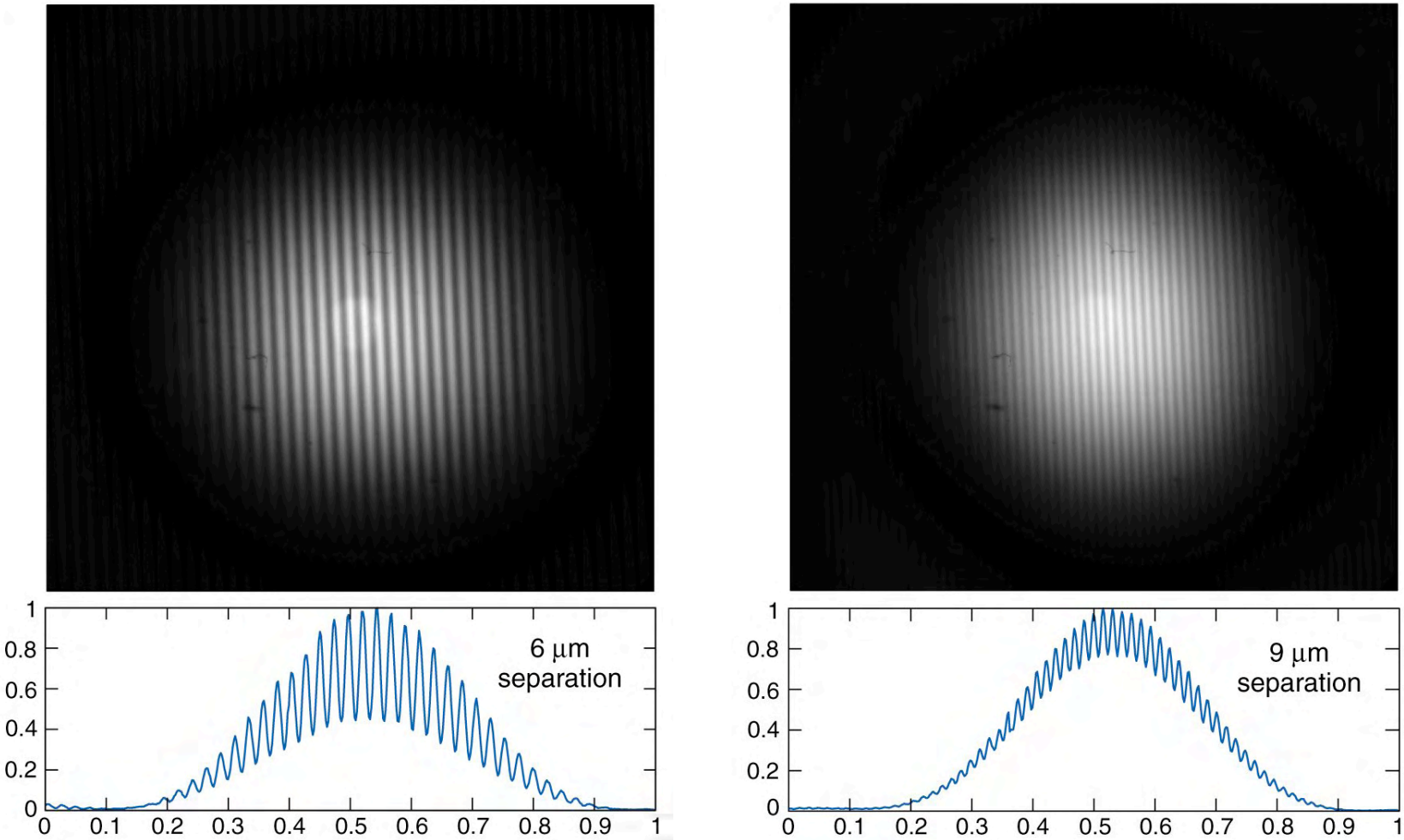

Courtesy of Chang Chang, UC Berkeley and LBNL.

λ = 13.4 nm, 450 nm diameter pinholes, 1024 x 1024 EUV/CCD at 26 cm ALS, 1.9 GeV, λ_u = 8 cm, N = 55

Spatial Coherence Measurements in the Vertical Plane

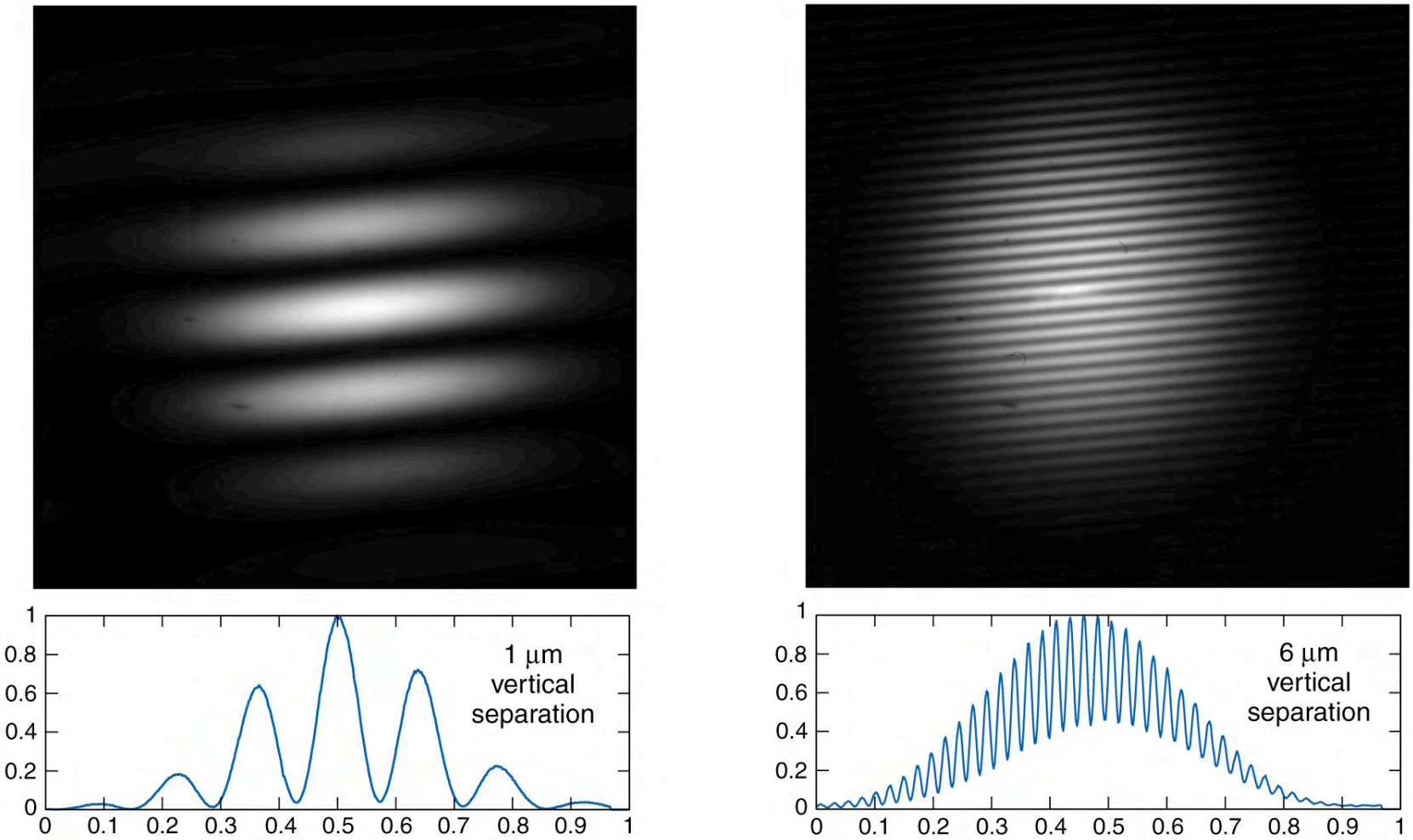

Courtesy of Chang Chang, UC Berkeley and LBNL.

λ = 13.4 nm, 450 nm diameter pinholes, 1024 x 1024 EUV/CCD at 26 cm ALS, 1.9 GeV, λ_u = 8 cm, N = 55

Coherent Undulator Radiation is Used for Interferometric Testing of Multilayer Coated Optics for EUV Lithography

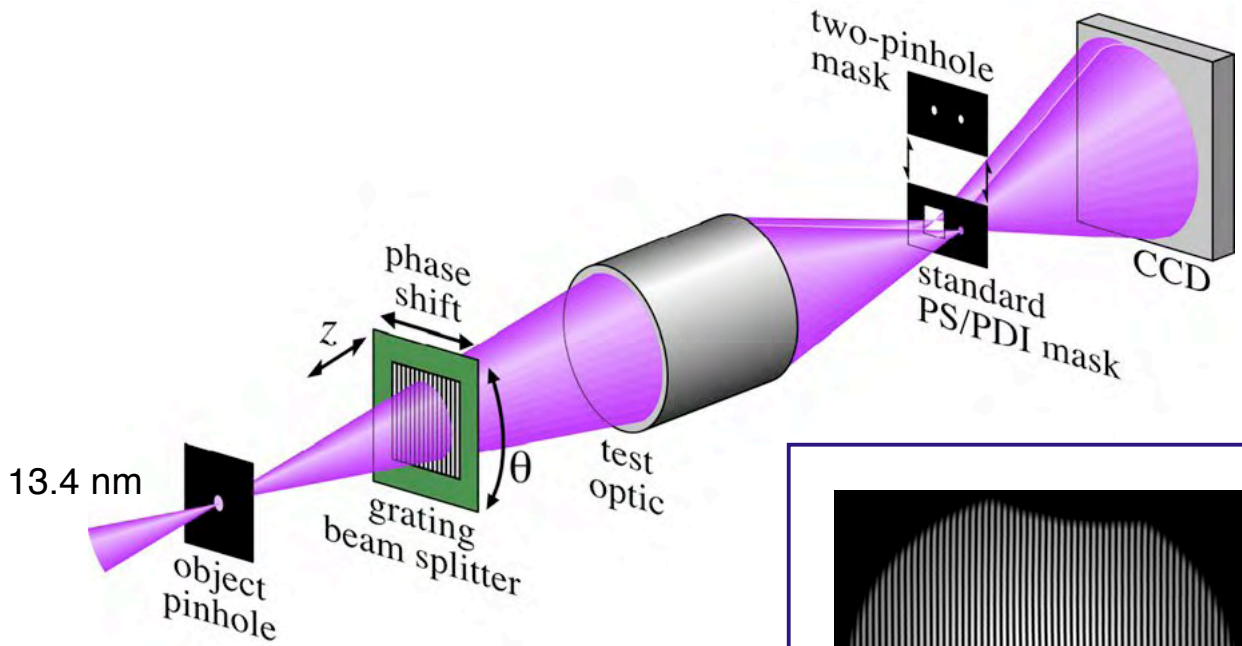

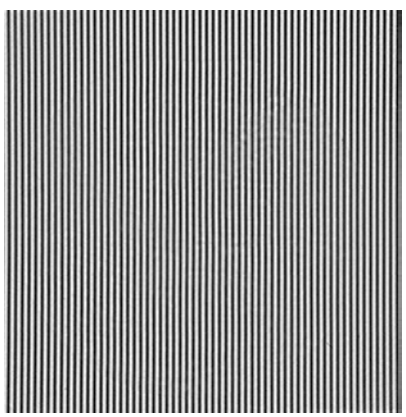

Null test interferogram

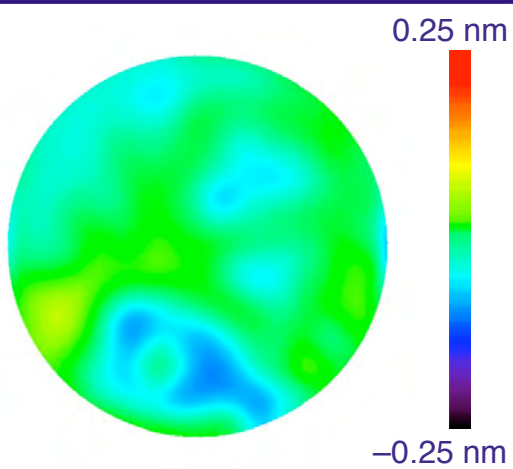

Reference wavefront

σ = 0.044 nm rms = λ_{euv} /300

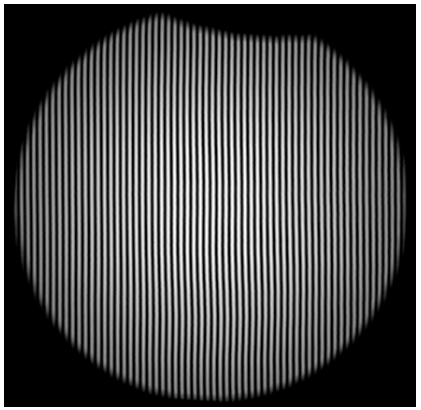

Interferogram

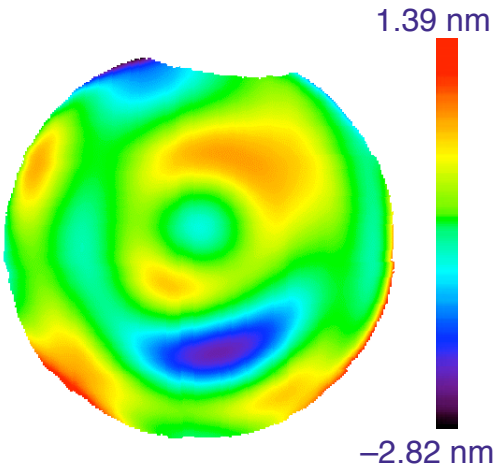

Wavefront

σ = 0.52 nm rms = λ_{euv} /26

Courtesy of K. Goldberg, P. Naulleau, J. Bokor, et al., LBNL.

EUV Interferometry of Projection Optics

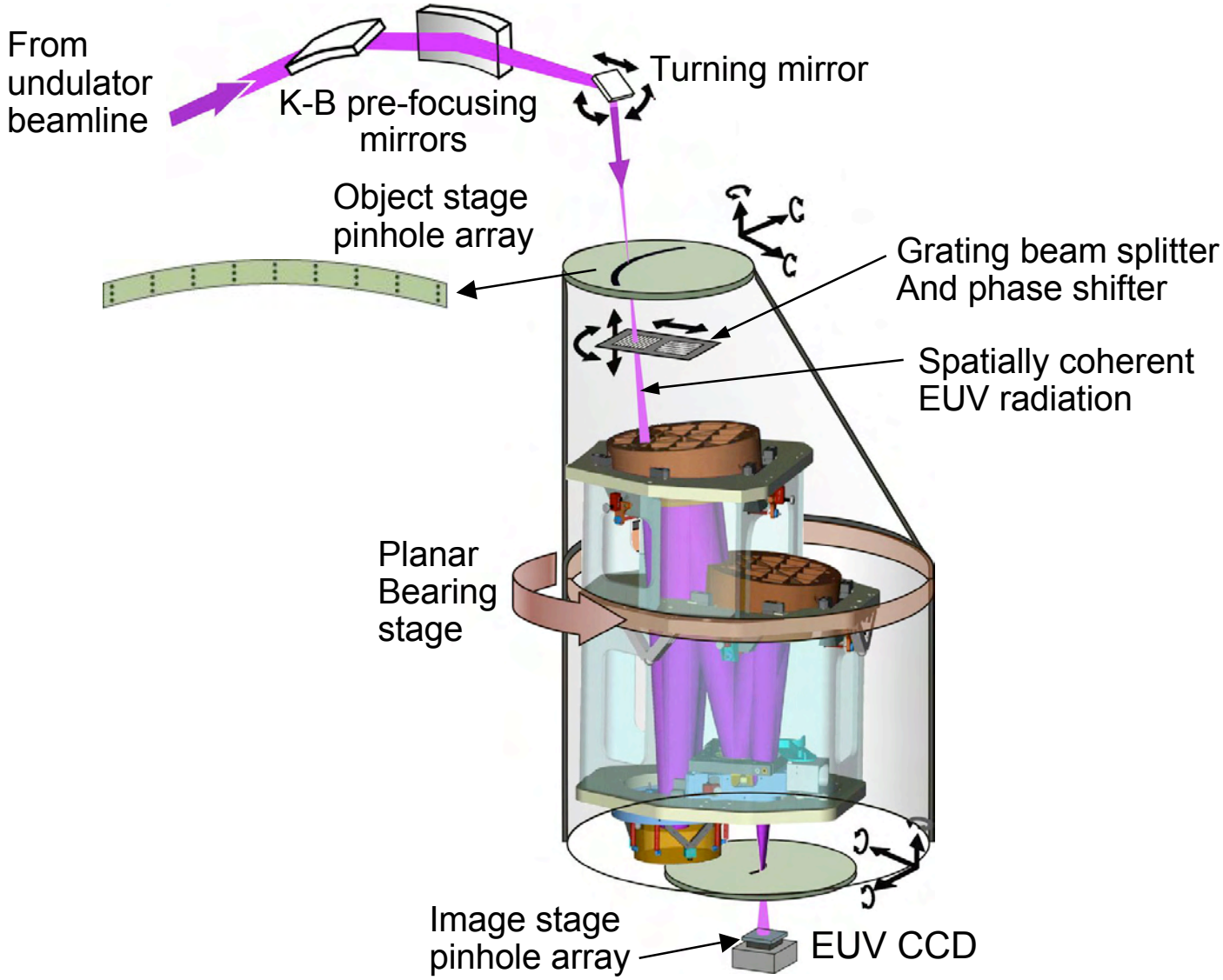

Courtesy of K. Goldberg, P. Naulleau and P. Batson (LBNL) and J. Bokor (UCB/LBL).

A 0.30 NA Micro-Exposure Tool (MET) for Testing EUV Resist Patterns to 12 nm Feature Size

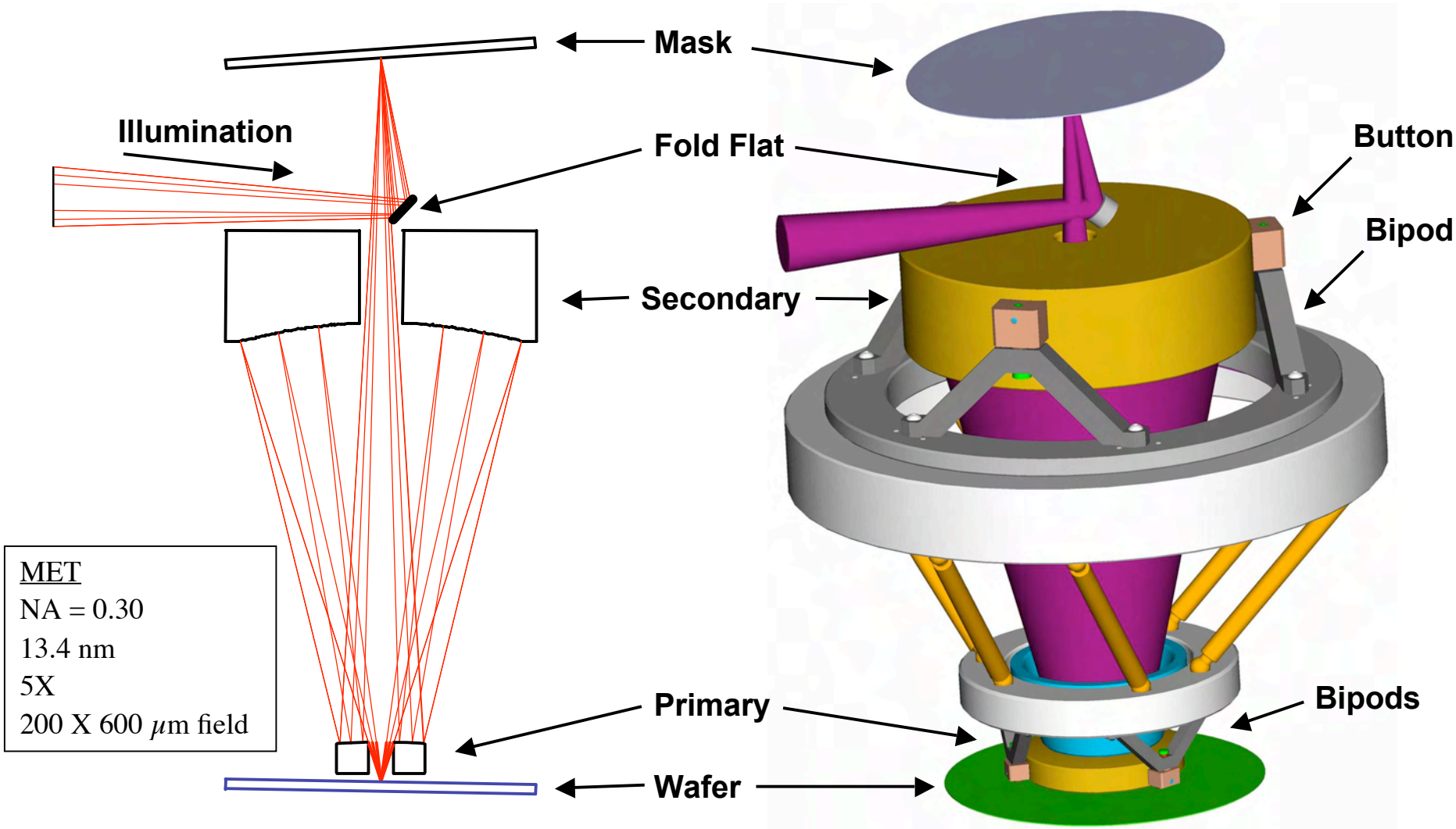

(Courtesy of J. Taylor, LLNL)

25 nm Pinhole Fabrication

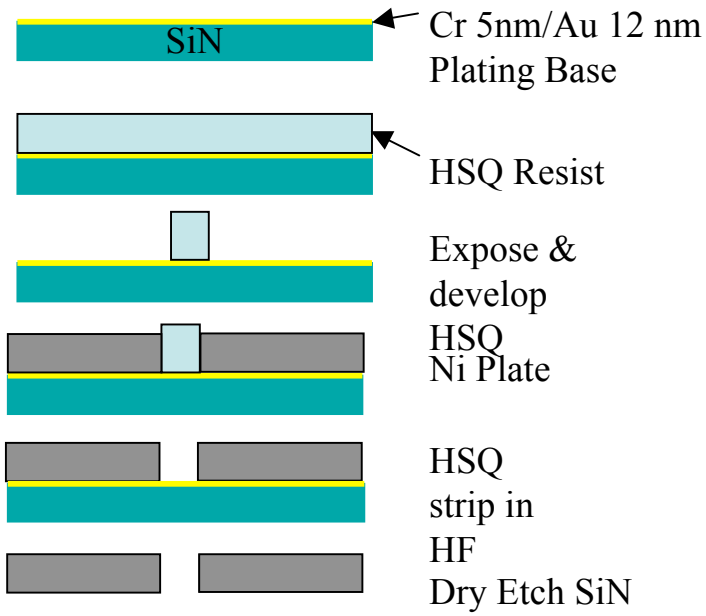

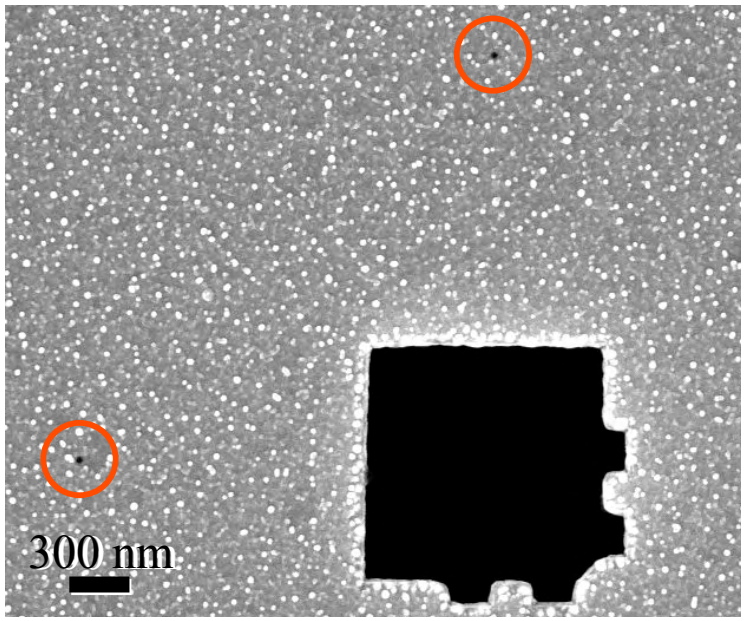

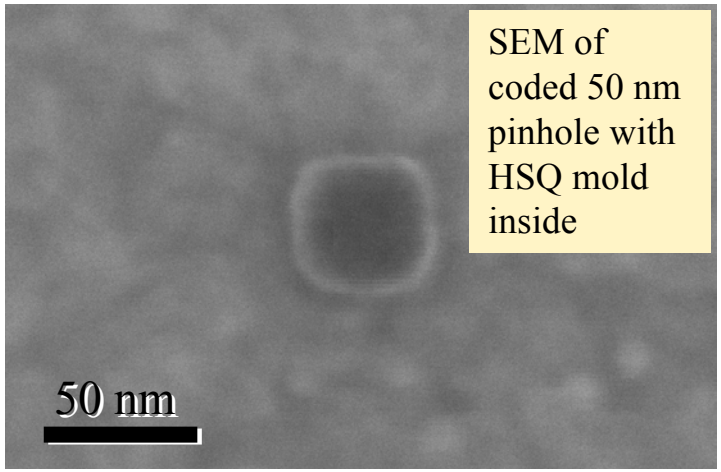

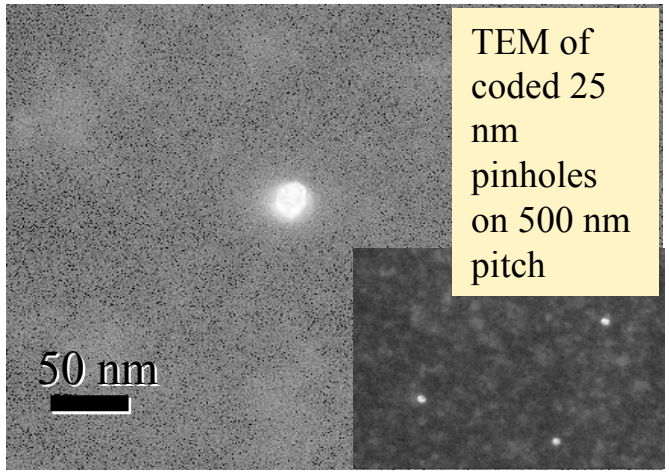

(Courtesy of J. Alex Liddle, Deirdre Olynick and Erik Anderson, LBNL)

MET At-Wavelength Interferometry and Alignment Preparation for Static Microfield Imaging

MET
Micro-Exposure Tool

2 mirrors
0.3 NA, 5x
13.5 nm

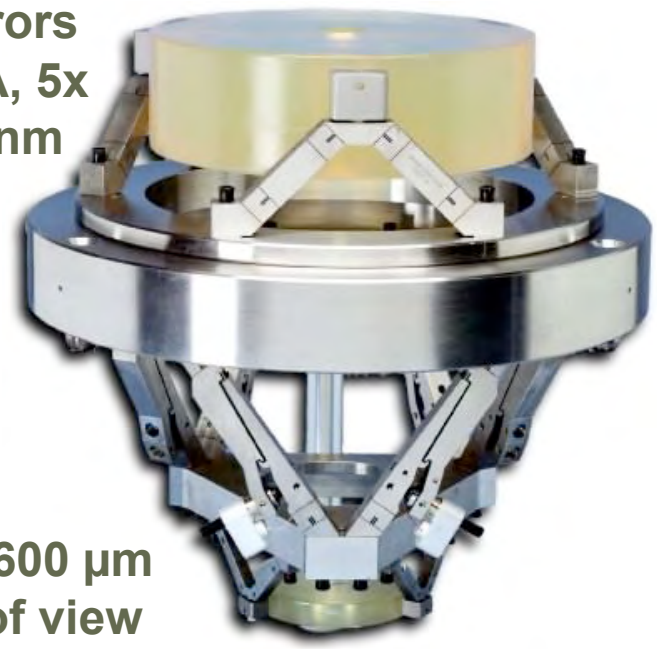

200 x 600 μm
field of view

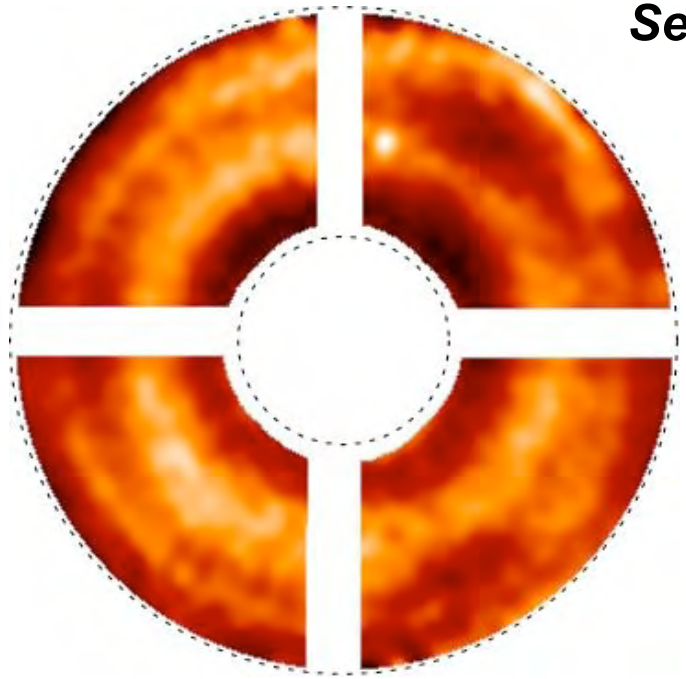

Alignment in progress
September 3, 2003
central field point

astig	0.1 nm
coma	0.3 nm
sph ab	0.4 nm
trifoil	0.2 nm
h-o s.	0.4 nm
RMS	0.8 nm
	$\lambda/17$

aberrations may be reduced in final alignment

- Visible-light alignment at Livermore
- EUV interferometry at Berkeley includes PS/PDI and shearing at 9 points across the field of view and in *z.*
- Higher-order spherical aberration dominates the wavefront
- A large part of the higher-order spherical is contained in Z35 and Z36. Higher-order spherical magnitude depends strongly on NA.

(Courtesy of K. Goldberg and P. Naulleau, LBNL)

Static Exposures with an Active Coherence Controlling Illuminator

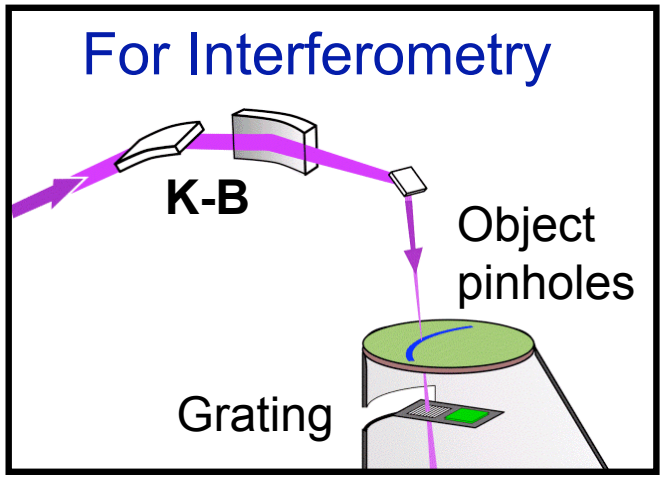

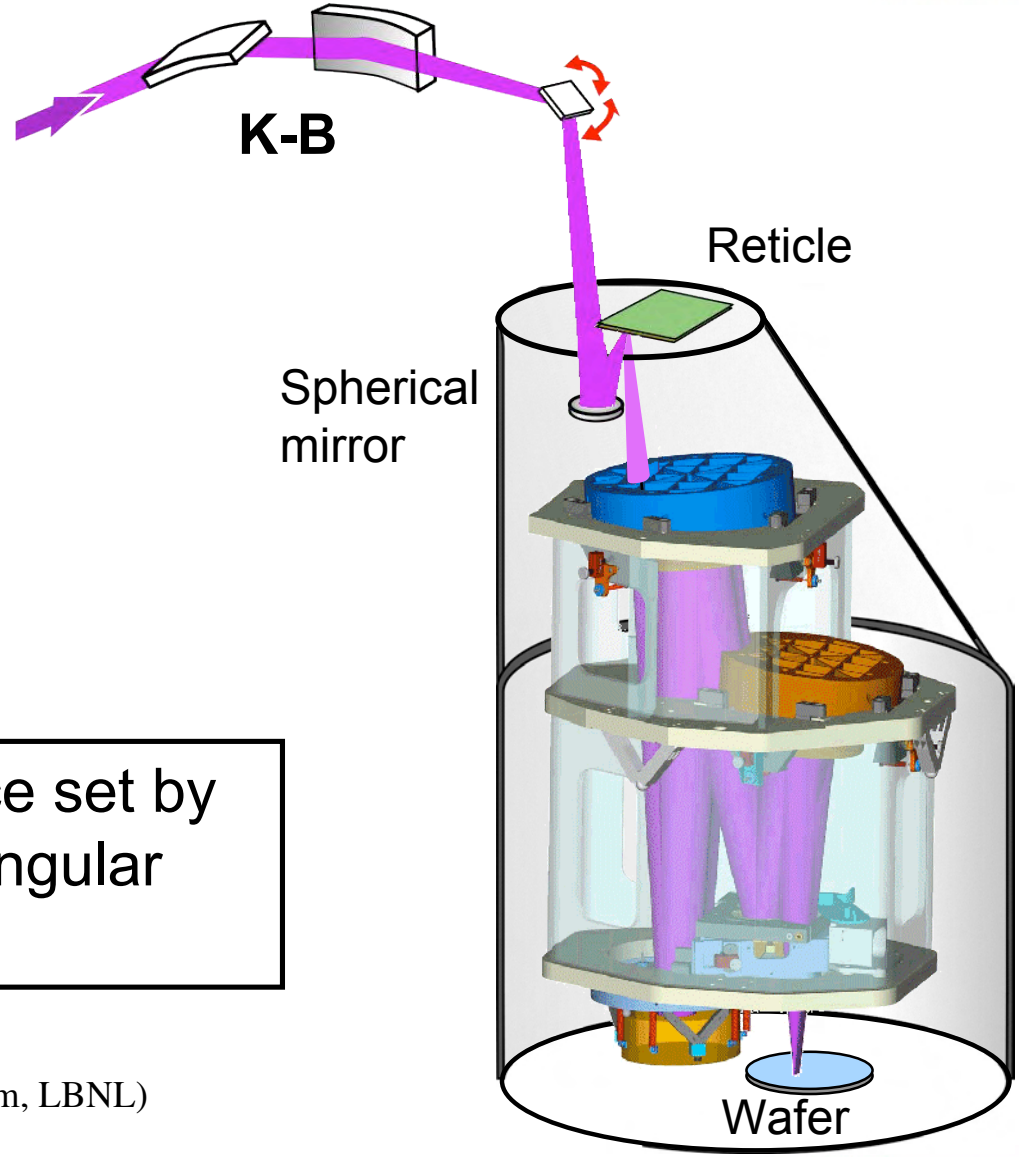

Partial coherence set by focal spot and angular scan

(Courtesy of P. Naulleau and P. Denham, LBNL)

Addressing critical EUV lithography issues for Sematech at the ALS: testing state-of-the-art EUV resists

Two-bounce, 0.3 NA, MET at ALS Beamline 12.0

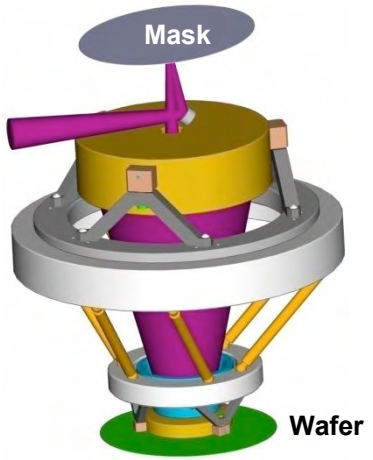

Programmable illumination

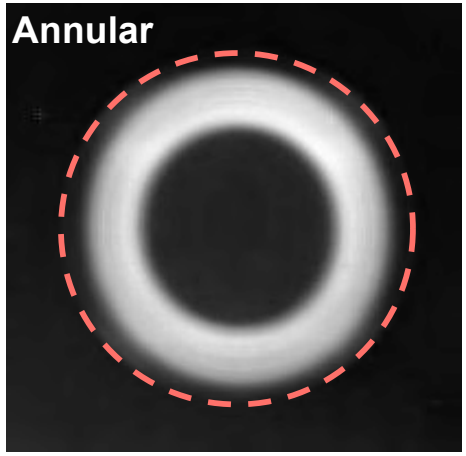

45 nm 40 nm 35 nm

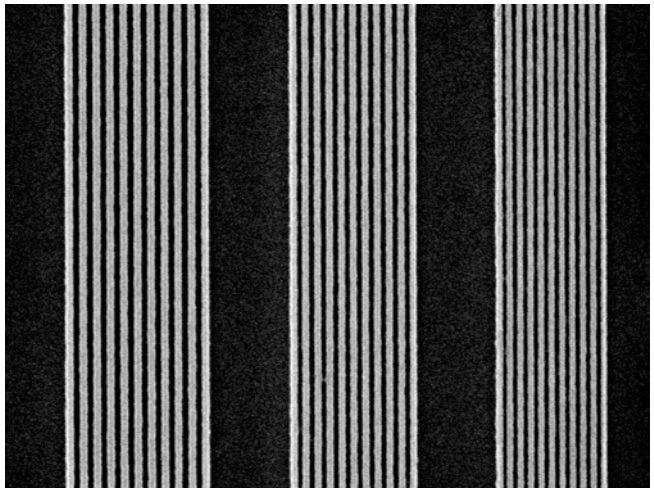

35 nm

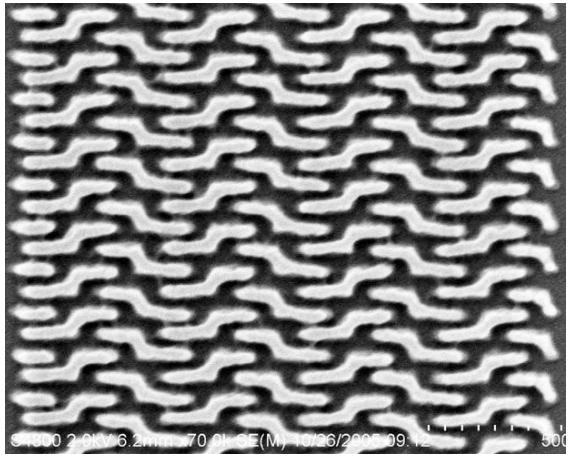

22 nm lines and spaces

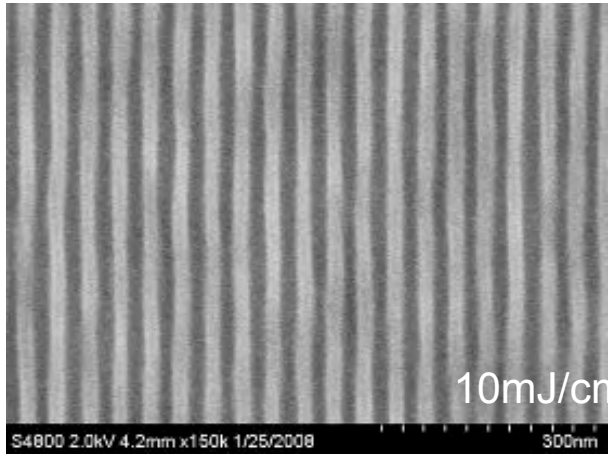

Major support and collaborators include Sematech, Intel, AMD, IBM, Samsung and others.
Courtesy of Patrick Naulleau, CXRO/LBNL.

Coherent Soft X-Ray Science Beamline

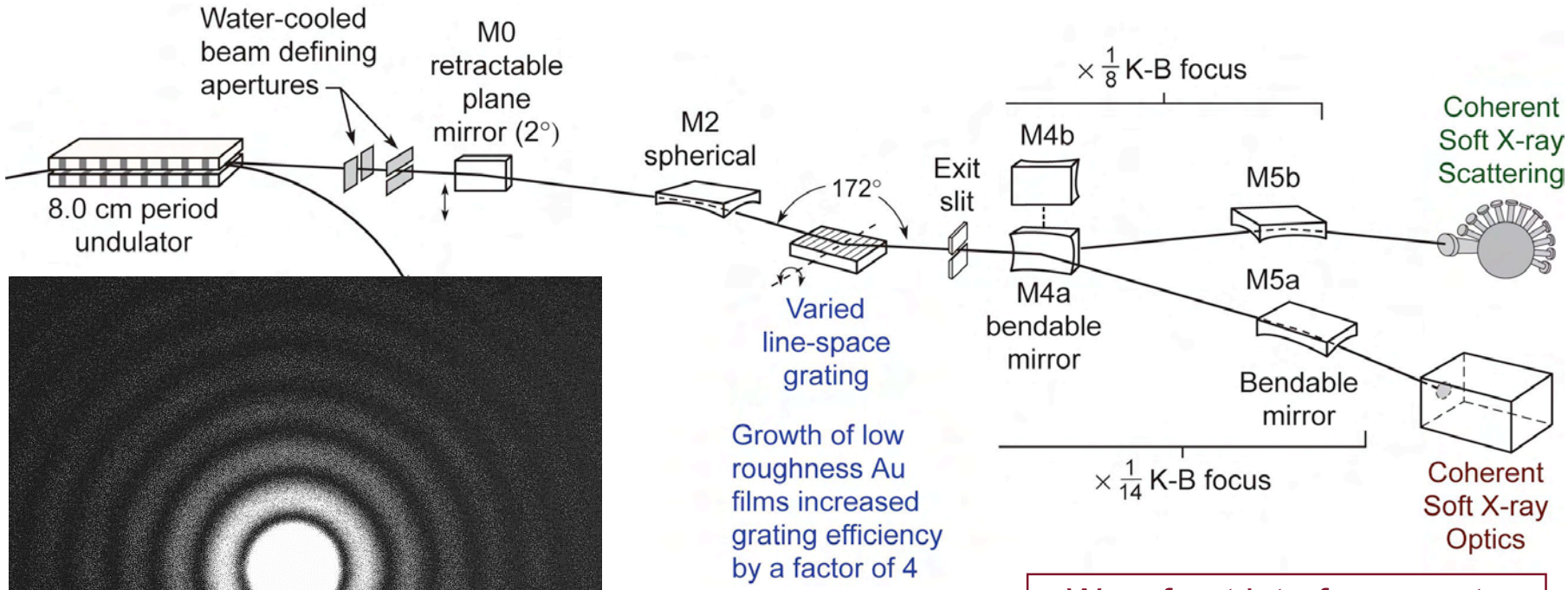

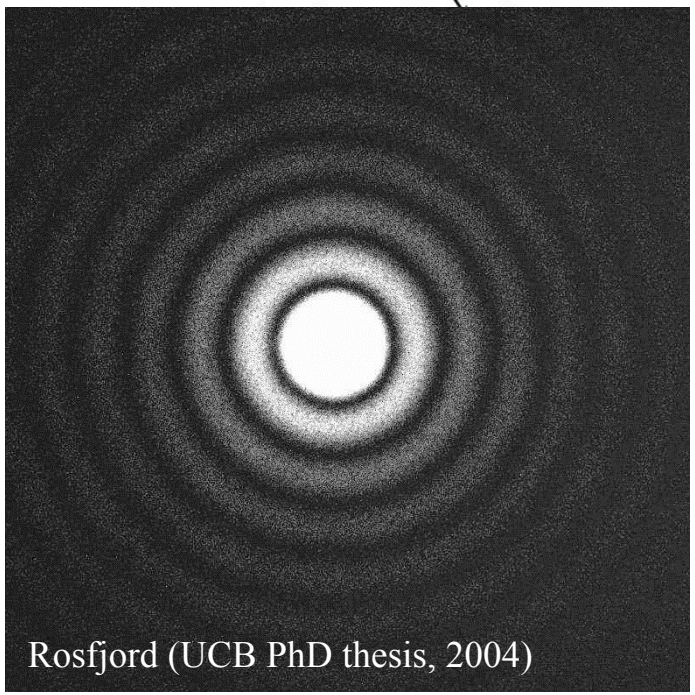

K. Rosfjord, Y. Liu, D. Attwood, "Tunable Coherent Soft X-Rays", IEEE J. Sel. Top. Quant. Electr.**10**, 1405 (Nov/Dec 2004)

Energy range 200-1000eV

Coherent flux at 600 eV:
2×10^{11} ph/sec/0.1%BW

λ = 2.07 nm (600 eV)

- Wavefront interferomery to measure aberrations in zone plate lenses
- Measure material properties (f_1 & f_2)
- Develop new coherent soft x-ray optical techniques (Fourier Optics)
- Coherent scattering from magnetic nanostructures

Coherent Soft X-Ray Beamline: Use of a Higher Harmonic (n = 3) to Access Shorter Wavelengths

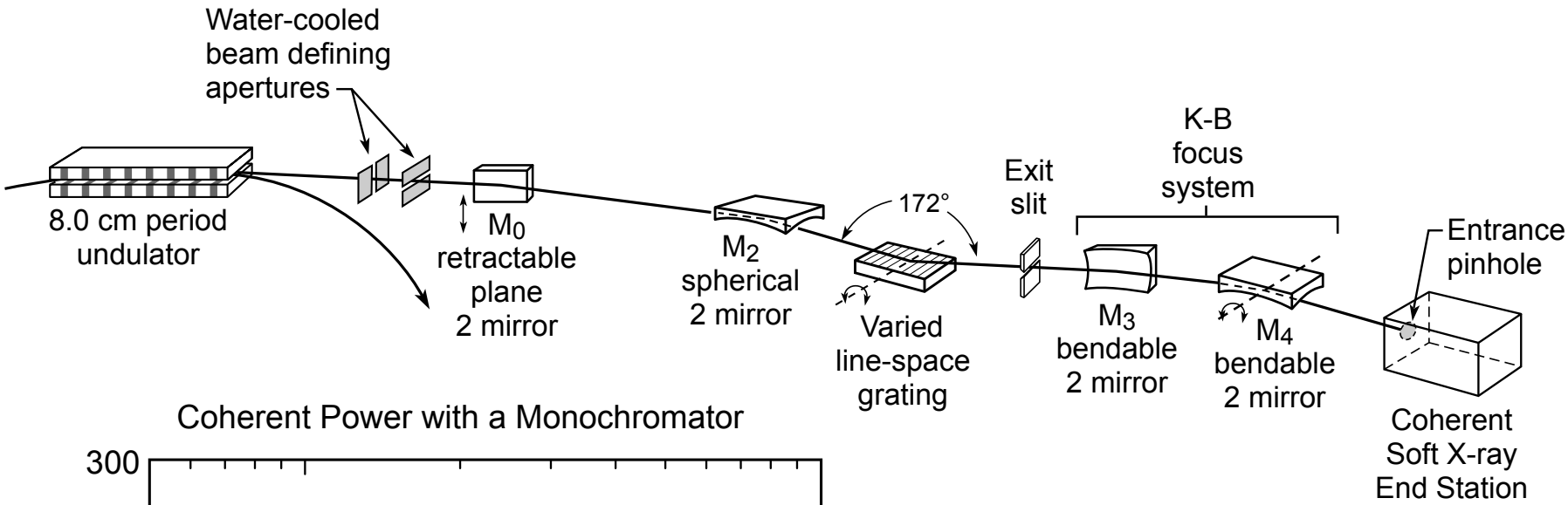

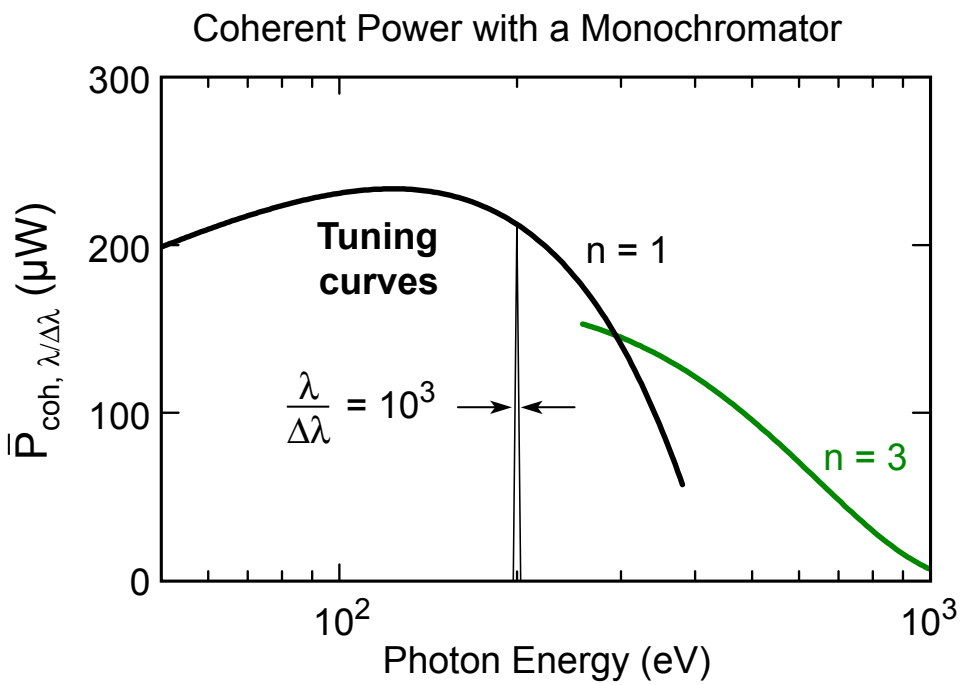

8.0 cm period, N = 55
1.9 GeV, 400 mA
$d \cdot \theta = \lambda/2\pi$
$\ell_{coh} = 1000\ \lambda/2$
$\eta_{euv} = 10\%$, $\eta_{sxr} = 10\%$

Coherent Soft X-Rays

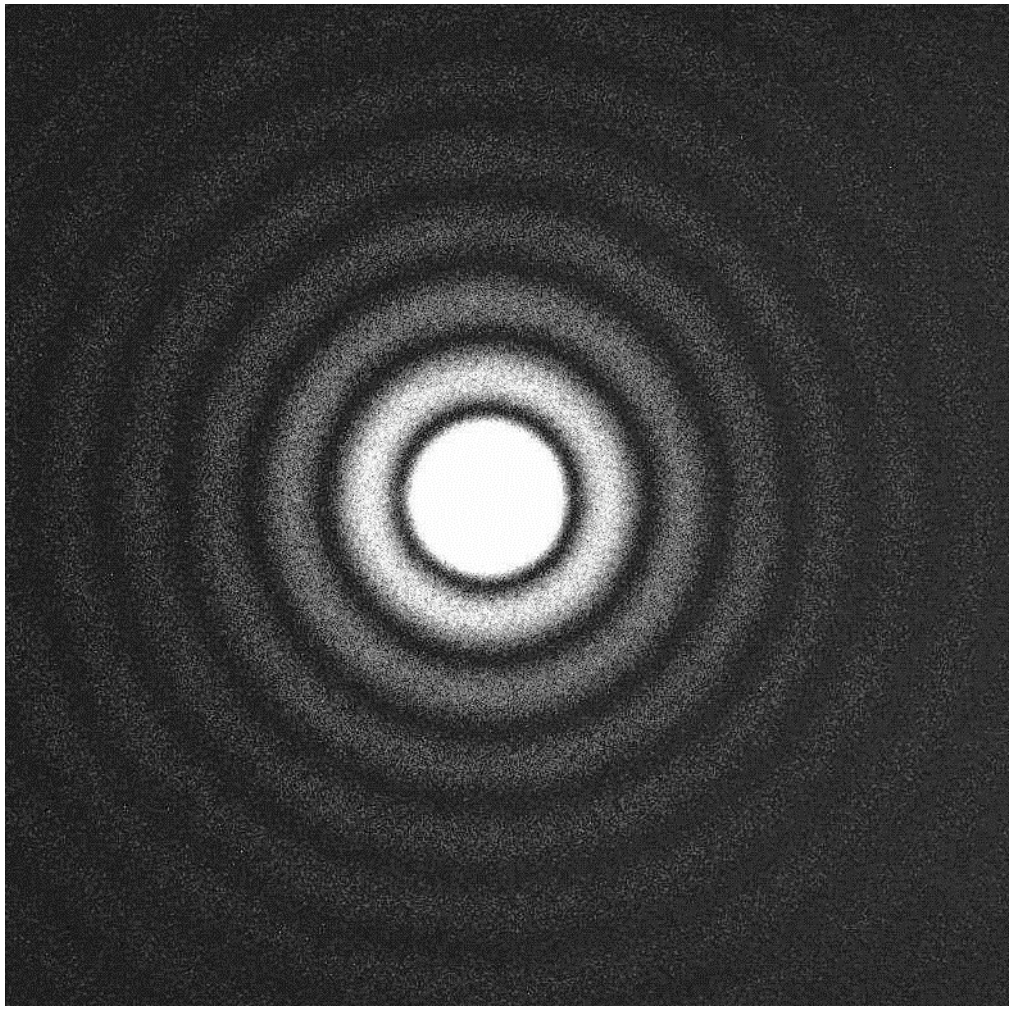

λ= 2.48 nm
(500 eV)
d = 2.6 µm
t = 40 msec
ALS beamline 12.0.2

Courtesy of Kris Rosfjord, CXRO/LBNL
K. Rosfjord et al., Coherent Soft X-Rays,
IEEE JSTQE **10**, 1405 (Nov/Dec 2004)

Beam Characterization: Double Pinhole Experimental Results

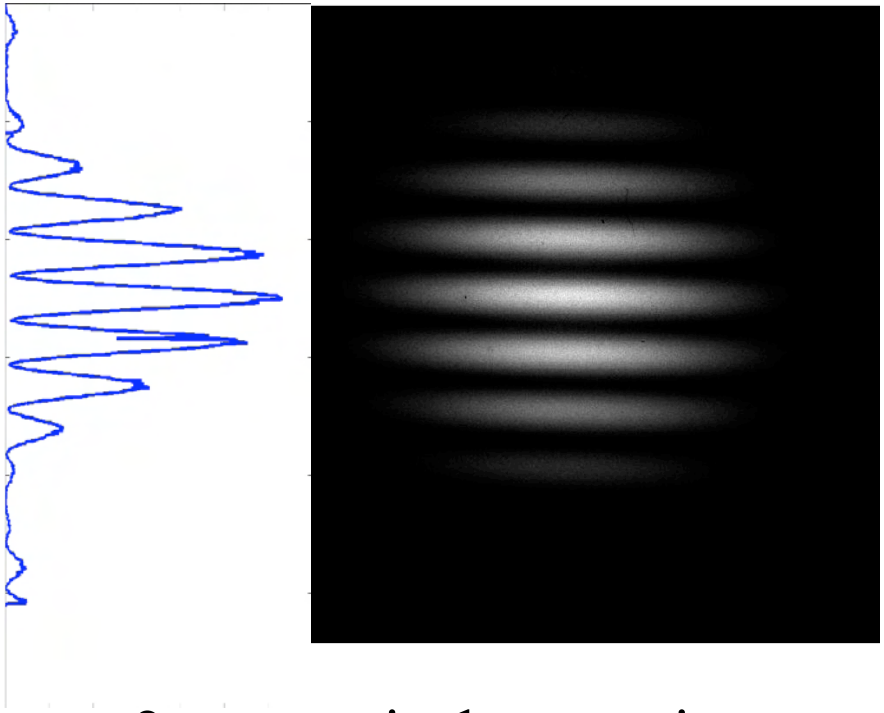

2 μm vertical separation
$|\mu| = 1.00$

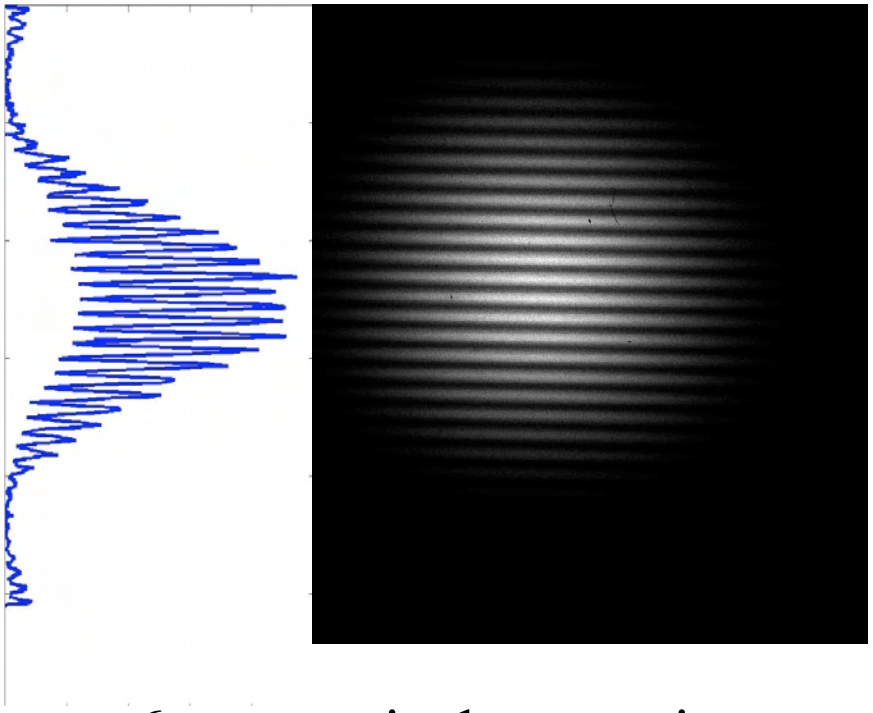

6 μm vertical separation
$|\mu| = .57$

d = 500nm diameter individual pinholes at 500eV
Focal spot size of 60um X 9.4um FWHM

Courtesy of Kris Rosfjord, CXRO/LBNL
K. Rosfjord et al., Coherent Soft X-Rays,
IEEE JSTQE **10**, 1405 (Nov/Dec 2004)

Interferometry of Material Properties (f_1 and f_2) Using the New XOR Fourier Optic

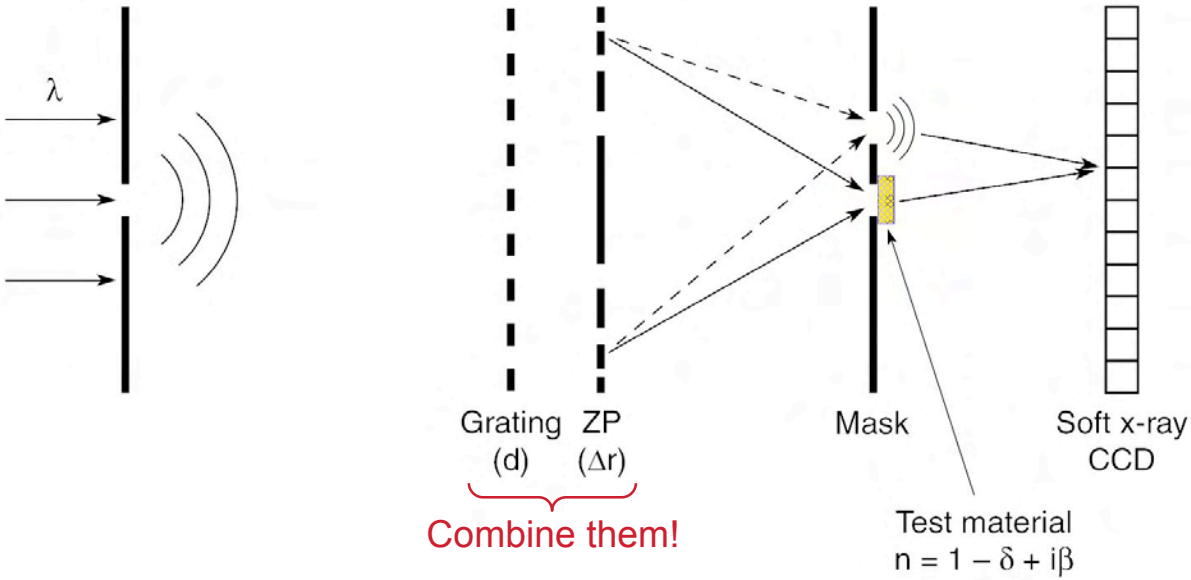

$$\delta = \frac{Na\ re\ \lambda^2}{2\pi} f_1^0(w)$$

$$\beta = \frac{Na\ re\ \lambda^2}{2\pi} f_2^0(w)$$

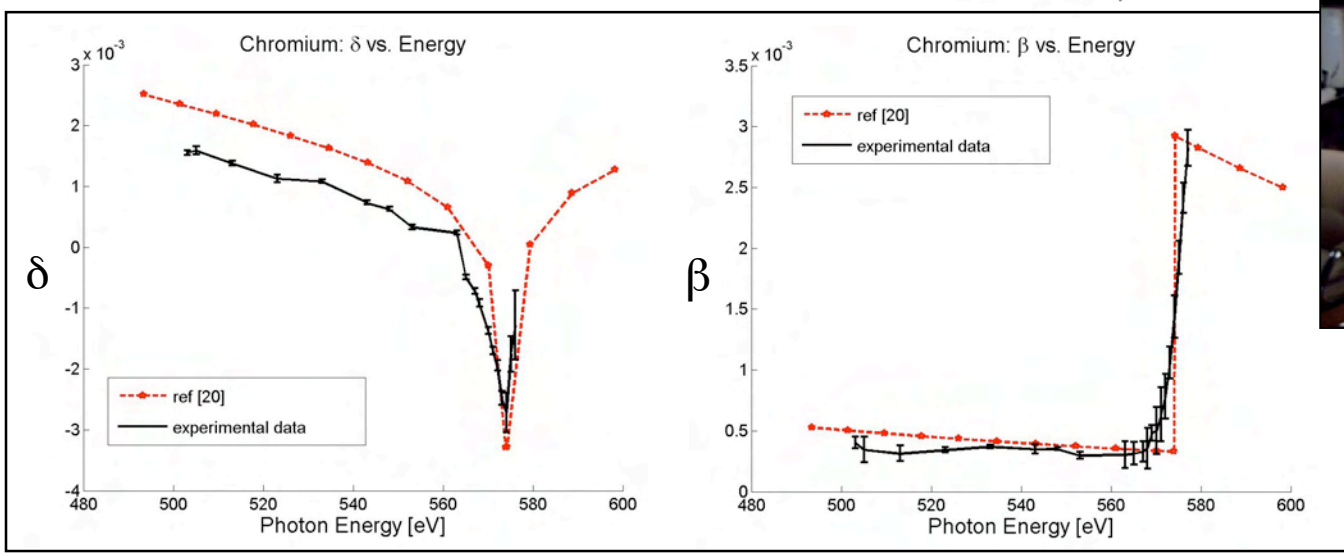

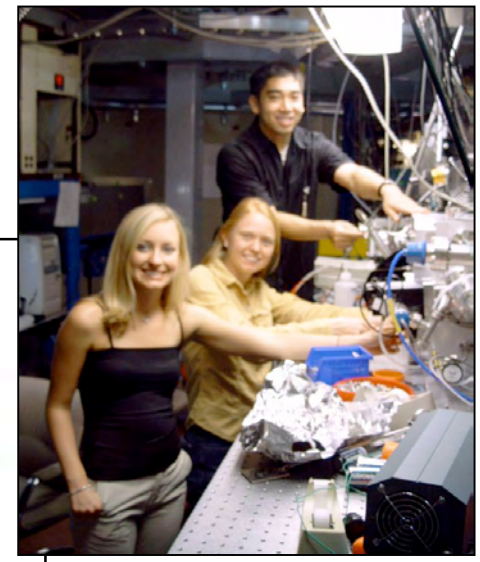

K. Rosfjord, C. Chang, R. Miyakawa, H. Barth, D. Attwood, Applied Optics (in press)

Coherent Soft X-Ray Science Beamline

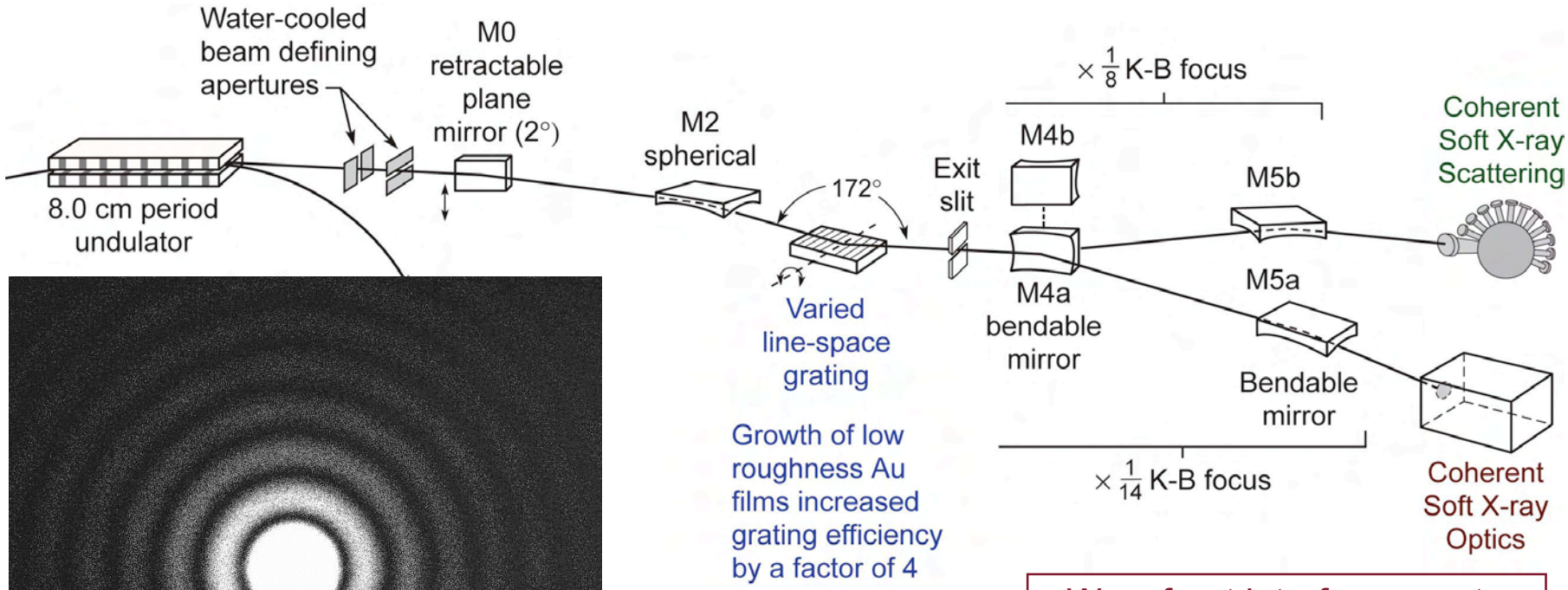

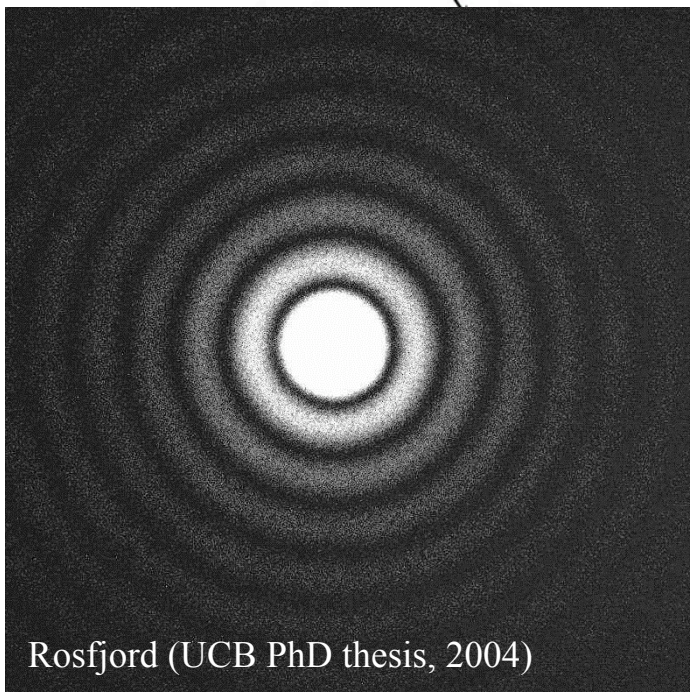

K. Rosfjord, Y. Liu, D. Attwood, "Tunable Coherent Soft X-Rays", IEEE J. Sel. Top. Quant. Electr.**10**, 1405 (Nov/Dec 2004)

Energy range 200-1000eV

Coherent flux at 600 eV:
2×10^{11} ph/sec/0.1%BW

λ = 2.07 nm (600 eV)

- Wavefront interferomery to measure aberrations in zone plate lenses
- Measure material properties (f_1 & f_2)
- Develop new coherent soft x-ray optical techniques (Fourier Optics)
- Coherent scattering from magnetic nanostructures

Coherent Soft X-Ray Scattering

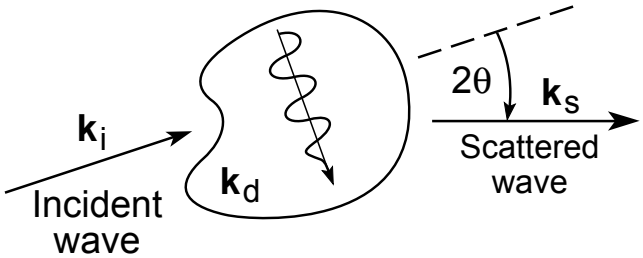

$|\mathbf{k}_d| = 2\pi/d$ represents a spatial non-uniformity in the medium, such as atoms of periodicity d, a grating, or a density distribution due to a wave motion.

If the density distribution is stationary, or near stationary, the scattering diagram is isosceles.

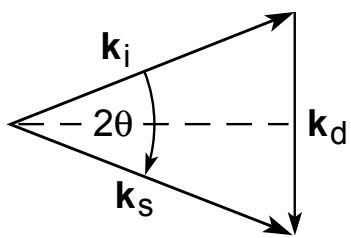

$$\hbar\omega_s = \hbar\omega_i + \hbar\omega_d$$
$$\hbar\mathbf{k}_s = \hbar\mathbf{k}_i + \hbar\mathbf{k}_d$$

- At a given angle one detects scattering from fluctuations of a specific spatial scale
- At that angle, the frequency content tells you the time structure of those fluctuations

Coherent Scattering from a Pt:Co Multilayer

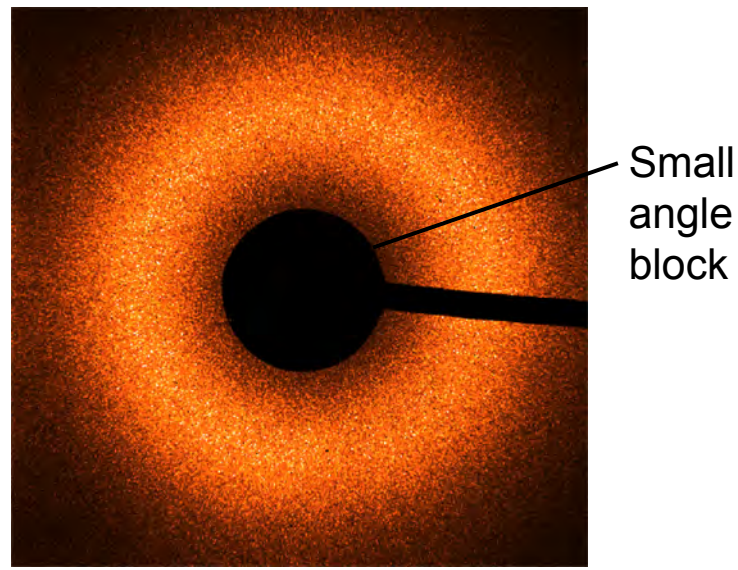

Soft x-ray speckle pattern: diffraction pattern of the magnetic domain structure

(Courtesy of Steve Kevan, University of Oregan)

Coherent Soft X-Ray Magnetic Scattering Endstation

Flangosaurus

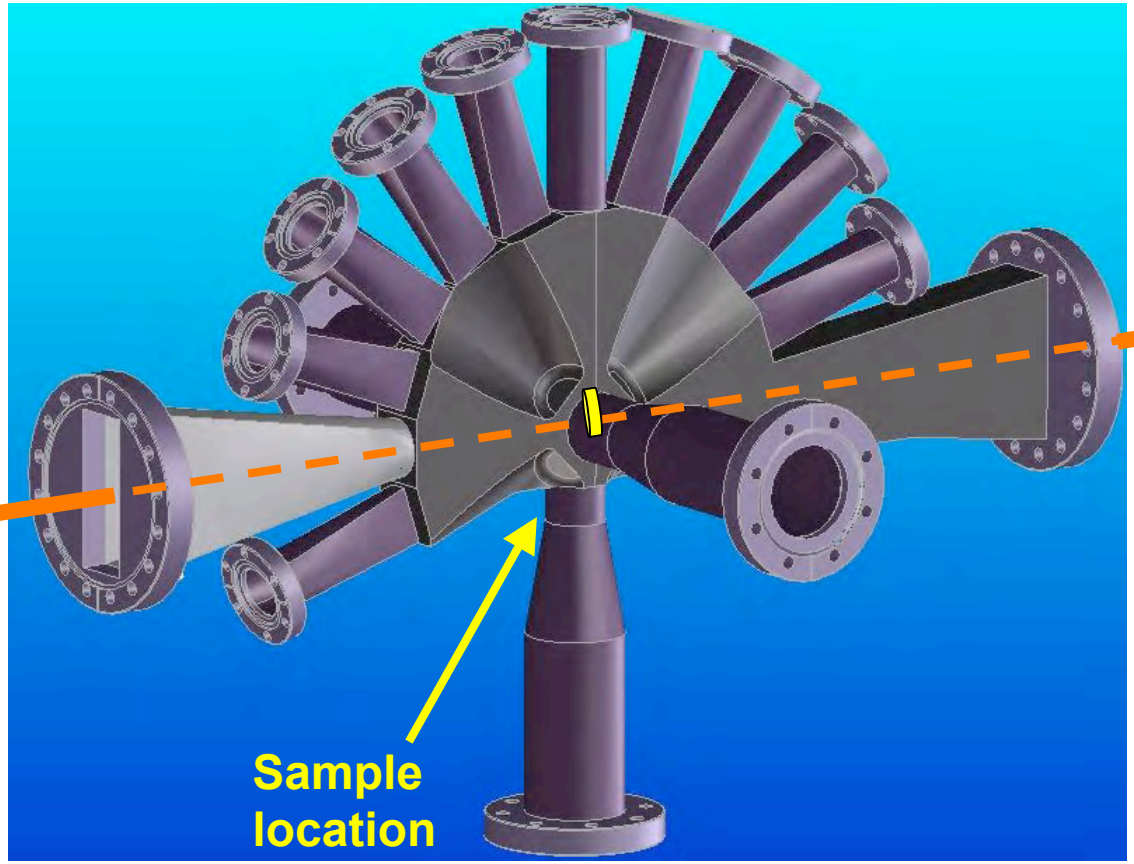

Courtesy of K.Chesnel, S. Kevan, U. Oregon

Example of Experiment in Transmission: Coherent Scattering from Nanoparticles

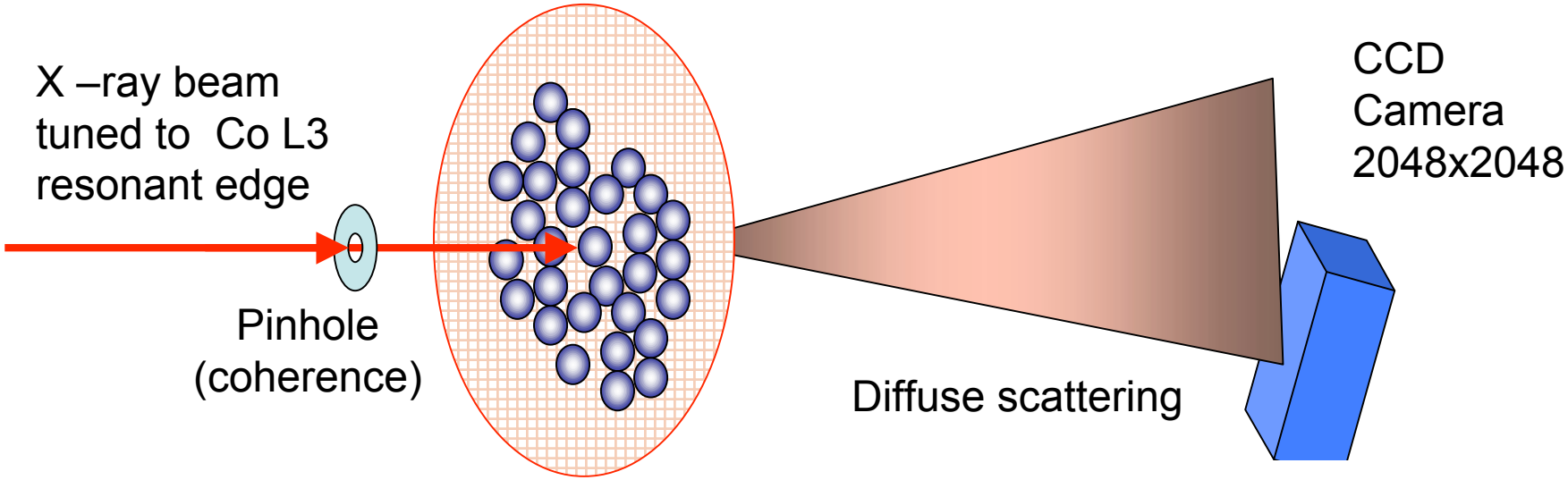

Co Nanoparticles assembly precipitated on TEM grid

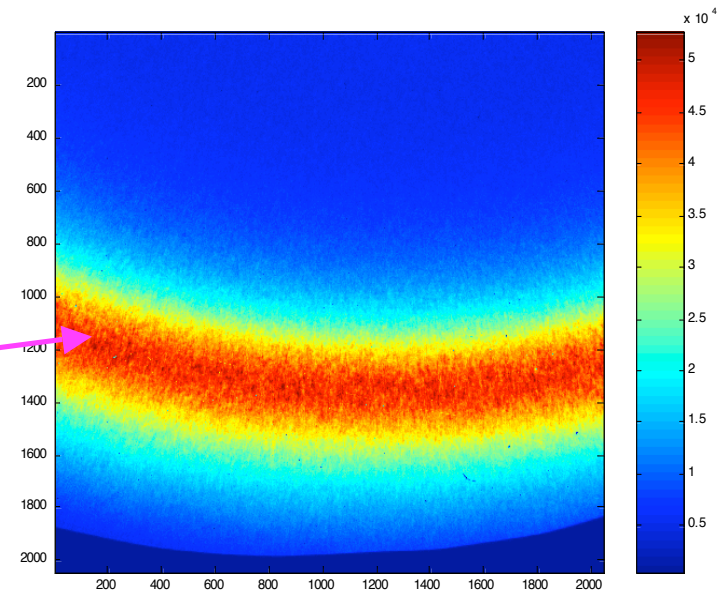

Scattering ring related to interparticle distance ~12nm

Courtesy of K.Chesnel, S. Kevan, U. Oregon

The Scanning Soft X-Ray Microscope Requires Spatially Coherent Illumination

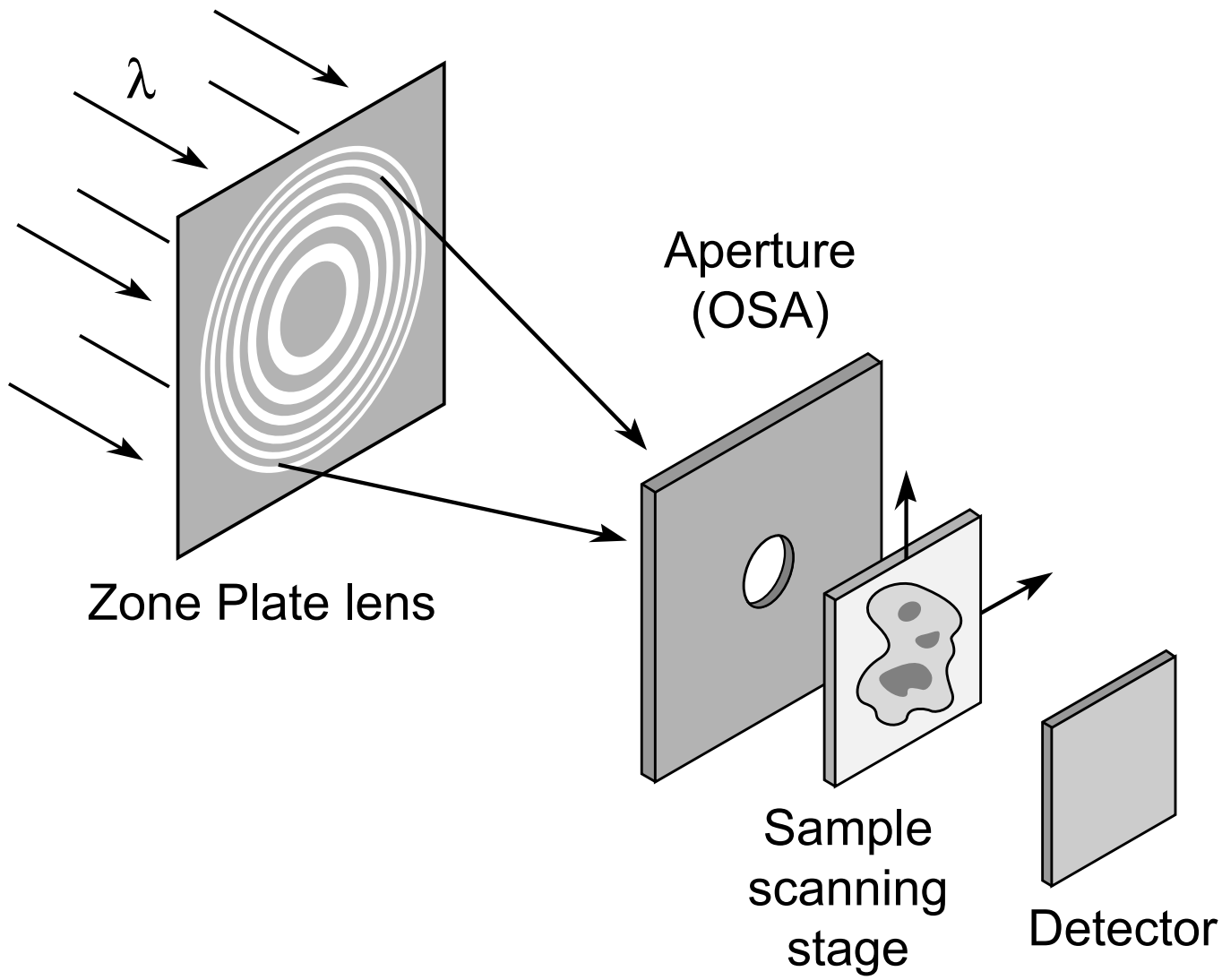

Professor David Attwood
Univ. California, Berkeley

An Undulator Beamline for Scanning X-Ray Microscopy

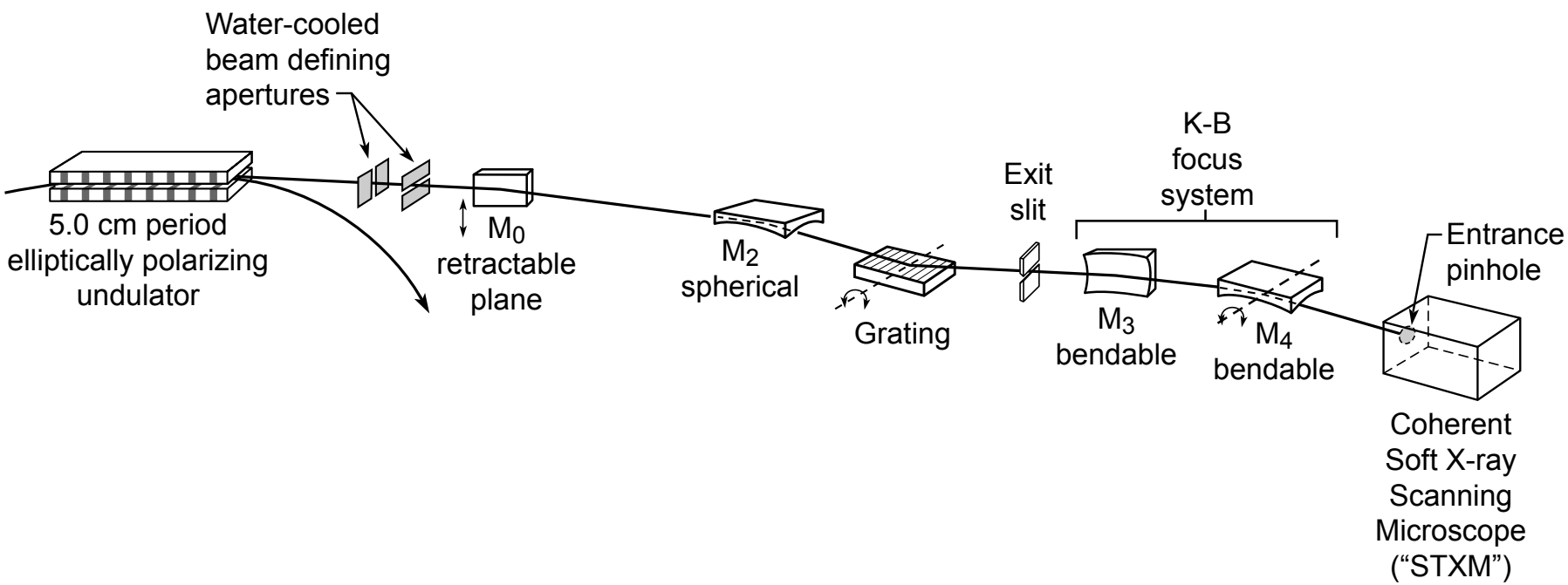

Coherent Power for an EPU at the ALS

U5 EPU

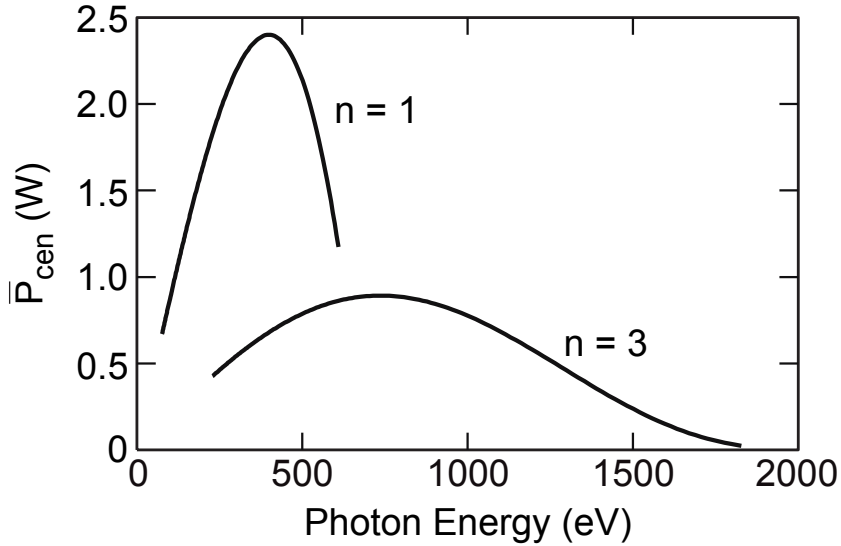

1.9 GeV, 400 mA

λ_u = 50 mm, N = 27

$0.5 \le K \le 4.0$

σ_x = 260 μm, σ_x' = 23 μr

σ_y = 16 μm, σ_y' = 3.9 μr

θ_{cen} = 61μr @ K = 0.87 (500 eV)

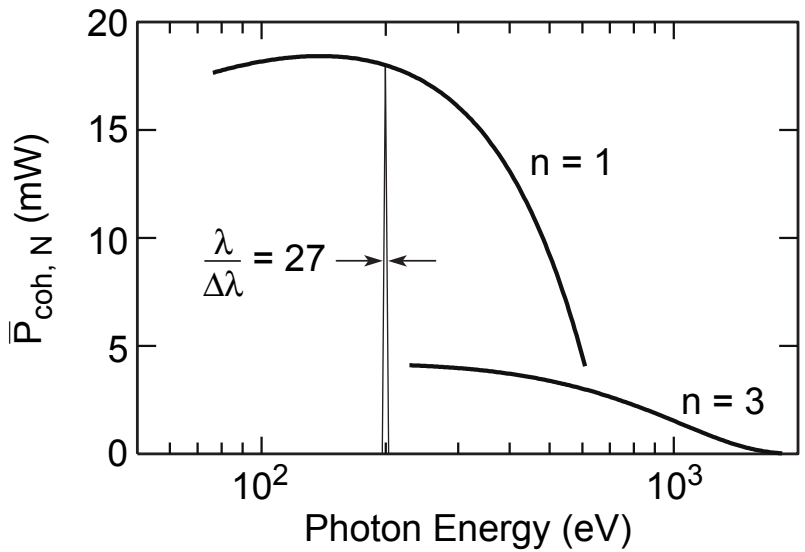

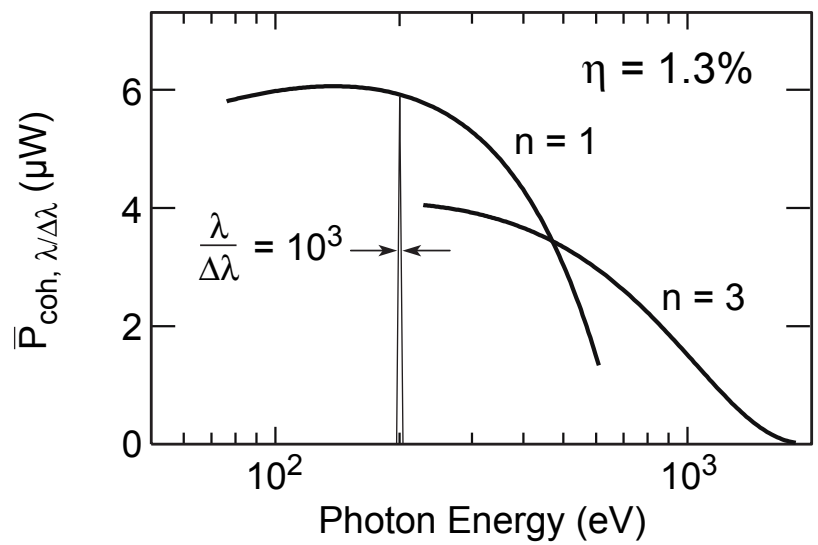

Biofilm from Saskatoon River

ALS-MES 11.0.2

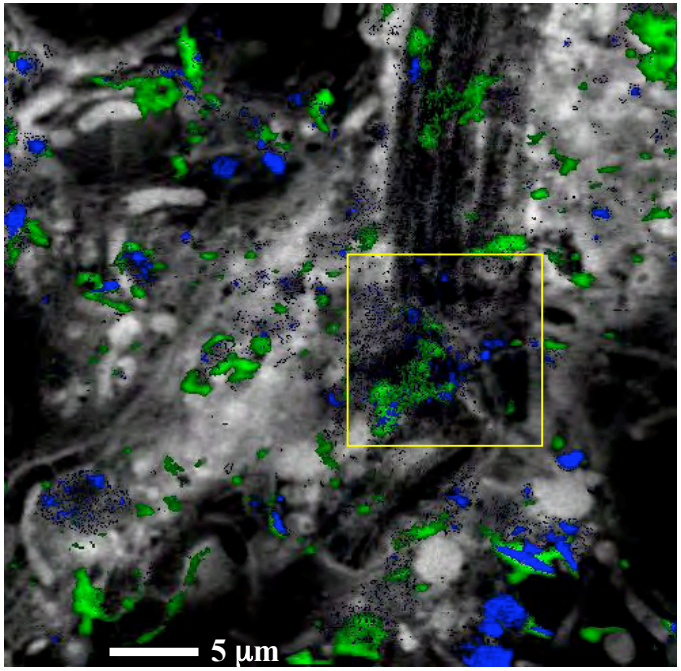

Protein (gray), Ca, K

RESULTS

•Ni, Fe, Mn, Ca, K, O, C elemental map,
(there was no sign of Cr.)

•Different oxidation states for Fe and Ni

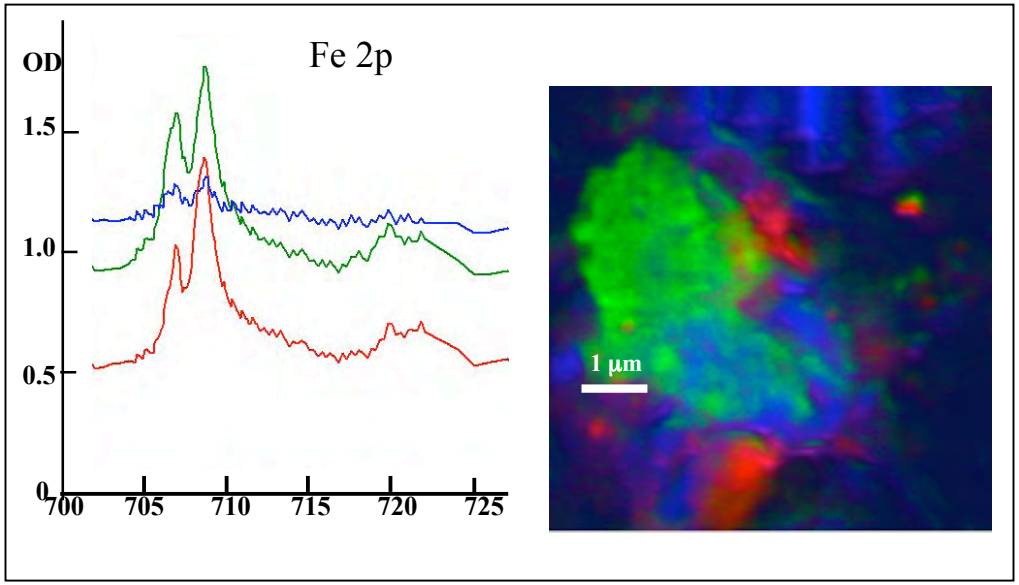

Different oxidation states (minerals) found for Fe & Ni

Tohru Araki, Adam Hitchcock (McMaster University)
Tolek Tyliszczak, LBNL
Sample from: John Lawrence, George Swerhone (NWRI-Saskatoon), *Gary Leppard* (NWRI-CCIW)

Patterned Polymer Photoresists

ALS-MES 11.0.2

M.K. Gilles, R. Planques, S.R. Leone
LBNL
Samples from B. Hinsberg, F. Huele
IBM Almaden

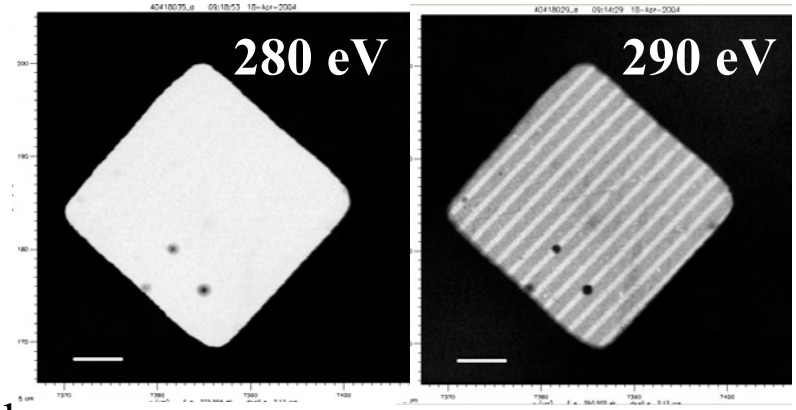

Exposure to UV light results in loss of carbonyl peak

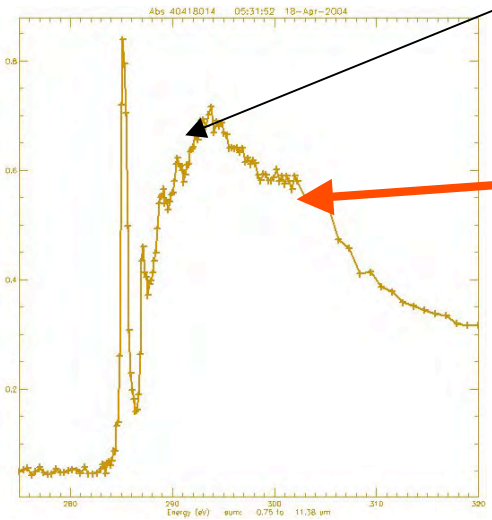

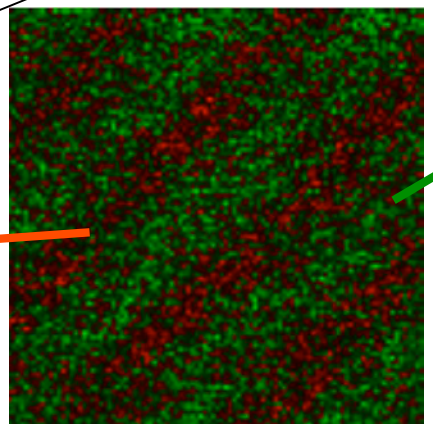

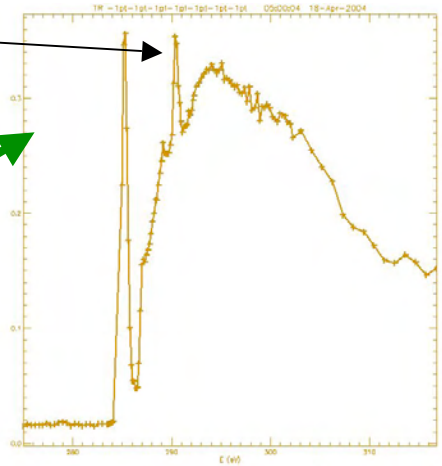

Map chemical spectra taken of pure samples
Onto a sample containing both components

Courtesy of Mary Gilles, LBNL

16 December 2004

International weekly journal of science

nature

$10.00

www.nature.com/nature

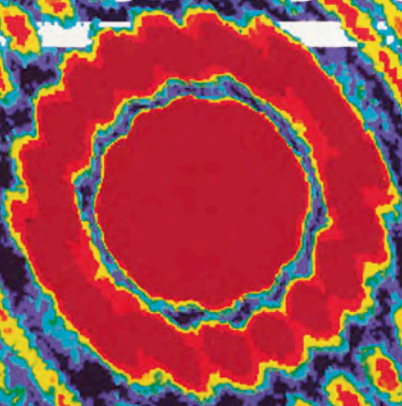

Inside this week

X-ray holography

Lensless imaging at the nanoscale

The 'Halloween storm'
How the Sun plays its tricks

Protein transport
Escape from the nucleus

Duck-billed platypus
Curiouser and curiouser

Locusts over Africa
Time for biological control?

$10.00US $12.99CAN

Coherent Power at BESSY II

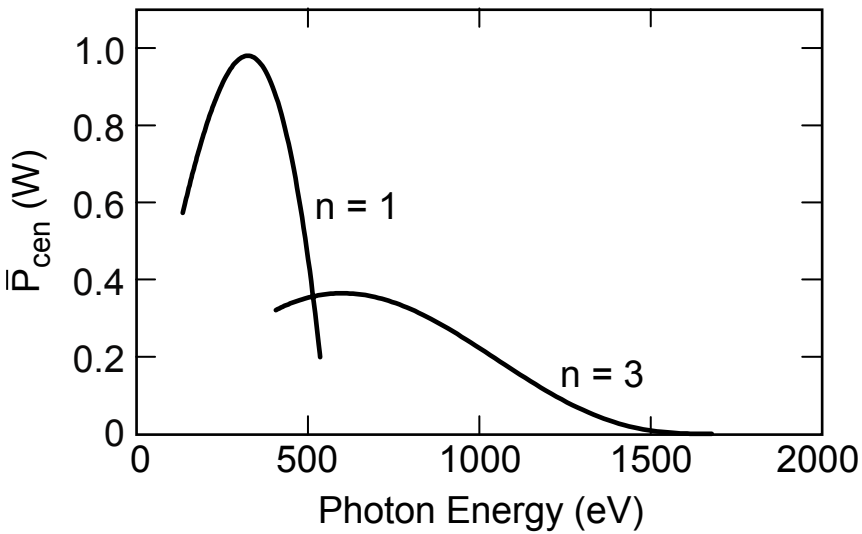

1.7 GeV, 200 mA

λ_u = 49 mm, N = 84

$0 \le K \le 2.5$

σ_x = 314 μm, σ_x' = 18 μr

σ_y = 24 μm, σ_y' = 2 μr

η_{euv} = 10% ; η_{sxr} = 10%

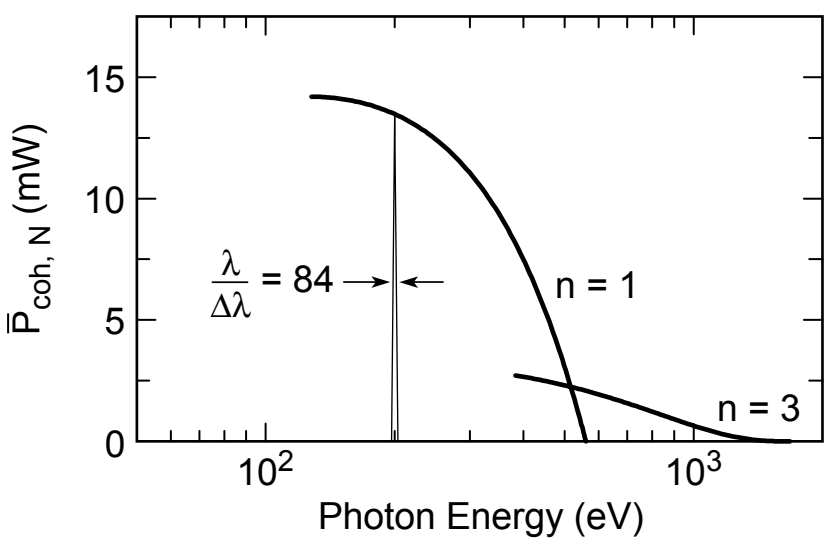

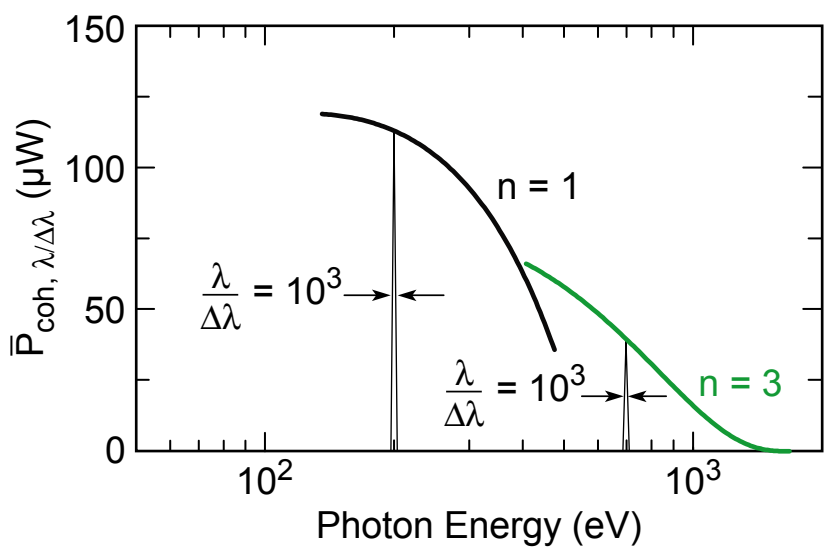

Lensless Imaging of Magnetic Nanostructures by X-Ray Spectro-Holography

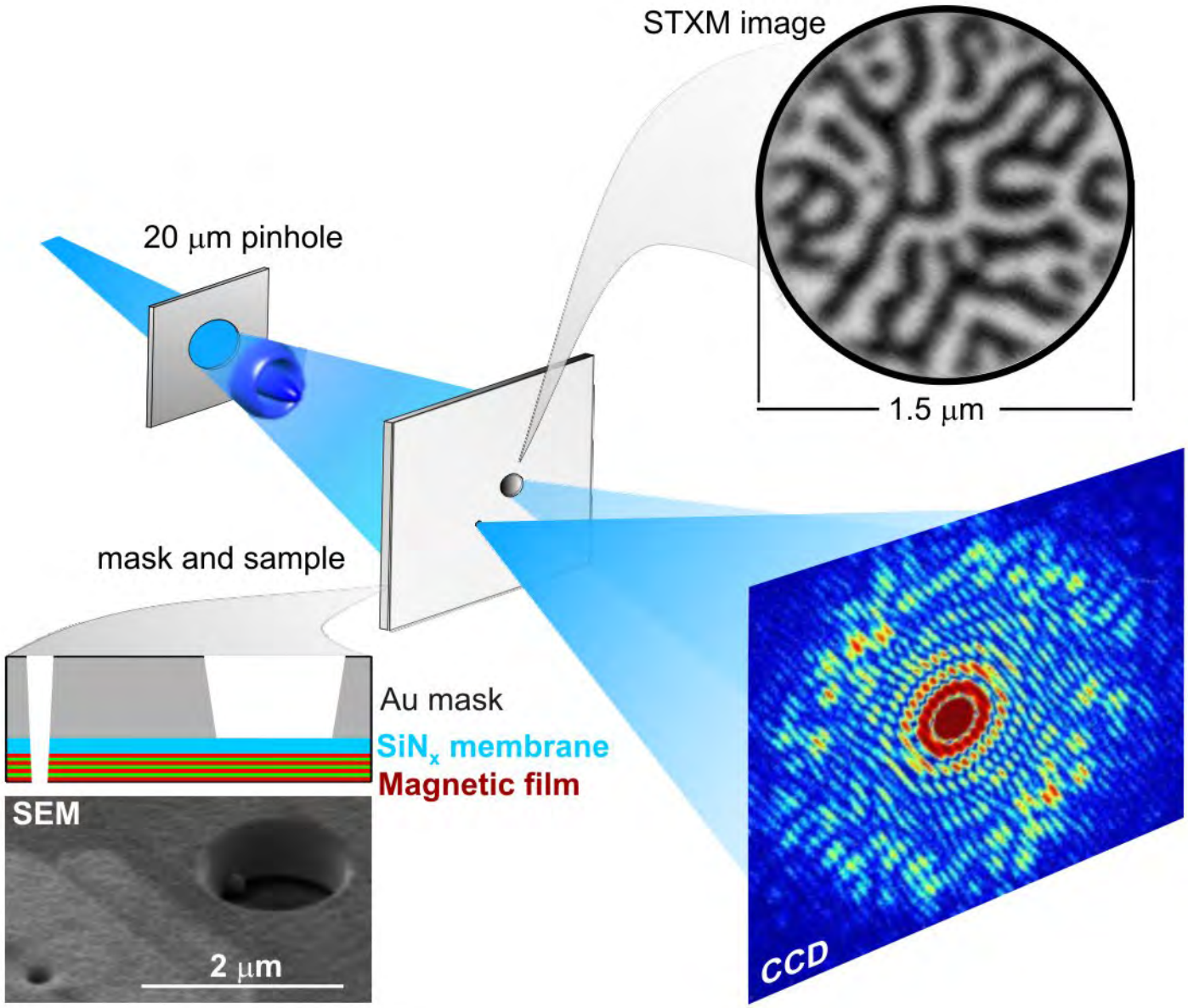

S. Eisebitt, J. Lüning, W.F. Schlotter, M. Lörgen, O. Hellwig, W. Eberhardt & J. Stöhr / *Nature*, 16 Dec 2004

X-Ray Hologram at 1.59 nm Wavelength Using Undulator Radiation at BESSY

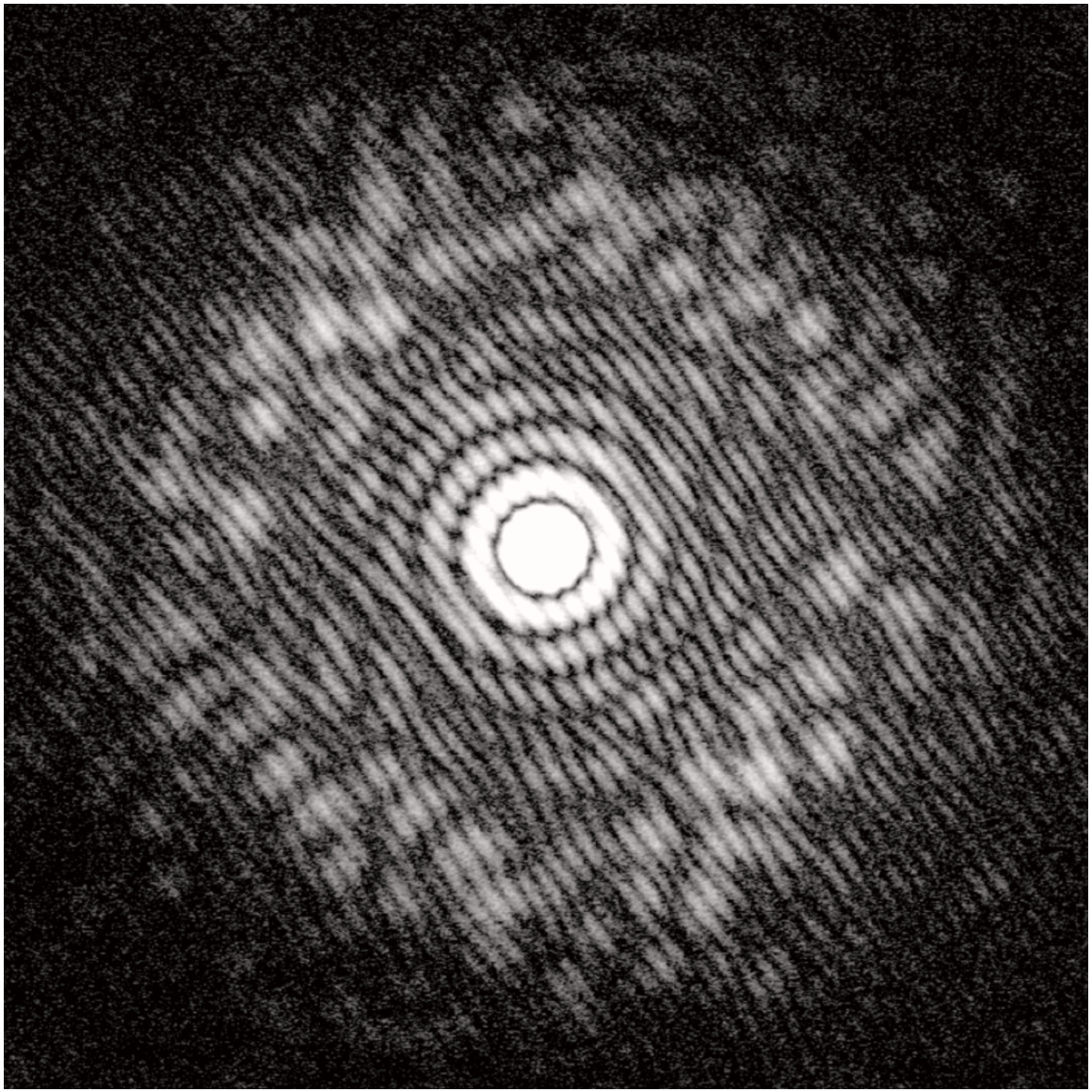

S. Eisebitt, J. Lüning, W.F. Schlotter, M. Lörgen, O. Hellwig,
W. Eberhardt & J. Stöhr / *Nature*, 16 Dec 2004

Recorded Pattern of Magnetic Nanostructures and Comparison to Scanning X-Ray Microscope

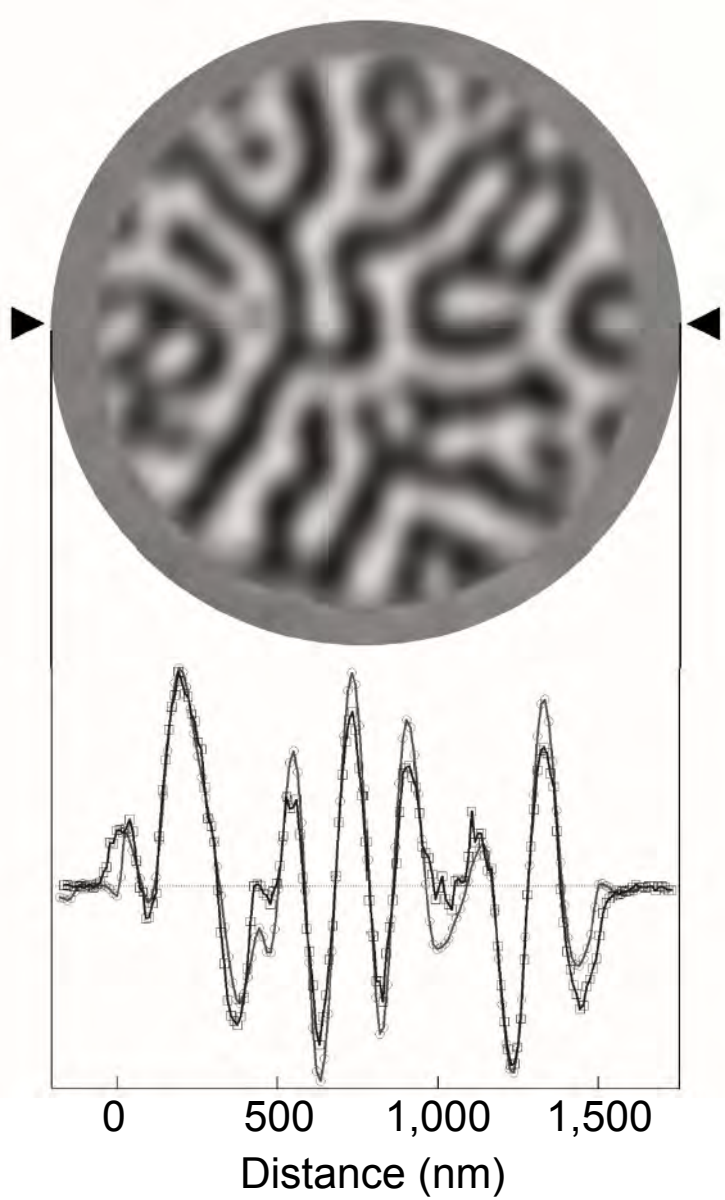

S. Eisebitt, J. Lüning, W.F. Schlotter, M. Lörgen, O. Hellwig, W. Eberhardt & J. Stöhr / *Nature*, 16 Dec 2004

Undulators, FELs and Coherence

- Spatial coherence
- Temporal coherence
- Partial coherence
- Full coherence
- Spatial filtering
- Uncorrelated emitters
- Correlated emitters
- True phase coherence and mode control
- Lasers, amplified spontaneous emission (ASE) and mode control
- Undulator radiation
- SASE FEL 100^{+} fsec soft/hard x-rays
- Seeded FEL true phase coherent x-rays
- High harmonic generation (HHG) compact fsec/asec EUV
- EUV lasers and laser seeded HHG
- Applications with uncorrelated emitters
- Applications with correlated emitters

Young's Double Slit Experiment: Spatial Coherence and the Persistence of Fringes

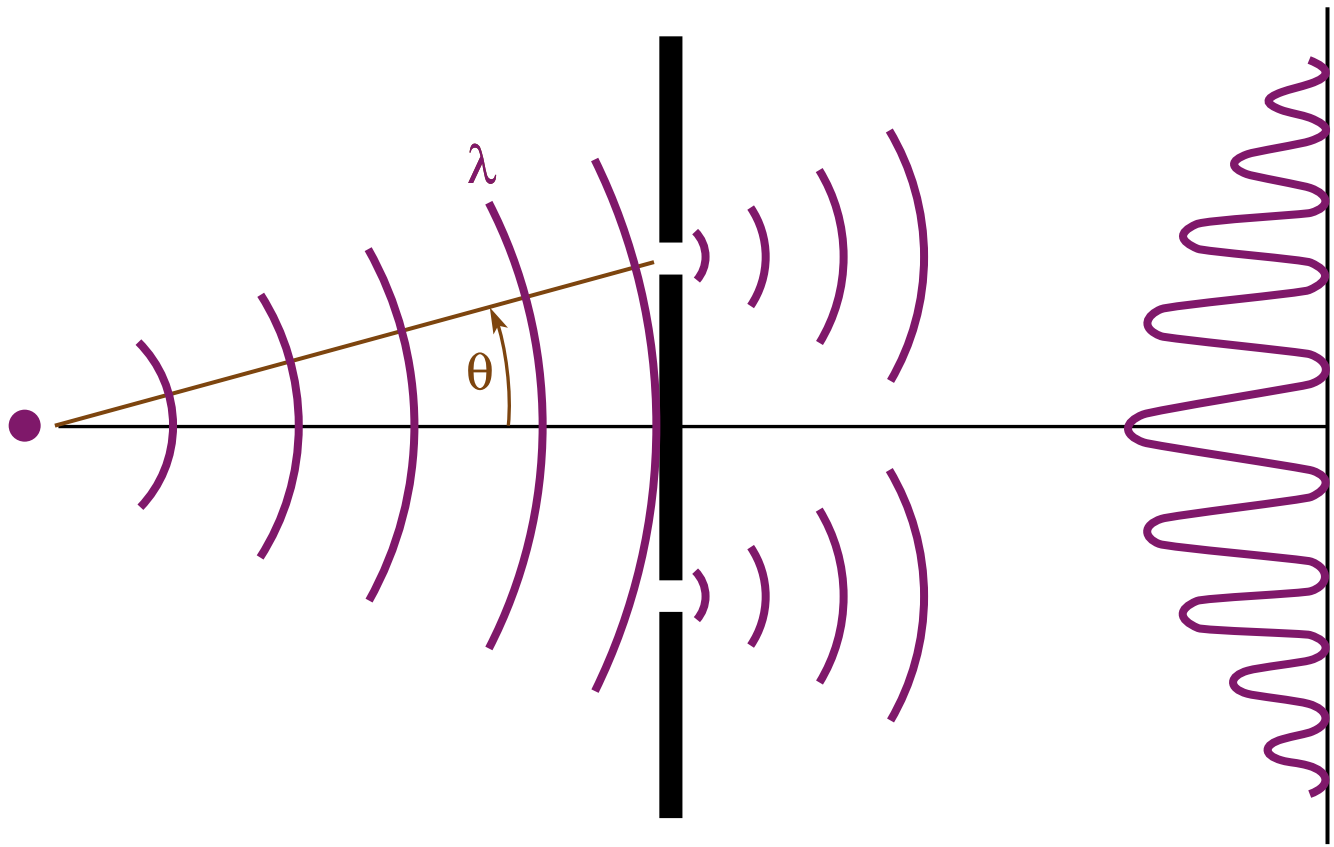

Professor David Attwood
Univ. California, Berkeley

Young's Double Slit Experiment: Spatial Coherence and the Persistence of Fringes

Persistence of fringes as the source grows from a point source to finite size.

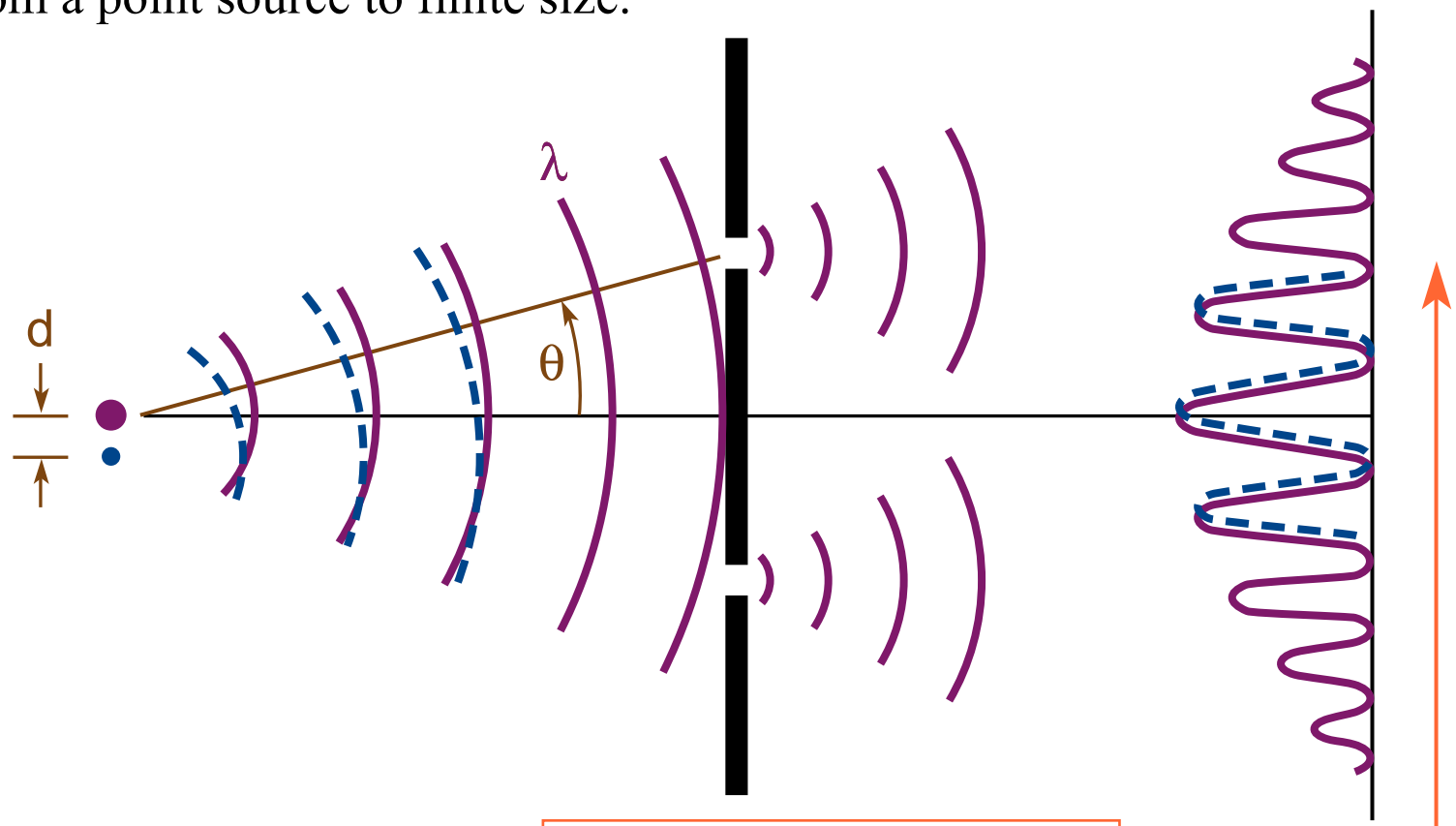

$$d \cdot 2\theta|_{FWHM} \simeq \lambda/2$$

$$\lambda_{coh} = \lambda^2/2\Delta\lambda = \frac{1}{2} N_{coh}\lambda$$

Professor David Attwood
Univ. California, Berkeley

Young's Double Slit Experiment with Random Emitters: Young did not have a laser

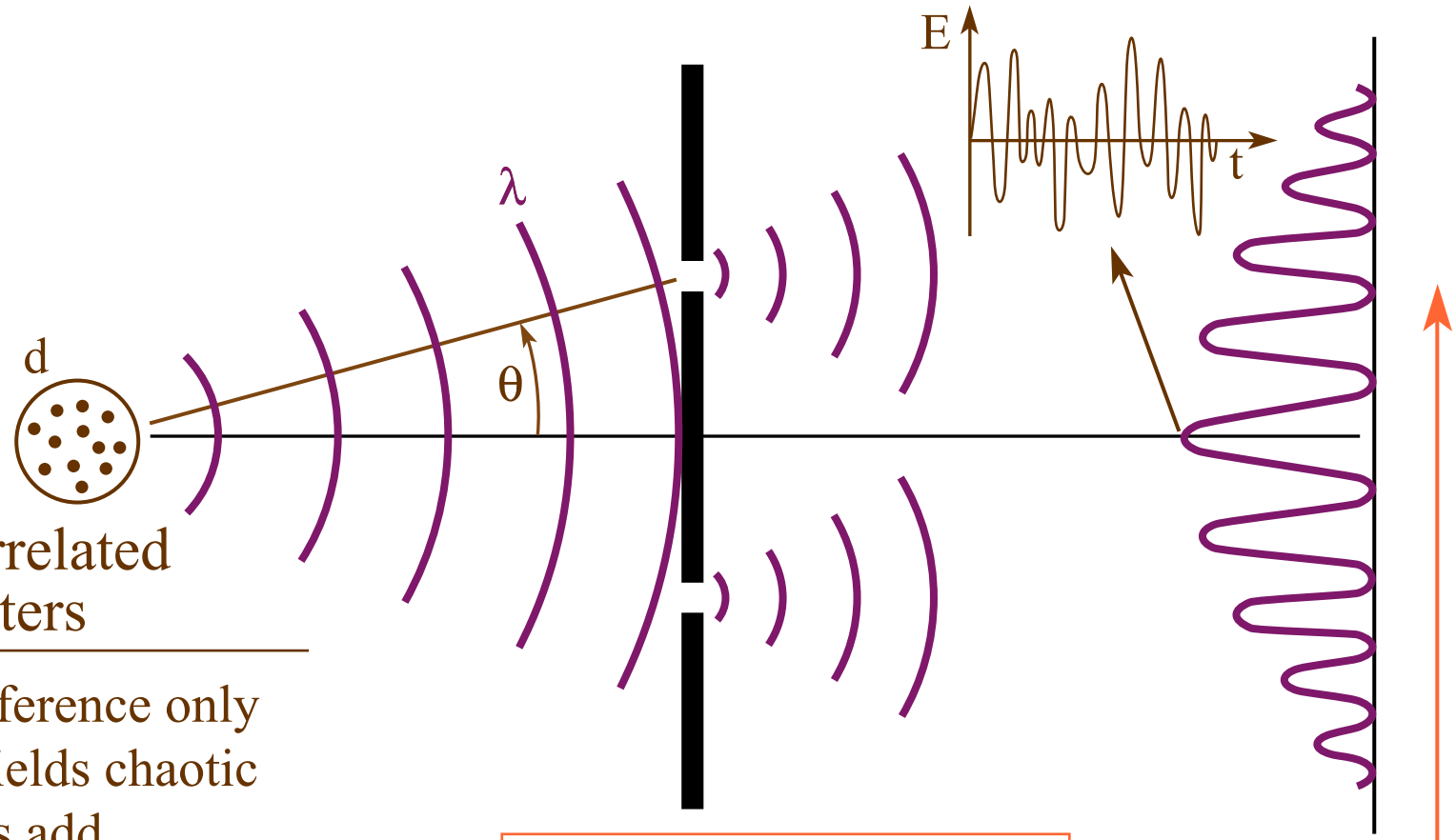

N uncorrelated emitters

- Self-interference only
- Electric fields chaotic
- Intensities add
- Radiated power ~ N

$$d \cdot 2\theta|_{FWHM} \simeq \lambda/2$$

$$\lambda_{coh} = \lambda^2/2\Delta\lambda = \frac{1}{2} N_{coh}\lambda$$

Professor David Attwood
Univ. California, Berkeley

Young's Double Slit Experiment with Phase Coherent Emitters (some lasers, or properly seeded FELs)

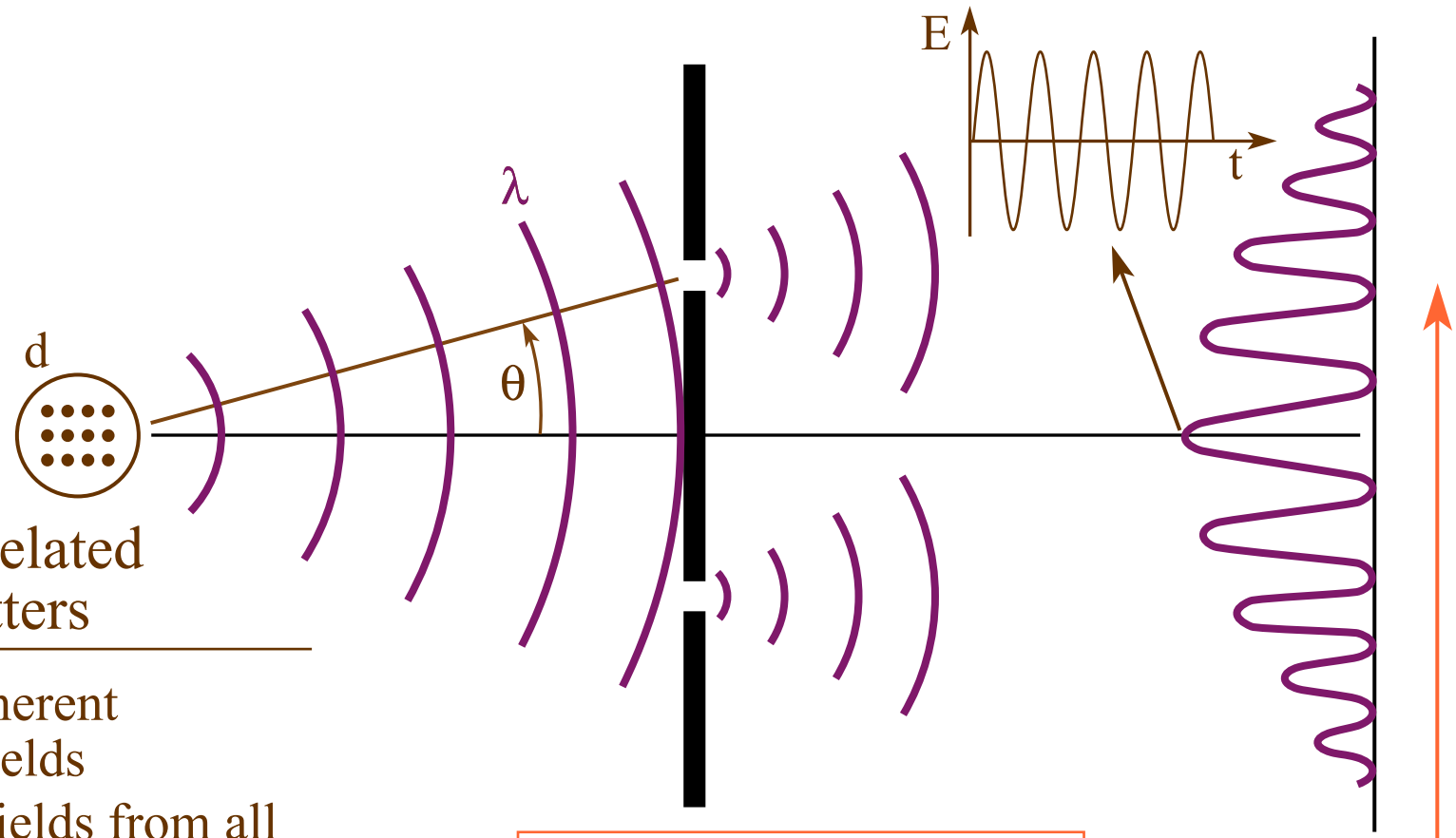

N correlated emitters

- Phase coherent electric fields
- Electric fields from all particles interfere constructively
- Radiated power ~ N^2
- New phase sensitive probing of matter possible

$$d \cdot 2\theta|_{FWHM} \simeq \lambda/2$$

$$\lambda_{coh} = \lambda^2/2\Delta\lambda = \frac{1}{2} N_{coh}\lambda$$

Professor David Attwood
Univ. California, Berkeley

The Lasing Process Begins with Amplified Spontaneous Emission (ASE)

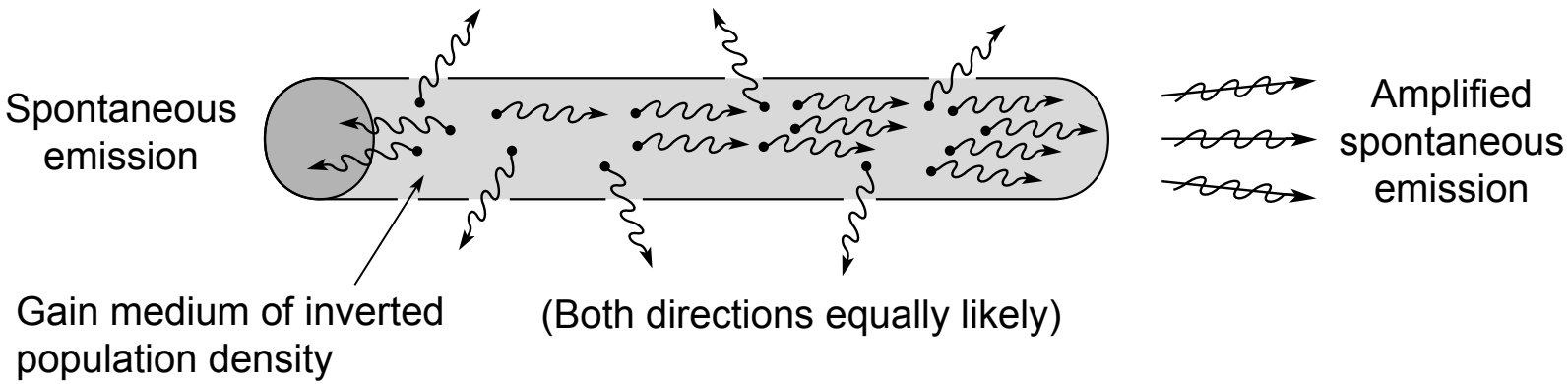

but with spatial and temporal filtering, true phase coherence and mode control can be achieved.

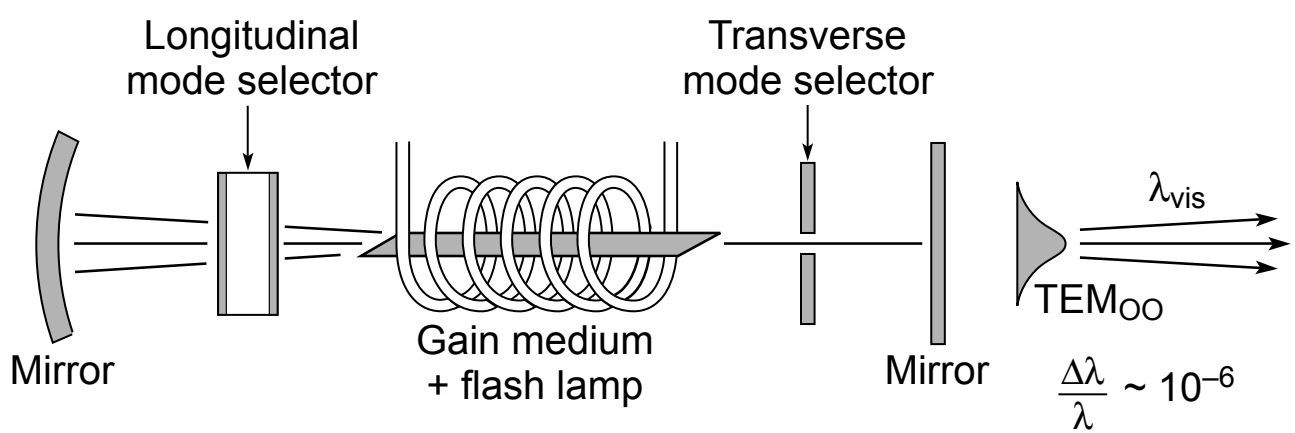

Undulators and FELs

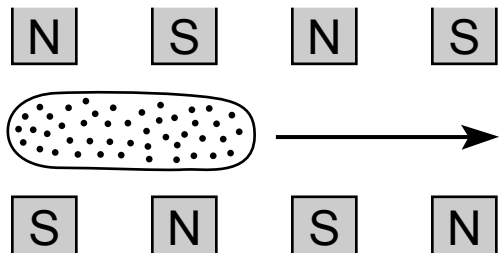

$$\frac{d\mathbf{p}}{dt} = -e(\mathbf{E} + \mathbf{v} \times \mathbf{B})$$

Undulator – uncorrelated electron positions, radiated fields uncorrelated, intensities add, limited coherence, power ~ N.

Undulators and FELs

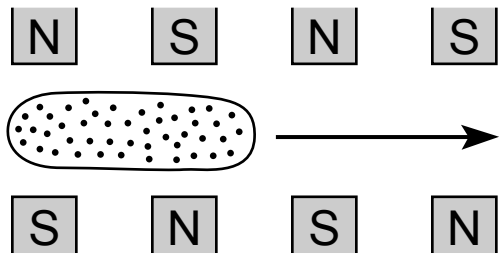

$$\frac{d\mathbf{p}}{dt} = -e(\mathbf{E} + \mathbf{v} \times \mathbf{B})$$

Undulator – uncorrelated electron positions, radiated fields uncorrelated, intensities add, limited coherence, power ~ N.

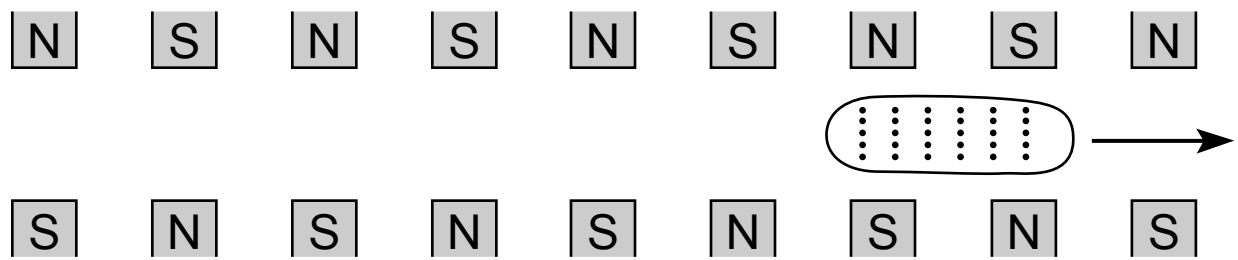

Free Electron Laser (FEL) – very long undulator, electrons are "microbunched" by their own radiated fields into strongly correlated waves of electrons, all radiated electric fields now add, spatially coherent, power ~ N^2

$$\frac{d\mathbf{p}}{dt} = -e(\mathbf{E} + \mathbf{v} \times \mathbf{B})$$

Undulators and FELs

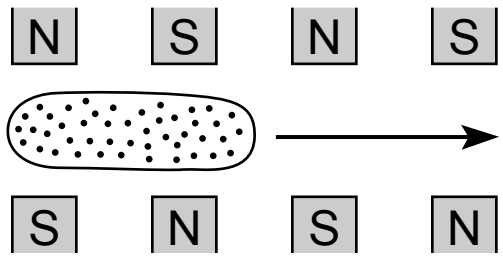

$$\frac{d\mathbf{p}}{dt} = -e(\mathbf{E} + \mathbf{v} \times \mathbf{B})$$

Undulator – uncorrelated electron positions, radiated fields uncorrelated, intensities add, limited coherence, power ~ N.

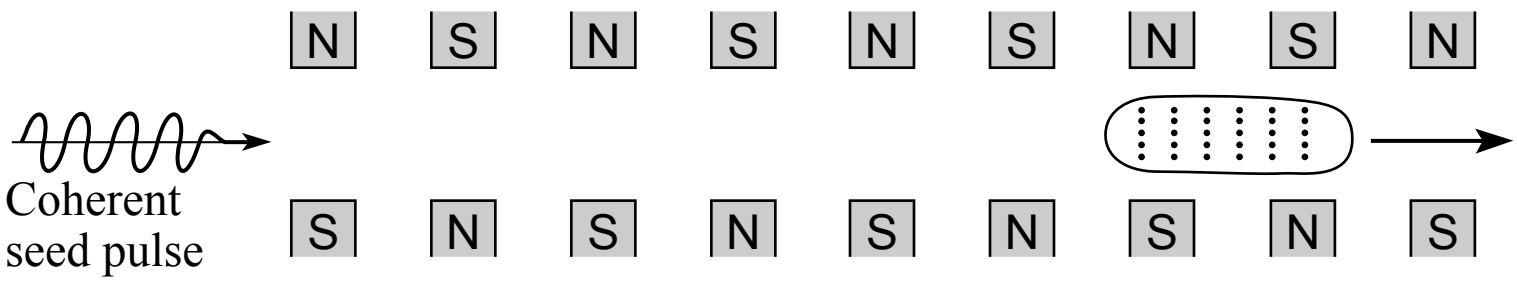

Free Electron Laser (FEL) – very long undulator, electrons are "microbunched" by their own radiated fields into strongly correlated waves of electrons, all radiated electric fields now add, spatially coherent, power ~ N^2

$$\frac{d\mathbf{p}}{dt} = -e(\mathbf{E} + \mathbf{v} \times \mathbf{B})$$

Gain and Saturation in an FEL

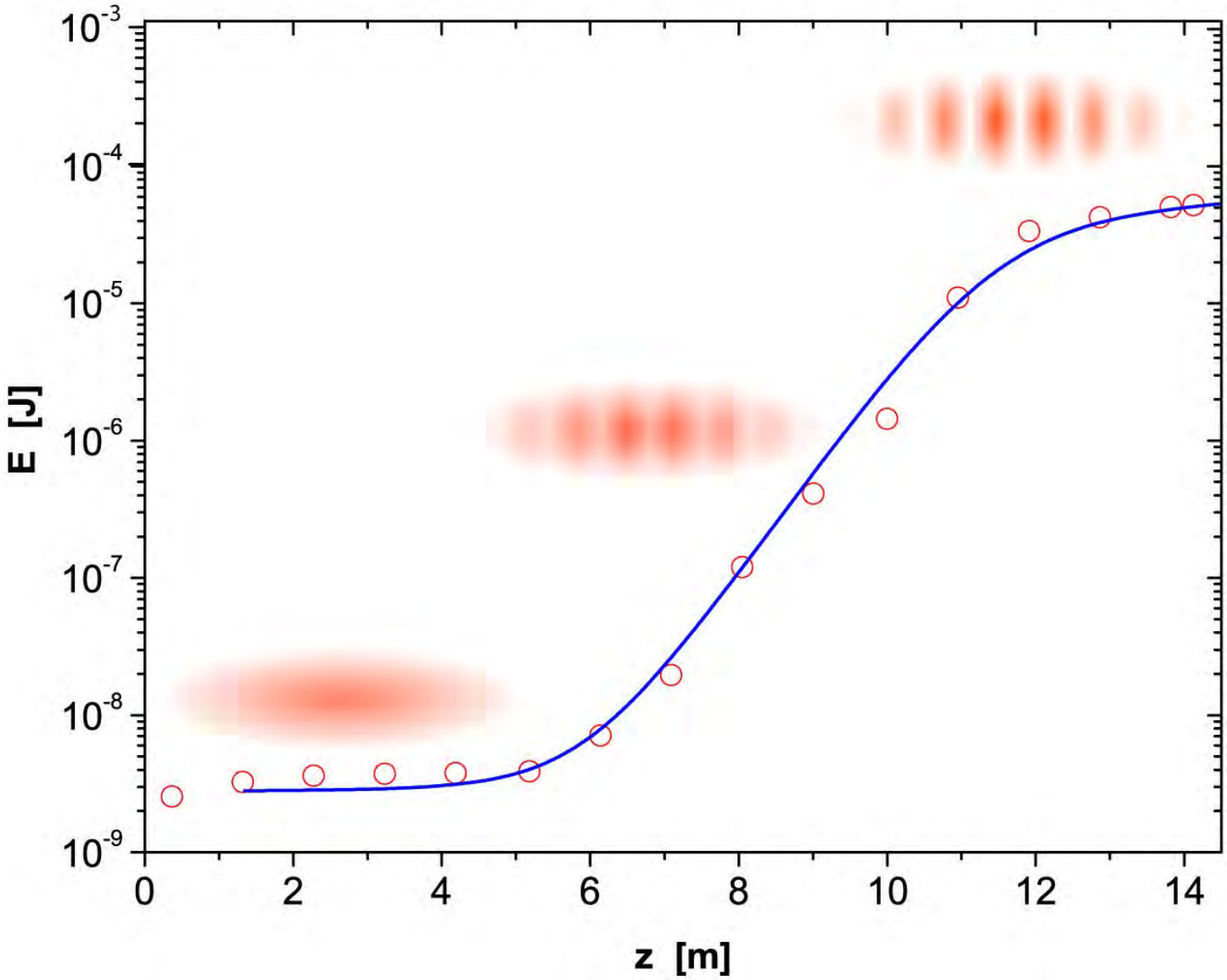

Courtesy of K-J. Kim

Professor David Attwood
Univ. California, Berkeley

FEL Microbunching

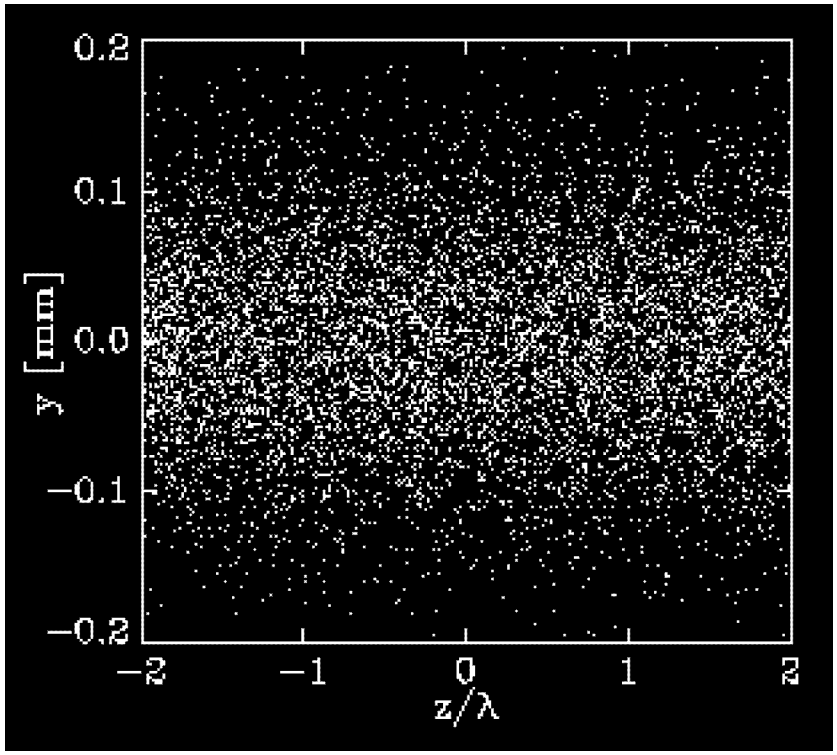

Courtesy of Sven Reiche, UCLA.

Free Electron Lasers

Parameters	Flash FEL (Hamburg)	LCLS (Stanford, 2010)	European XFEL (Hamburg, Schenefeld; 2014)
E_e	230/1000 MeV	13.6 GeV	17.5 GeV
γ	450/2000	26,600	35,000
λ_u	2.73 cm	3 cm	5 cm
N	500/1100	3700	4000
L_u	30 m	112 m	200 m
$\hbar\omega$	50-200 eV	1-10 keV	4-12 keV
$\lambda/\Delta\lambda$	100	350	1000
e^-/bunch	10^9	6×10^9 (1 nC)	6×10^9
$\Delta\tau$	25 fsec	160 fsec	100 fsec
$\dot{\mathcal{F}}$	3×10^{12} ph/pulse	2×10^{12} ph/pulse	$10^{12} - 10^{14}$ ph/pulse
rep rate	1 Hz	120 Hz	10 Hz
$\hat{I}$	1.3 kA	3.4 kA	
$\hat{P}$	0.3 GW	8 GW	20-100 GW
$\hat{B}$	1×10^{28}	1×10^{33}	5×10^{33}
L	260 m	5 km	3.4 km

FLASH EUV/soft x-ray FEL at DESY Lab, Hamburg

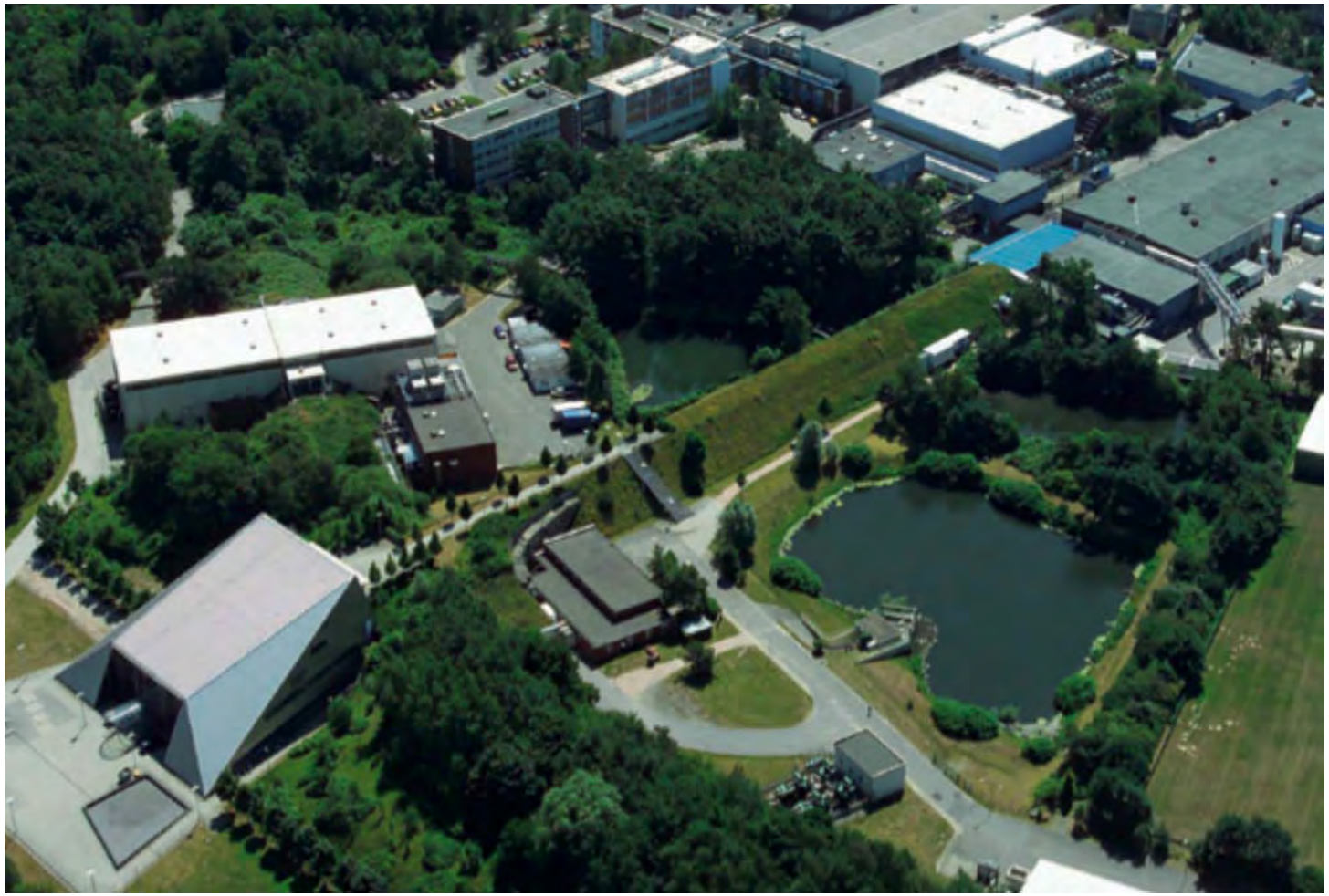

6.5-32 nm wavelength in 1st harmonic
20 fsec, 10^{12} photons per pulse

Courtesy of Henry Chapman (LLNL, now Hamburg) and Stefano Marchesini (LLNL, now LBL).

Coherent X-ray Diffractive Imaging with the FLASH free-electron laser (FEL) in Hamburg, Germany

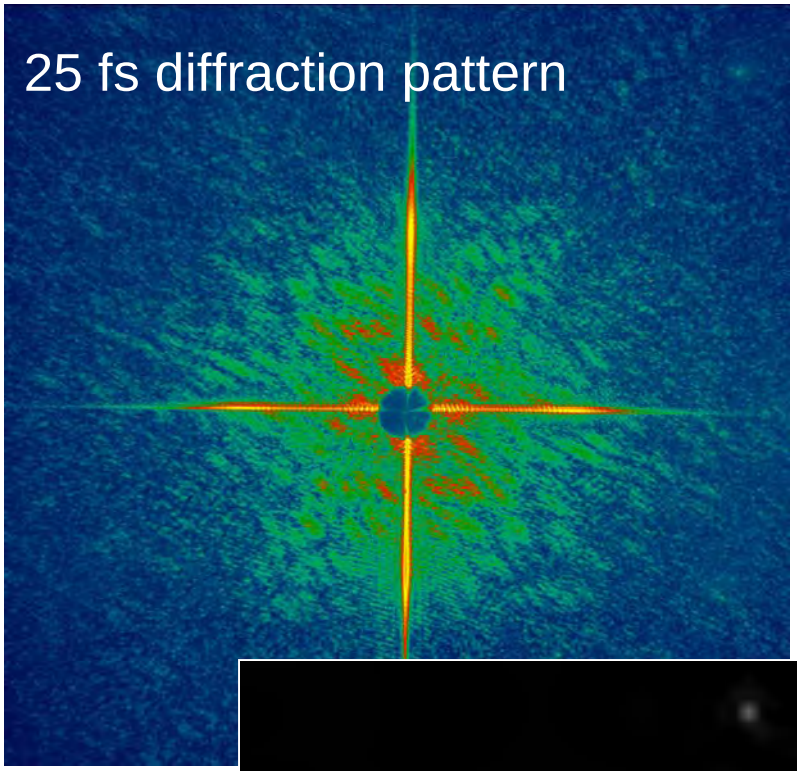

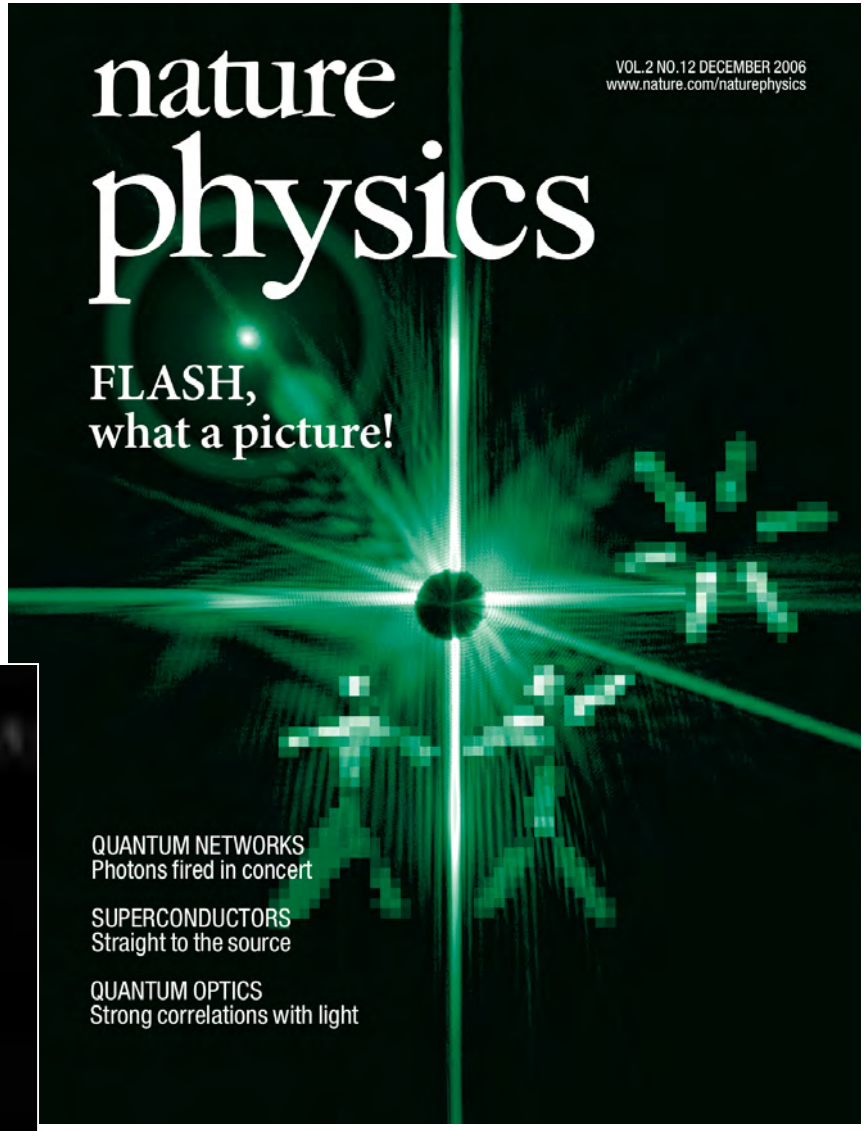

Chapman et al, *Nature Phys* **2** 839 (2006)